EUROPEAN COMMISSION

Community Research

SEVENTH FRAMEWORK PROGRAMME

ARCHER

Collaborative Project

Co-funded by the European Commission under the
Euratom Research and Training Programme on Nuclear Energy
within the Seventh Framework Programme

Grant Agreement Number: 269892
Start date: 01/02/2011 Duration: 48 Months

www.archer-project.eu

Archer
Advanced Reactor for Cogeneration of Heat & Electricity-R&D

Report on graphite selection and recommended design properties.

Part III - Graphite Selection and Recommended Design Properties.

Deliverable D41-18

M W Davies (AMEC)

ARCHER project – Contract Number: 269892
Advanced High-Temperature Reactors for Cogeneration of Heat and Electricity R&D
EC Scientific Officer: Dr. Panagiotis Manolatos

Document title	Report on graphite selection and recommended design properties. Part III – Graphite Selection and Recommended Design Properties
Author(s)	M W Davies (AMEC)
Number of pages	66
Document type	Report
Work Package	WP41
Document number	D41-18
Issued by	AMEC
Date of completion	29/01/15
Dissemination level	Restricted to the partners of the ARCHER project

Summary

A number of graphites have been irradiated to a high fluence in the High Flux Reactor at Petten at two different temperatures, namely at 750°C and at 950°C. An assessment of the data from these experiments has been carried out in two companion reports to this report (Refs 1 and 2). The assessments looked at the dimensional change behaviour of the graphites tested, along with the changes in dynamic Young's modulus, coefficient of thermal expansion and thermal conductivity with fluence. A comparison was made between the dimensional change behaviour and the property variations for each graphite at each temperature, and both qualitative and quantitative observations were made. This report considers the data in its entirety and compares and contrasts the differences in behaviour between the graphites. It also provides an insight as to how these differences could affect their suitability for the two different high temperature reactor (HTR) types, namely the prismatic/block type reactor and the pebble bed type reactor.

It is not the intention of this report to recommend the use any of the graphites tested for a particular reactor design nor to state that any of them should be discounted. It is entirely up to the designer to make the selection and to justify this. The report concludes that the 'ideal' graphite does not exist yet and is unlikely to ever exist. Therefore the designer needs to take advantage of the favourable behaviour/attribute of a particular graphite and minimise the effect of the unfavourable ones.

For each graphite tested, the fluences to reach cross-over were found to be dramatically reduced on going from 750°C to 950°C, generally by a factor of ~2. This could have implications for the VHTR, where the graphite temperatures will be significantly higher than for a HTR, and so it is essential that the highest temperatures in the graphite do not coincide with the highest fluences.

Approval

Rev.	Short description	First author	WP Leader	Domain leader	Coordinator
0	First issue	M W Davies AMEC	A Vreeling (NRG)	D Buckthorpe (AMEC)	S Knol (NRG)

Distribution list

Name	Organisation	Comments
P. Manolatos	EC DG RTD	
All technical participants	ARCHER	
Steering Committee members	ARCHER	

DOCUMENT ISSUE RECORD
(engineering documents)

Document Title :	**Reports on graphite selection and recommended design properties. Part III – Graphite Selection and Recommended Design Properties**
Project Reference:	100525

Purpose of Issue : Issue to client

Security Class : Not protectively marked

Issue	Description of Amendment	Originator/ Author	Checker	Approver	Date
01	First Issue	M W Davies	D Buckthorpe	J O'Keefe	Jan 2015

Total number of pages:	Intro:		Text	66	Tables		Figures		Appendices	

Previous issues of this document shall be destroyed or marked **SUPERSEDED**

Distribution: ARCHER partners, M W Davies, D Buckthorpe, A Grainger

Table of contents

1 Introduction & Scope

In order to support the development of a future European High Temperature Reactor (HTR), a number of candidate graphites were selected for an irradiation programme. This programme was undertaken by NRG using the high flux reactor (HFR) at Petten and was aimed at establishing the irradiation behaviour of selected graphites over the fluence and temperature range appropriate for a HTR. This would allow the 'best' graphite(s) to be selected and would provide a significant amount of the data necessary to undertake a graphite core design.

Based on the reference design for the Pebble Bed Modular Reactor (PBMR), the peak fluence to be achieved for the irradiation programme was set at 25 displacements per atom (dpa), i.e. ~200 x 10^{20} n.cm^{-2} Equivalent DIDO Nickel Dose (EDND), and the temperature range was set at 550°C to 950°C. It was decided to carry out the first irradiation experiment at the mid-point of the temperature range i.e. 750°C, and to a maximum fluence of ~ 1/3 of the target peak fluence i.e. 8-9 dpa (~65-70 x 10^{20} n.cm^{-2} EDND). This was referred to as INNOGRAPH 1A and was carried out within the 5th Framework Programme (HTR-M1). The follow-up experiment at 750°C was planned to achieve a maximum fluence of ~2/3 of the target peak fluence i.e..15-16 dpa (~125-130 x 10^{20} n.cm^{-2} EDND), This was referred to as INNOGRAPH 1B and was carried out in the 6th Framework Programme (RAPHAEL). After the PIE of the INNOGRAPH 1A samples was carried out, around half of the samples were placed in the INNOGRAPH 1B experiment, the remaining positions being filled with fresh graphite specimens. With this arrangement, the fresh samples would see ~2/3 of the peak fluence and the samples previously irradiated in INNOGRAPH 1A would be irradiated up towards the peak fluence. Due to the flux buckling of the HFR, each experiment would see a range of fluences, with the samples at the top and bottom seeing about 0.65 of the fluence in the centre. A full post-irradiation examination (PIE) of the samples was carried out after each stage. This involved measuring their new dimensions and mass (from which their new volumes and densities were calculated) as well as dynamic Young's modulus (DYM), coefficient of thermal expansion (CTE) and thermal diffusivity (from which their thermal conductivity was calculated). The results are assessed in Ref 1, which is a companion report to this one.

Another two irradiation experiments, referred to as INNOGRAPH 2A and 2B, were also carried out in the 6th Framework Programme These are the equivalent of INNOGRAPH 1A and 1B, but at a temperature of 950°C, and to a peak fluence of only ~14 dpa (~120 x 10^{20} n.cm^{-2} EDND). The lower fluence was specified at the outset because the higher temperature would result in a lower fluence to dimensional change turnaround and to positive growth, referred to as 'cross-over', which is a limiting feature of the capsule design. The planned PIE of all the specimens was also carried out within ARCHER and the assessment of the data, including dimensional change, DYM, CTE and thermal conductivity is carried out in Ref 2, which is also a companion report to this one.

The first aim of this report is to make a comparison of the dimensional change behaviour and property variations for the graphites to ascertain their similarities and differences. A comparison is done between the different manufacturing methods (extrusion, iso-moulding and vibro-moulding), the different grain sizes (medium, fine and super-fine), and the different coke sources (petroleum and pitch). A comparison is also done between the 'same' graphite made by two different manufacturers. The graphite grades/samples used in the INNOGRAPH 1A/1B and 2A/2B experiments are summarised in Section 2, and the pre-characterisaiton and post-irradiation measurements carried out on them are summarised in Section 3. The comparisons for the 750°C experiments are done in Section 4, and those for the 950°C experiments are done in Section 5. The second aim of the report is to compare the differences in dimensional change behaviour and property variations at the two different temperatures i.e. at 750°C and 950°C and this is carried out in Section 6. This allows the implications of moving from a HTR to a VHTR, where the graphite temperature range will be significantly higher, to be quantified and discussed. The third aim is to provide a judgment on wherether or not a particular graphite would be a suitable candidate from the point of view of a prismatic/block type reactor, where the blocks are replaced at regular intervals and so only see a low fluence, and also for a pebble bed reactor where the intent is to keep the blocks in the reactor for as long as possible, thereby minimising the number of core changes required (preferably to zero, but no more than one). This is done in Section 7. The fourth aim is to recommended initial design data for the individual graphites and this is done in Section 8.

2 Graphite grades/samples

A total of 11 candidate graphites from 3 manufacturers were chosen for INNOGRAPH. These are shown in Table 1 below, grouped in terms of manufacturer. It can be seen that they are a mixture of petroleum and pitch coke graphites made by extrusion, iso-moulding and vibro-moulding. The grain size ranges from medium, through fine, down to super-fine. Some of these grades were classified as 'major' and ~30 samples were tested for each (~15 for each grain direction). The others were classified as 'minor' and ~14 samples were tested for each (~7 for each grain direction). A small number of grades were interchanged between 'major' and 'minor' and vice versa before the INNOGRAPH 2A, 1B and 2B experiments had started. This is indicated my 'major/minor' and 'minor/major' in the table. Those that were not in the INNOGRAPH 1A experiment have a '------' for the first classification. NBG-20 was dropped after INNOGRAPH 1A and so has a '------' for the second classification.

Manufacturer	Grade	Coke	Grain size	Process	Classification
GrafTech	PCEA	Petroleum	Medium	Extrusion	Minor/Major
	PPEA	Pitch	Medium	Extrusion	Major/Major
	PCIB-SFG	Petroleum	Super-fine	Iso-moulding	Major/Minor
	LPEB/BAN	Petroleum	Medium	Extrusion	-------/Minor
SGL	NBG-10	Pitch	Medium	Extrusion	Major/Major
	NBG-20	Petroleum	Medium	Extrusion	Minor/-------
	NBG-25	Petroleum	Fine	Iso-moulding	Major/Minor
	NBG-17	Pitch	Medium	Vibro-moulding	-------/Minor
	NBG-18*	Pitch	Medium	Vibro-moulding	-------/Major
Toyo Tanso	IG-110	Petroleum	Fine	Iso-moulding	Major/Minor
	IG-430	Pitch	Fine	Iso-moulding	Minor/Minor

Table 1 – Selected graphites for the INNOGRAPH irradiation experiment

3 Pre-characterisation and post-irradiation measurements

3.1 Pre-characterisation measurements

The graphite blocks supplied by the manufacturers for each grade were sectioned and machined to produce the required number of samples. Each sample was cylindrically shaped with a nominal diameter of 8 mm and a nominal length of 6 or 12 mm. The samples were machined from both the central and outer regions of each block, to take account of the known variability in properties throughout it. In addition, a small flat was also machined on each sample so that it could be uniquely identified with an alphanumeric code, and its orientation within the block would be known for recording the measurements (Figure 1). In this way, initial property variations as a function of position and orientation in the block, could be determined (as well as for the irradiated properties).

The dimensions of each sample (see Section 3.2) were measured together with its DYM, CTE and thermal diffusivity (used to calculate thermal conductivity). The mass of each sample was also measured, which together with the dimensions, allowed the initial density to be determined. Details of the testing methods used are given in Ref 3. All the measurements (together with specific properties derived from them) were recorded in an Excel spreadsheet developed by NRG.

[Note - Although strength is a very important property from a core design point of view, it cannot be measured on the samples to be irradiated as this will involve a destructive test. Nevertheless, strength

measurements can be made on other suitable samples obtained from a disc/block, and the strength distribution thus obtained should be representative of those being irradiated. Measurements of non-irradiated and irradiated strength were carried out within the ARCHER programme and the results are reported in Ref 4. All show the typical behaviour, which is an initial sharp increase at low fluence, followed by a plateau and then a further rise to a peak, after which it falls at an increasing rate..

3.2 Sample Orientations

Given the need to cover both principal directions (WG and AG), the cylindrical shape of the samples with the machined flat meant that great care had be used to ensure that the principal directions were maintained for each sample during manufacture. Figure 2 shows the orientations of the samples taken from both an extruded block and an iso-/vibro-moulded block. It can be seen that the extruded block has one principal WG direction and two principal AG directions, whereas the iso-/vibro-moulded block has two principal WG directions and one principal AG direction. The figure also shows the three dimensions measured, namely the axial length (L), the major diameter (D) and the smaller diameter perpendicular to the flat (X). The samples are classified as WG or AG according to the axial direction, hence the axial length L is always in this (assigned) orientation. The classification of the other two dimensions however depends on its orientation and also which type of block it came from. Table 2 below gives the appropriate classifications.

Process	**Sample orientation**	**Classification**		
		L	**D**	**X**
Extrusion	WG	WG	AG	AG
	AG	AG	AG*	WG*
Iso-moulding, Vibro-moulding	WG	WG	WG*	AG*
	AG	AG	WG	WG

Table 2 – Classification of sample dimensions with respect to sample orientation

* These classifications rely on the flat being machined with the sample in (or very close to) the correct orientation. If this was not the case for any sample, these particular measurements will not be 100% WG or AG, but will be somewhere in between, and this would reduce their usefulness.

4 Comparison of graphite irradiation behaviour at 750°C

4.1 Dimensional change behaviour

In this section, a comparison is made between the dimensional change behaviour of the 7 different graphites tested in both INNOGRAPH 1A and 1B. These are the ones that reached the full fluence of ~23 dpa, namely NBG-10, NBG-25, PCEA, PPEA, PCIB, IG-110 and IG-430. Figure 3 is a plot for all the graphites in the WG direction, Fig. 4 is the equivalent plot for the AG direction and Fig. 5 is the plot for the volume change. It can be seen that there is a very large difference in behaviour across all 7 graphites in terms of the maximum shrinkage observed, the fluence at which this (turnaround) occurs, the fluence at which cross-over occurs (which is when the original dimensions/volume return to their pre-irradiated values), and the maximum dimensions/volume attained at the peak fluence,

Because the graphites cover the spectrum of coke source, grain size and manufacturing methods used to manufacture nuclear grade graphite at the time, the data can be used to investigate the effect of each of these on dimensional change behaviour. First of all a comparison is made between the extruded and iso-moulded graphites, which is also effectively a comparison between the different grain sizes – the extruded graphites having a medium grain size and the iso-moulded graphites having a fine and super-fine grain size. Next, a comparison is made between similar petroleum coke and the pitch coke graphites. Finally a comparison is made for the ‘same’ graphite made by two different manufacturers.

4.1.1 Comparison between the extruded and iso-moulded graphites

The extruded grades are NBG-10, PCEA and PPEA, and the iso-moulded grades are NBG-25, PCIB, IG-110 and IG-430. The comparison of these graphites in terms of dimensional change behaviour is shown in Fig. 6 for the WG direction, Fig. 7 for the AG direction and Fig. 8 for the volume change. It can be seen that in all three cases, the extruded graphites generally shrink more than the iso-moulded graphites, and reach both turnaround and cross-over at a higher fluence.

4.1.2 Comparison between the petroleum coke and pitch coke graphites

The comparison between the petroleum coke and pitch coke graphites is best carried out for the two pairs of 'sister' graphites namely PCEA & PPEA and IG-110 & IG-430. PCEA and PPEA are both extruded graphites made by the same company (GrafTech), and densified using the same number of pitch impregnations. The first is made out of a petroleum coke and the second is made out of a pitch coke. IG-110 and IG-430 are both iso-moulded graphites made by the same company (Toyo Tanso), and densified using the same number of pitch impregnations. The first is made out of a petroleum coke and the second is made out of a pitch coke.

Figure 9 shows the WG, AG and volume changes for PCEA and PPEA. It can be seen that the petroleum coke graphite (PCEA) shrinks more than the pitch coke graphite (PPEA), and reaches both turnaround and cross-over at a higher fluence for the WG and AG directions as well as the volume change. Figure 10 shows the WG, AG and volume changes for IG-110 and IG-430. It can be seen that the petroleum coke graphite (IG-110) again shrinks more than the pitch coke graphite (IG-430), and reaches both turnaround and cross-over at a higher fluence for the WG and AG directions as well as the volume change

4.1.3 Comparison between the 'same' graphite made by different manufacturers

NBG-10 is an extruded pitch coke graphite made by SGL, and PPEA is an extruded graphite made by GrafTech. Both use the same source coke and both are densified with two impregnations. The 'graphite' is actually that currently used for the fuel sleeves in the UKs Advanced Gas-cooled Reactors and was known at the time of selection to have a good irradiation behaviour at temperatures at least up to 550^{o}C (which is around the peak temperature seen by the fuel sleeves). This was one of the reasons for its inclusion in the INNOGRAPH programme.

Figure 11 shows the WG, AG and volume changes for NBG-10 and PPEA. It can be seen that in all three cases, the behaviour of the two graphites is very similar, which is reassuring.

4.2 DYM variations

The DYM variations with irradiation fluence for the extruded graphites are shown in Fig 12, and the fractional changes, or multiplying factors (expressed as DYM_{irr} / DYM_{unirr}) are shown in Fig 13. The DYM variations for the iso-moulded graphites are shown in Fig 14, and the fractional changes are shown in Fig 15. It can be seen from DYM variations plots that all graphites show a similar behaviour. First of all there is a sharp rise in DYM over the range 0-1 dpa. This is followed by a plateau up to around 5-6 dpa, after which there is a more gradual increase in DYM until a peak is reached. Thereafter the DYM falls off at an ever-increasing rate, and this is due to the graphite structure breaking down. [It should be noted that available strength data on previously irradiated graphites have shown that the strength follows a similar trend, with the initial sharp increase, followed by a plateau, which in turn is followed by a gradual increase to a peak, before undergoing a reduction at an ever increasing rate. The samples eventually fell apart due to an almost total loss of strength].

The only real difference between the extruded and iso-moulded graphites is evident from the fractional change plots. These show that the extruded graphites have an initial fractional increase of ~1.45 whereas the iso-moulded graphites have a higher initial increase of between 1.6 and 1.7. In a similar fashion, the factorial increase corresponding to the peak DYM ranges from 2.70 to 2.82, whereas the iso-moulded graphites have a higher peak value ranging from 3.15 to 3.48. The difference is attributed to the grain size rather than the manufacturing method, the larger effect being seen by the smaller grain size.

4.3 CTE variations

The variations in CTE with irradiation fluence for the extruded graphites are given in Fig 16 and the fractional changes are shown in Figure 17. The CTE variations for the iso-moulded graphites are shown in Fig 18 and the fractional changes in Fig 19. The fractional changes (f) are expressed as (CTE_{irr} / CTE_{unirr}) – 1, which is the customary way of doing this [thus CTE_{irr} = (1 - f)*CTE_{unirr}]. Each plot shows the value of the mean CTE over 3 temperature ranges, 30-120°C, 30-200°C and 30-750°C. The five graphites that were irradiated up to the peak fluence of ~23 dpa show the familiar trend seen for all graphites irradiated in the past. There is a small initial increase in CTE over a fluence range of 0-2 dpa, after which there is a progressive decrease until a plateau is reached. For all five graphites, this continues up to at least the peak fluence reached (~23 dpa). Unfortunately, there was insufficient data for IG-110 and IG-430 to establish their CTE variation at fluences beyond 10 dpa, but it would expected to be similar to that of the other five graphites.

4.4 Thermal conductivity variations

The variations in thermal conductivity with irradiation fluence for the extruded graphites are given in Fig 20 and the fractional changes are shown in Figure 21. The thermal conductivity variations for the iso-moulded graphites are shown in Fig 22 and the fractional changes in Fig 23. The fractional changes are expressed as ($TCon_{irr}$ / $TCon_{unirr}$) – 1, which is the customary way of doing this. Each plot shows the value of the instantaneous thermal conductivity at temperatures of 27, 100, 200, 300, 400, 500, 600 and 700°C. It can be seen from Figures 20 and 22 that the unirradiated thermal conductivity of each graphite decreases with increasing temperature. When irradiated, all 7 graphites show the familiar trend seen for all graphites irradiated in the past. There is a very rapid decrease in thermal conductivity over a fluence range of 0-1 dpa, after which a plateau is reached. At higher fluences, a further decrease is observed, and this continued up until the peak fluence was reached.

It is interesting to note that, although there is a large spread in the unirradiated thermal conductivity over the measured temperature range (27° to 700°C), the variation is significantly reduced after a relatively small amount of irradiation. For example, Figure 20a shows that the spread in thermal conductivity for NBG-10 over the temperature range is ~160 W/m/K (at 27°C) to ~65 W/m/K at (700°C), a range of ~95 W/m/K. However, after only a few dpa of irradiation the thermal conductivity is ~40 W/m/K (at 27°C) to ~25 W/m/K at (700°C), a range of only ~15 W/m/K. At higher fluences, it can be seen that the range reduces to ~10 W/m/K.

5 Comparison of graphite irradiation behaviour at 950°C

5.1 Dimensional change behaviour

In this section, a comparison is made between the dimensional change behaviour of the 5 major grade graphites tested in INNOGRAPH 2A and 2B, namely NBG-10, NBG-18, NBG-25, PCEA and PPEA. Figure 24 is a plot for all the graphites in the WG direction, Fig. 25 is the equivalent plot for the AG direction and Fig. 26 is the plot for the volume change. It can be seen that there is a large difference in behaviour across all 5 graphites in terms of the maximum shrinkage observed, the fluence at which this (turnaround) occurs, the fluence at which cross-over occurs (which is when the original dimensions/volume return to their pre-irradiated values), and the maximum dimensions/volume attained at the peak fluence.

Because the graphites cover the spectrum of coke source, grain size and manufacturing methods used to manufacture nuclear grade graphite, the data can be used to investigate the effect of each of these on dimensional change behaviour. First of all a comparison is made between the extruded and moulded graphites, which is also effectively a comparison between the different grain sizes – the extruded and vibro-moulded graphites having a medium grain size and the iso-moulded graphite having a fine grain size. Next, a comparison is made between similar petroleum coke and the pitch coke graphites. Finally a comparison is made for the 'same' graphite made by two different manufacturers.

5.1.1 Comparison between the extruded and moulded graphites

The extruded grades are NBG-10, PCEA and PPEA, the iso-moulded grade is NBG-25, and the vibro-moulded grade is NBG-18. A comparison of these graphites in terms of dimensional change behaviour is shown in Fig. 27 for the WG direction, Fig. 28 for the AG direction and Fig. 29 for the volume change. The line types and colours have been chosen to group the graphites together in terms of manufacturing method and grain size. The extruded graphites are shown in different shades of blue and in solid lines to indicate they have a medium grain size. The moulded graphites are shown in red. NBG-18 is shown in a solid line to indicate that is also has a medium grain size, and IG-110 is shown in a dotted line to indicate that it is different to the others in that it has a fine grain size.

It can be seen that in all three cases, the extruded graphites shrink in a similar way and at a faster rate than the moulded graphites, reaching a higher shrinkage before turnaround. This was also the case for the 750°C irradiations. Of the three extruded graphites, PCEA, which is the petroleum coke graphite, shrinks the most. After turnaround the behaviour of all three graphites is similar for the AG direction and volume but the differences are more pronounced for the WG directions. The two moulded graphites both shrink at a similar rate and reach turnaround and cross-over at about the same time. Thereafter, however, the dimensions/volume increase at a faster rate for NBG-18. The cross-over fluences are similar for all five graphites in the WG direction and for volume, but in the AG direction the moulded graphites cross-over at significantly lower fluences than the extruded graphites.

5.1.2 Comparison between the petroleum coke and pitch coke graphites

The comparison between the petroleum coke and pitch coke graphites is best carried out for pairs of 'sister' graphites as was the case for the 750°C experiments. In this case however, only the data for PCEA and PPEA were sufficient to make a meaningful comparison. Figure 30 shows the WG, AG and volume changes. It can be seen that the petroleum coke graphite (PCEA) shrinks more than the pitch coke graphite (PPEA), and reaches both turnaround and cross-over at a higher fluence for the WG and AG directions as well as the volume change. This was also found to be the case for the 750°C experiments.

5.1.3 Comparison between the 'same' graphite made by different manufacturers

As described in Section 4.1.3, NBG-10 and PPEA are essentially the 'same' graphite. Figure 31 shows the WG, AG and volume changes for both. It can be seen that in all three cases, the behaviour of the two graphites at the higher temperature is again very similar, although there is a more noticeable difference after cross-over this time compared to the 750°C case.

5.2 DYM variations

The DYM variations with irradiation fluence for the five graphites are shown in Fig 32, and the fractional changes are shown in Fig 33. It can be seen from the DYM variation plots that all graphites show a similar behaviour, as was the case for the 750°C experiments. As there was no low dose experiment at 950°C, equivalent to the INNOGRAPH 1C experiment at 750°C, the initial sharp rise in DYM and the plateau that follows is not evident from the plots. Each curve begins at a fluence between 3 and 4 dpa, and the data points suggest that for NBG-10, NBG-18 and PCEA, which have data at ~3 dpa, the second increase phase is just starting. For NBG-25 and PPEA, the data starts at ~4 dpa and this is clearly part of the more gradual increase in DYM seen after the plateau. As expected the data show that a peak is reached and thereafter the DYM falls off at an ever-increasing rate. (As mentioned in Section 4.2, the strength is expected to follow a similar trend).

The only real difference between the graphites is evident from the fractional change plots. Unlike for the 750°C experiments, it is not possible to compare the initial factorial increase for the graphites as the there is no low dose data available, although it is shown in Section 8.2 the values can be reasonably inferred based from the 750°C data. However, the fractional increase corresponding to the peak DYM ranges show there is a difference, it is with respect to coke source rather than manufacturing method/grain size. The pitch coke graphites (NBG-10, NBG-18 and PPEA) have increase by a factor of ~2.75, whereas the petroleum coke graphites (NBG-25 and PCEA) have increased by a factor of ~3.35. This was an interesting observation.

5.3 CTE variations

The variations in CTE with irradiation fluence for the five graphites are given in Fig 34 and the fractional changes are shown in Figure 35. The fractional changes (f) are expressed as (CTE_{irr} / CTE_{unirr}) – 1, which is the customary way of doing this [thus CTE_{irr} = (1 - f)*CTE_{unirr}]. Each plot shows the value of the mean CTE over 3 temperature ranges, 30-120°C, 30-200°C, 30-750°C and 30-950°C. Unlike the assessment carried out on the 750°C experiment (Ref 1), which had the benefit of the low fluence data, it was not possible to see the initial small increase at the lower fluences. Nevertheless, it can be assumed that this small initial increase did occur, after which there is a progressive decrease until a plateau is reached, which is evident from the data. As the fluence increases further, there are differences in behaviour between the different graphites. For the petroleum coke graphite (NBG-25), there appears to be a further decrease in CTE with increasing fluence, whereas for the pitch coke graphites, the CTE appears to be increasing. This is a very interesting observation.

5.4 Thermal conductivity variations

The variations in thermal conductivity with irradiation fluence for the five graphites are given in Fig 36 and the fractional changes are shown in Figure 37. The fractional changes are expressed as ($TCon_{irr}$ / $TCon_{unirr}$) – 1, which is the customary way of doing this. Each plot shows the value of the instantaneous thermal conductivity at temperatures of 27, 100, 200, 300, 400, 500, 600, 800, 900 and 950°C. It can be seen from Fig 36 that the unirradiated thermal conductivity of each graphite decreases with increasing temperature. Unlike for the assessment carried out on the 750°C (Ref 1), which had the benefit of the low fluence data, it was not possible to see the initial very large reduction in thermal conductivity at the lower fluences (0-2 dpa range). Nevertheless, it can be assumed that this rapid decrease in thermal conductivity did occur, after which a plateau is reached, which is evident from the data. At higher fluences, a further decrease in thermal conductivity is observed, and this is consistent with the behaviour of other graphites irradiated in the past.

It is interesting to note that, although there is a large spread in the unirradiated thermal conductivity over the measured temperature range (27° to 950°C), the variation is significantly reduced after a relatively small amount of irradiation as was the case for 750°C. For example, Figure 36a shows that the spread in thermal conductivity for NBG-10 over the temperature range is ~150 W/m/K (at 27°C) to ~60 W/m/K at (950°C), a range of ~90 W/m/K. However, after only a few dpa of irradiation the thermal conductivity is ~50 W/m/K (at 27°C) to ~40 W/m/K at (950°C), a range of only ~10 W/m/K. At higher fluences, it can be seen that the range reduces even further to ~7 W/m/K.

6 Comparison of dimensional change graphite behaviour at 750°C and 950°C

By far the largest effect on graphite behaviour in going from 750°C to 950°C was clearly with regard to dimensional changes. To illustrate this Figs 38 to 40 show the effect on an extruded graphite and Figs 41 to 43 show the effect on one of the iso-moulded graphites. Figure 38 compares the behaviour for an extruded graphite in the WG direction. It can be seen that the peak shrinkage reached at both temperatures was similar, but at 950°C the graphite shrinks much faster than at 750°C (by a factor of ~2) and a reaches the peak shrinkage after only ~5 dpa, compared to ~11 dpa at 750°C. The fluence to cross-over is also much less, being ~9 dpa at 950°C compared to ~18 dpa at 750°C. A similar story can be seen in Fig 39 for the AG direction. It can be seen that the peak shrinkage reached at both temperatures was also similar, but at 950°C the graphite shrinks much faster than at 750°C and reaches the peak shrinkage after only ~4.5 dpa, compared to ~10 dpa at 750°C. The fluence to cross-over is also much less, being ~8 dpa at 950°C compared to ~16 dpa at 750°C. As would be expected the volume changes replicate the dimensional changes.

The behaviour of the iso-moulded graphite is similar in one aspect, but different in another. Figure 41 compares the behaviour for the graphite in the WG direction. It can be seen that the initial shrinkage rate for the two was very similar at the two temperatures, but at 950°C the graphite shrinks to about a half of what it does at 750°C and reaches its peak shrinkage after only ~6 dpa, compared to ~12 dpa at 750°C. The fluence to cross-over is also much less, being ~10 dpa at 950°C compared to ~20 dpa at 750°C. A similar story can be seen in Fig 42 for the AG direction where turnaround occurs at only ~3.5 dpa at 950°C compared to ~7 dpa at 750°C and cross-over occurs after only ~7 dpa at 950°C, compared to ~12.5 dpa at 750°C. As would be expected the volume change replicates the dimensional changes

7 Graphite selection

There are a number of factors that will influence the choice of graphite for a core design, whether it be a prismatic/block design or a pebble bed design. In the prismatic/block design, the fuel blocks are expected to be replaced every 2/3 years of operation, the reflector blocks adjacent to the fuel perhaps every 10/15 years of operation, and the outer reflector/shielding blocks should never need replacing. The lifetime of the plant should therefore not be limited by the graphite behaviour, but as the lifetime of the fuel blocks, the reflector blocks, and the structures these form, will be affected, this will just change the frequency at which the blocks need replacing. For the pebble bed design, it would be hoped that the reflector blocks adjacent to the fuel will last the lifetime of the plant. However, it can be seen from the data presented that the fluence at which cross-over occurs will be the ultimate limit for the core before it will need partial replacement (assuming that other ageing effects such as block cracking do not limit the life of the core to less than the cross-over fluence). Depending on the desired lifetime of the plant, this might require one (or more) core changes.

The important irradiation induced effects for the designer to consider are covered in this report, namely, the dimensional change behaviour and the variation of DYM, CTE and thermal conductivity. Also important, but not covered earlier in this report, is the variation in strength. This is known to be closely related to the DYM variation and so one can be inferred from the other. Of these, the dimensional change behaviour is without doubt the most important from a designer's point of view and so would be top of the list in terms of selection criteria. This is covered in section 7.1 below. DYM/strength is also an important consideration and is covered in Section 7.2 below. The CTE and thermal conductivity variations are not as important for selection and these are fairly similar for all the graphites tested.

[Note - It is not the intention of this report to recommend the use any of the graphites tested for a particular reactor design nor to state than any of them should be discounted. It is entirely up to the designer to make the selection and to justify this. For example, there is also the oxidation behaviour of the graphite in air and steam to consider (which is of particular importance with regard to air ingress and steam ingress situations), as well as the within-brick, brick-to-brick and batch-to-batch variability in properties. Another important factor to consider is the cost of the graphite, with pitch coke graphites being more expensive than the equivalent petroleum coke graphites. The designer would also need to take account of the availability of the graphite both in the short term (for design/construction) and in the long term (for fuel block/reflector replacement in any given reactor or for the construction of future reactors of the same design). All of the other factors mentioned above are beyond the scope of this report and so are not considered further].

7.1 Dimensional change behaviour

Excessive shrinkage could lead to an unacceptable reduction in the height of graphite columns over time, or unacceptable gaps developing between components which could have a significant effect on core geometry and flow paths. Excessive growth in late life could lead to unacceptable increases in the height of graphite columns and the closure of initial gaps between components, the latter leading to gross expansion of the core diameter. It is important that the core design can accommodate these dimensional changes without causing any overloading of components, disengagement between components, or overheating of the fuel. [Note – the designer also has to deal with differential expansion between the graphite and the steelwork, the CTE of graphite being ~1/3 to 1/4 of that of steel. However, the steelwork will interface with graphite that will see very low irradiation and so any changes over life will be negligible].

Differential shrinkage strains within components give rise to stresses that could ultimately lead to cracks developing in the fuel and/or reflector brocks. The stresses are likely to be higher, and therefore result in cracks occurring at an earlier time in life, if the graphite has high anisotropy (i.e. a large difference between the WG and AG behaviour), and/or a large variability in its behaviour (i.e. scatter in the data). Overall component distortions affect the stability and hence loading of the whole structure, which could be made worse by cracking. Excessive cracking is unlikely to be tolerable and could therefore result in a much shorter core life if the wrong graphite is used.

Therefore, from a designer's point of view, the 'ideal' graphite would have the following dimensional change behaviour:

(i) a relatively low initial shrinkage rate

(ii) a relatively small peak shrinkage

(iii) a moderately high fluence at which turn-around occurs,

(iv) a high fluence at which cross-over occurs (i.e. original WG/AG dimensions attained)

(v) a low anisotropy (difference between WG and AG behaviour)

(vi) a low variability (low scatter in the data)

It can be seen from the dimensional change data presented in this report that the 'ideal' graphite does not yet exist, and is unlikely to ever exist for a future graphite because improving one attribute will inevitable have a detrimental effect on another. Nevertheless, the designer should take advantage of the favourable attributes and minimise the effects of the unfavourable ones. All candidate graphites for a HTR will exhibit shrinkage over the temperature range of interest. However, there is clearly a large difference in the initial shrinkage rate between the graphites tested as well as the maximum shrinkage reached. For a prismatic/block design in which the fuel blocks only see a relatively small fluence, it is preferable to have a low initial shrinkage rate so that gaps of an unacceptable size do not arise between components as this could lead to core instability and unwanted flow paths. This would point towards fine grain graphites. For the pebble bed reactor, however, the desire is to have a graphite that has a high fluence to cross-over. The problem is that this would mean that a larger peak shrinkage would have to be tolerated and all the issues that would generate in terms of stability and flow paths.

7.2 DYM/strength

The strength of a graphite is important as this dictates the levels of stress that can be tolerated before crack initiation. In this respect fine grain graphites are stronger than medium grain graphites and so for components with a purely core support function, the fine grain graphites may be the better choice. However, for irradiated components the benefits are not so clear because higher strength generally means higher DYM. The shrinkage and thermal strains that arise in a component are converted into stresses by multiplying by the (static) modulus, which means that a given local strain results in a higher stress local stress if the modulus is higher. Therefore, although the local strength will be higher, so will be the stress. As the graphite gets irradiated, the increase in modulus is higher than that for the strength and so the margin against crack initiation may be higher for a lower strength/lower modulus graphite, which would point towards the medium grain graphites.

[Note - Another factor considered by the designers of the German HTRs was fracture toughness. This governs how fast a crack will grow/propagate through a component. Cracks were shown to grow/propagate much faster through finer grain graphites than through medium grain graphites. There was a strong belief by some involved with the German designs, and subsequently with the design of the South African PMBR, that fine grain graphites should not be used for HTRs for this reason. However, if there are sufficient margins between the stresses in a component and its strength, the initiation of a crack will not occur and so the rate of growth/propagation of a crack is not a concern, and therefore neither is its fracture toughness].

8 Recommended design properties

8.1 Dimensional change

The dimensional change curves for each of the graphites in the WG and AG directions for the two temperatures have been determined using the Excel 'add trendline' feature. Although fourth order polynomials could be fitted through the 750°C data, because of the low fluence data available, it was only possible to fit third order polynomials through the 950°C data. It was therefore decided to fit third order polynomials through both to allow meaningful comparisons to be made. The polynomial fits are of the form:

$$\text{Dimensional change (\%)} = a * (dpa)^3 + b * (dpa)^2 + c* (dpa)$$

Where

'a',' b' and 'c' are coefficients (see Tables 3 and 4 below), and 'dpa' is the fluence

Grade	750°C WG			750°C AG		
	a	b	c	a	b	c
NBG-10	0.0009	-0.0050	-0.2192	0.0011	-0.0089	-0.1520
NBG-25	0.0008	-0.0069	-0.1767	0.0006	0.0020	-0.1212
PCEA	0.0006	0.0008	-0.3080	0.0007	0.0015	-0.2771
PPEA	0.0010	-0.0076	-0.2208	0.0012	-0.0106	-0.1453
PCIB	0.0002	0.0082	-0.1629	0.0001	0.0106	-0.1362
IG-110	0.0013	-0.0180	-0.1262	0.0015	-0.0220	-0.0494
IG-430	0.0015	-0.0253	-0.0150	0.0008	0.0025	-0.0951

Table 3 – Coefficients for 750°C dimensional change behaviour

Grade	950°C WG			950°C AG		
	a	b	c	a	b	c
NBG-10	0.00101	0.05928	-0.62858	0.00181	0.05764	-0.57907
NBG-25	0.00414	-0.02708	-0.13157	0.00416	-0.00818	-0.14910
NBG-18	0.01020	-0.10550	0.09360	0.00560	-0.01920	-0.09360
PCEA	0.00830	-0.07334	-0.21805	0.00724	-0.04097	-0.25821
PPEA	0.00782	-0.04395	-0.30588	0.00602	-0.00941	-0.30736

Table 4 – Coefficients for 950°C dimensional change behaviour

The above give the mean curves through the data. To account of the scatter in the data it is recommended that ±10% be applied to the mean dimensional change curves for design purposes.

8.2 DYM

The DYM changes can be considered in two parts. The first part is the initial factorial increase that occurs in the first 0-1 dpa, and the second part is the more gradual increase and then decrease that occurs at higher fluences. The initial factor can be defined explicitly for the 750°C due to the low fluence data, but not for the 950°C data due to the absence of any low fluence data. However, for those graphites that were irradiated at

both temperatures, there appears to be no difference in these factors, and so the 750°C values are also deemed to be applicable for 950°C for the other graphites. The 'add trendline' feature in Excel has been used to generate polynomial fits to the medium/high fluence data. Third order fits were the best for the 750°C data but second order fits were the best for the 950°C data. The polynomial fit is of the form:

DYM multiplying factor = $a * (dpa)^3 + b * (dpa)^2 + c*(dpa) + d$

Where

'a', ' b', 'c' and 'd' are coefficients (see Table 5 and 6 below), and 'dpa' is the fluence

Grade	Initial multiplying factor	a	b	c	d
NBG-10	1.45	0.00005	-0.0137	0.4380	-0.6308
NBG-25	1.60	0.0002	-0.0298	0.7324	-1.6036
PCEA	1.45	-0.0086	0.1252	2.7589	-2.1012
PPEA	1.45	0.0006	0.0066	0.1804	0.4885
PCIB	1.60	0.0002	0.0225	0.5773	-0.8999
IG-110	1.69	-0.0002	0.0084	0.4175	-0.3862
IG-430	1.60	-0.00004	-0.0211	0.6175	-1.1502

Table 5 – Multiplying factors for the increases in DYM at 750°C

Grade	Initial multiplying factor	a	b	c	d
NBG-10	1.46	0	-0.0572	0.9016	-0.0823
NBG-25	1.60	0	-0.0563	0.9587	-0.7008
NBG-18	1.45	0	-0.0578	0.9160	-0.8861
PCEA	1.45	0	-0.0817	1.3359	-2.1714
PPEA	1.45	0	-0.0566	0.8870	-0.7399

Table 6 – Multiplying factors for the increases in DYM at 950°C

The above give the mean curves through the data. To account of the scatter in the data it is recommended that ±10% be applied to the mean factorial increase for design purposes.

8.3 CTE

The CTE variation is very similar between the different graphites. For 750°C, the CTE of all the graphites increases by a factor (f) of ~0.1 after 2 dpa. From 2 to 12 dpa, the (27-700) CTE factor reduces approximately linearly to ~0.55 (±0.05). It remains at around this factor up to the peak fluence of 23 dpa. For 950°C, there are no low fluence data but it can be assumed that the (27-950) CTE of all the graphites increases by a factor of ~0.1 after 2 dpa (as for 750°C). From 2 to 6 dpa, the CTE factor reduces approximately linearly to ~0.40 (±0.10). It then increases again up to factor of ~0.25 (±0.10) at the peak fluence of 14 dpa. It is recommended that these values be used over the specified fluence ranges at each temperature.

8.4 Thermal conductivity

The thermal conductivity variation is also very similar between the different graphites. Although there is a wide spread in values over the temperature range for the unirradiated condition, the range collapses down after a small amount of irradiation. For 750°C, the thermal conductivity of all the graphites falls to ~35 (±5) W/m/K after 2 dpa. From 2 to 10 dpa, the thermal conductivity remains fairly constant, and thereafter reduces approximately linearly to ~20 (±3) W/m/K at 23 dpa. For 950°C, the thermal conductivity of all the graphites falls to ~45 (±5) W/m/K after 2 dpa. From 2 to 7 dpa, the thermal conductivity remains fairly constant, and thereafter reduces approximately linearly to ~25 (±2) W/m/K at 12 dpa. It is recommended that these values be used over the specified fluence ranges at each temperature.

9 Conclusions

A number of graphites have been irradiated to a high fluence in the High Flux Reactor at Petten at two different temperatures, namely at 750°C and at 950°C. An assessment of the data from these experiments has been carried out in two companion reports to this report (Refs 1 and 2). The assessments looked at the dimensional change behaviour of the graphites tested, along with the changes in dynamic Young's modulus, coefficient of thermal expansion and thermal conductivity with fluence. A comparison was made between the dimensional change behaviour and the property variations for each graphite at each temperature, and both qualitative and quantitative observations were made. This report considers the data in its entirety and compares and contrasts the differences in behaviour between the graphites. It also provides an insight as to how these differences could affect their suitability for the two different high temperature reactor (HTR) types, namely the prismatic/block type reactor and the pebble bed type reactor.

It is not the intention of this report to recommend the use any of the graphites tested for a particular reactor design nor to state than any of them should be discounted. It is entirely up to the designer to make the selection and to justify this. The report concludes that the 'ideal' graphite does not exist yet and is unlikely to ever exist. Therefore the designer needs to take advantage of the favourable behaviour/attribute of a particular graphite and minimise the effect of the unfavourable ones.

For each graphite tested, the fluences to reach cross-over were found to be dramatically reduced on going from 750°C to 950°C, generally by a factor of ~2. This could have implications for the VHTR, where the graphite temperatures will be significantly higher than for a HTR, and so it is essential that the highest temperatures in the graphite do not coincide with the highest fluences.

10 References

Ref	Title
1	M W Davies. Reports on graphite selection and recommended design properties. Part II - results for the 750°C INNOGRAPH irradiation experiments (2A and 2B). ARCHER deliverable D41-16
2	M W Davies. Reports on graphite selection and recommended design properties. Part II – results for the 950°C INNOGRAPH irradiation experiments (2A and 2B). ARCHER deliverable D41-17
3	F. Schmalz et al., Preliminary irradiation testing of selected graphite grades for HTR, Final report on HTR-M1 WP3, 20787/05.71179/P, 19 December 2005
4	M Heijna. Report on strength measurements of irradiated graphite. ARCHER deliverable D41-15

Figure 1 – Sample machining and dimensions

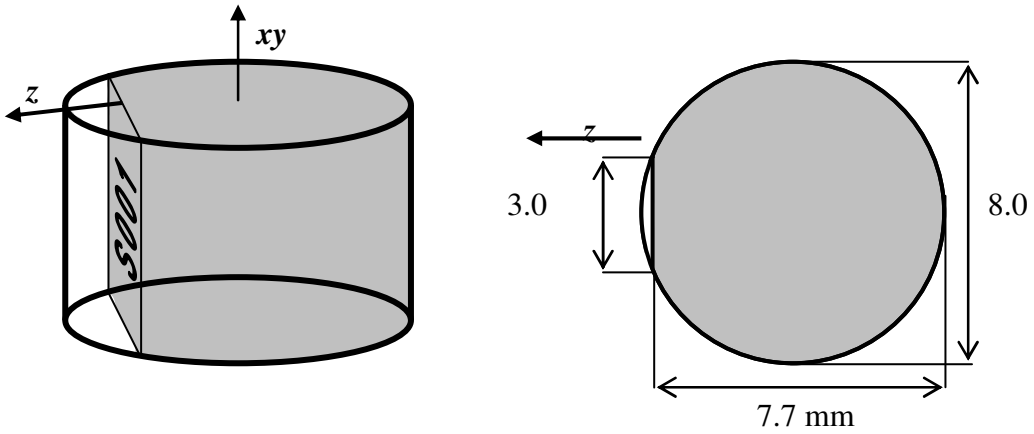

The figure on the left-hand side exaggeratedly shows the machined flat on the side of the cylinder. The milled plane is perpendicular to the *z*-direction when the axial direction of the cylinders in the *xy*-direction. The specimen number is engraved on the plane. The figure on the right-hand side is a top-view of the specimen. The important dimensions are indicated.

Figure 2 – Orientation of dimensions with grain directions

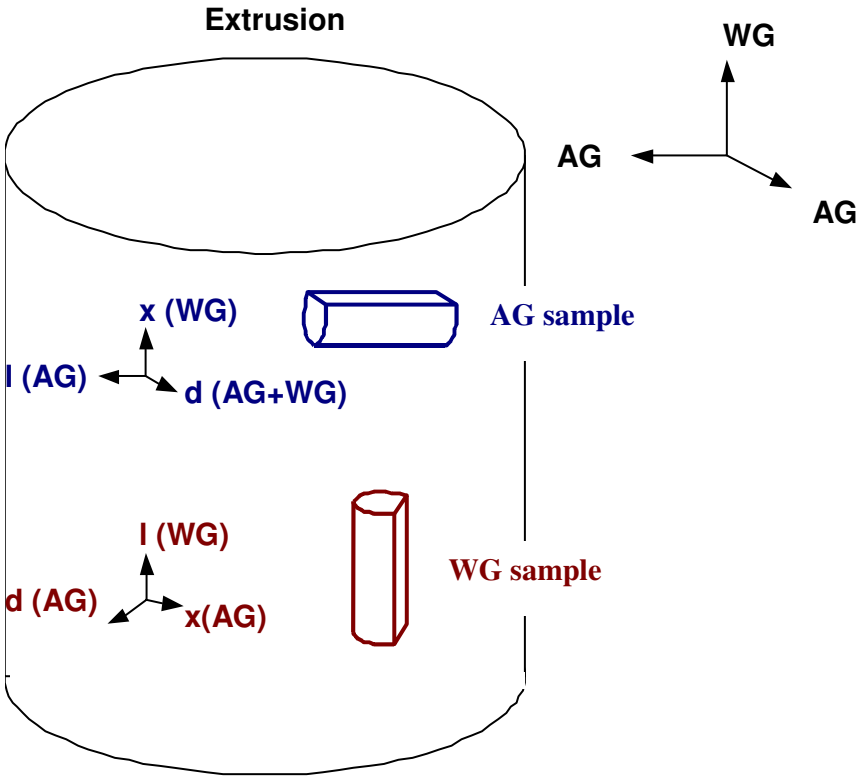

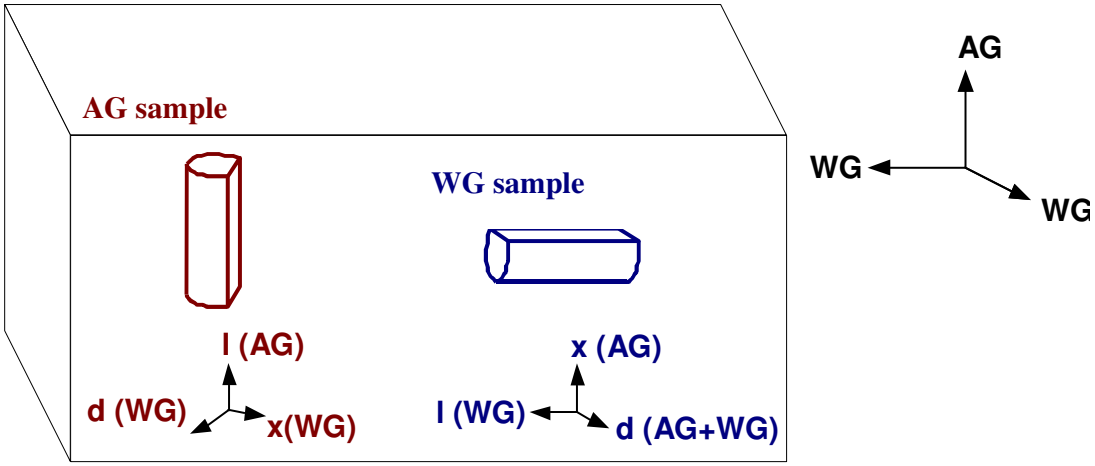

Iso-moulding

Figure 3 - Dimensional change behaviour at 750°C - WG

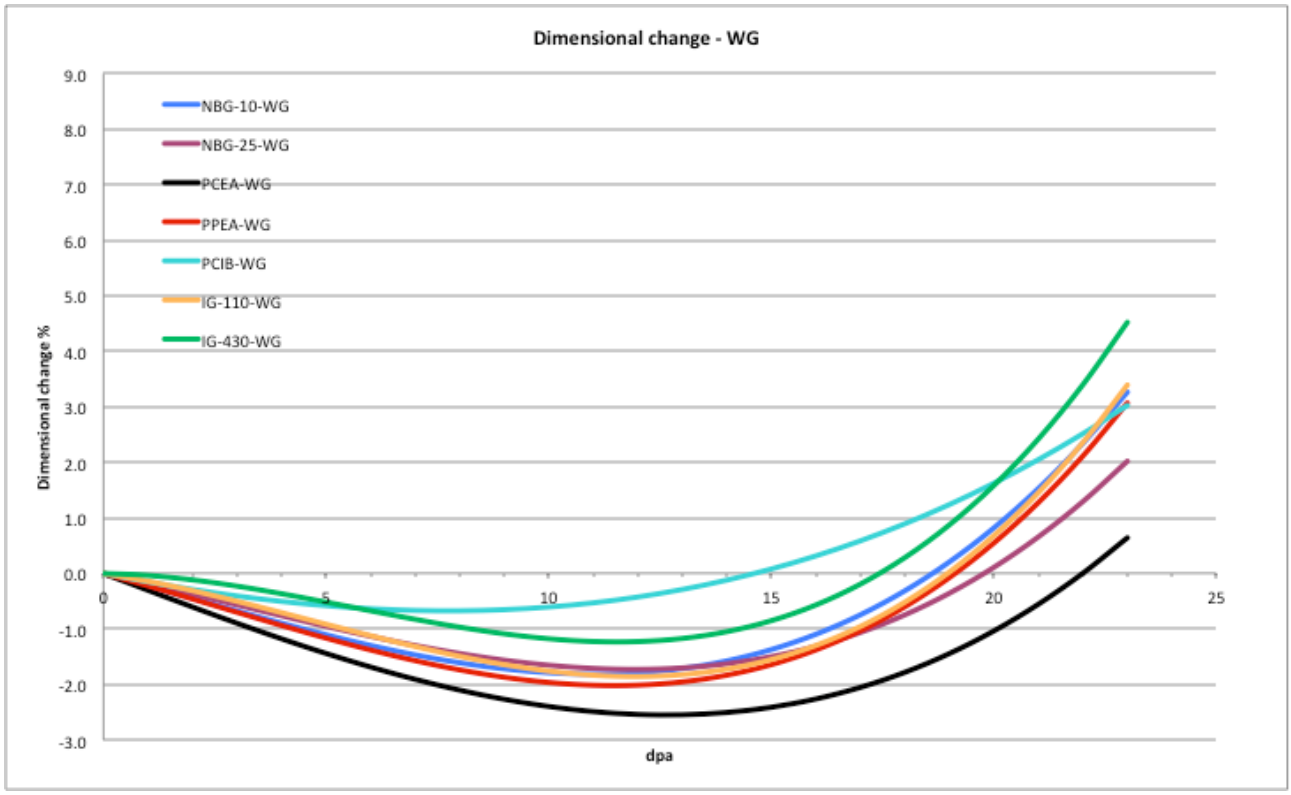

Figure 4- Dimensional change behaviour at 750°C - AG

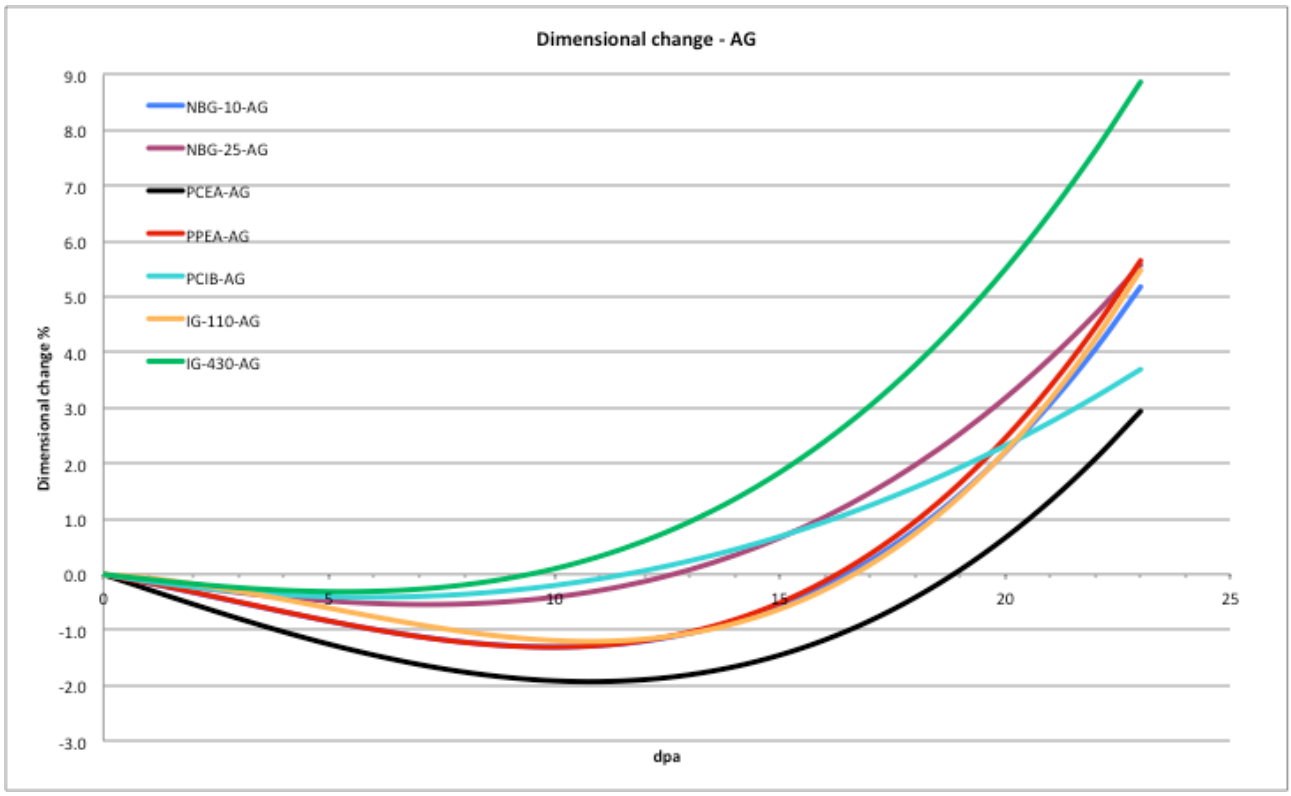

Figure 5- Volume change behaviour at 750°C

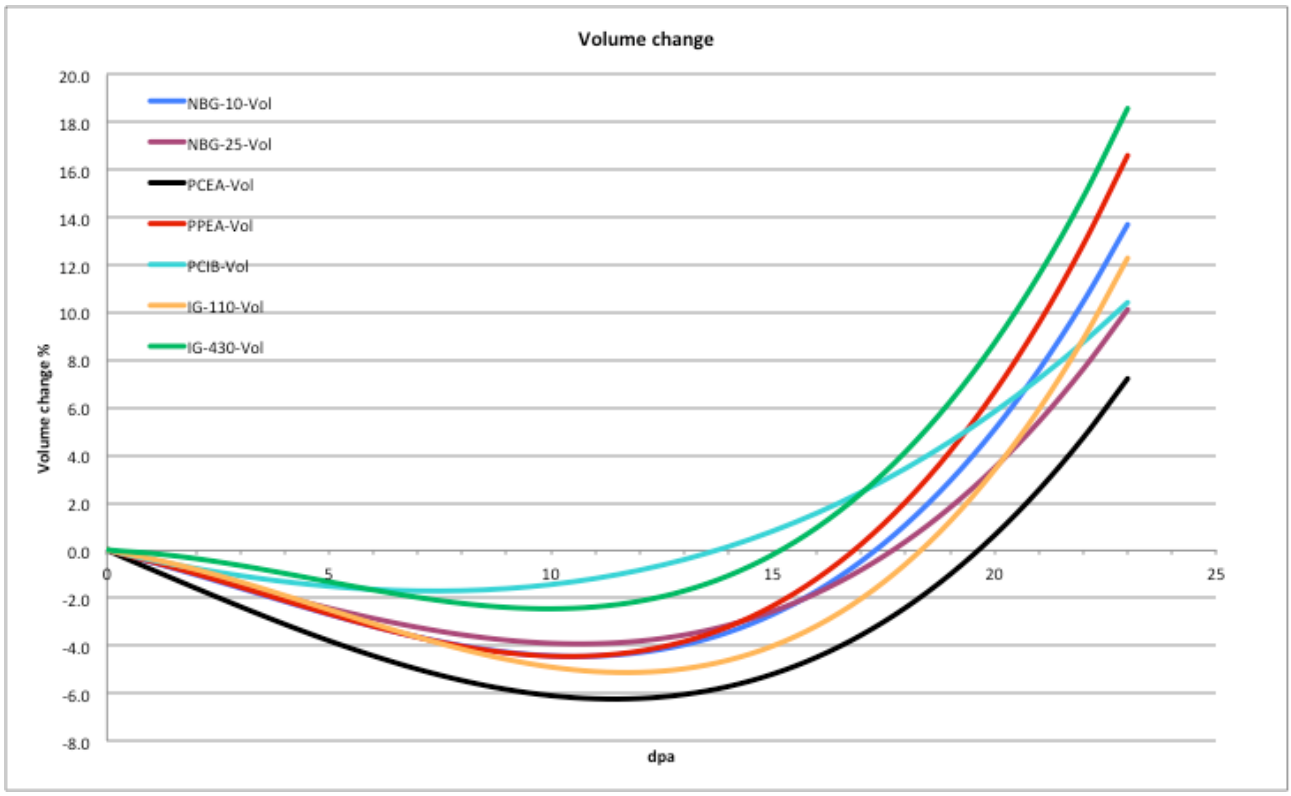

Figure 6- Comparison of extruded and iso-moulded at 750°C - WG

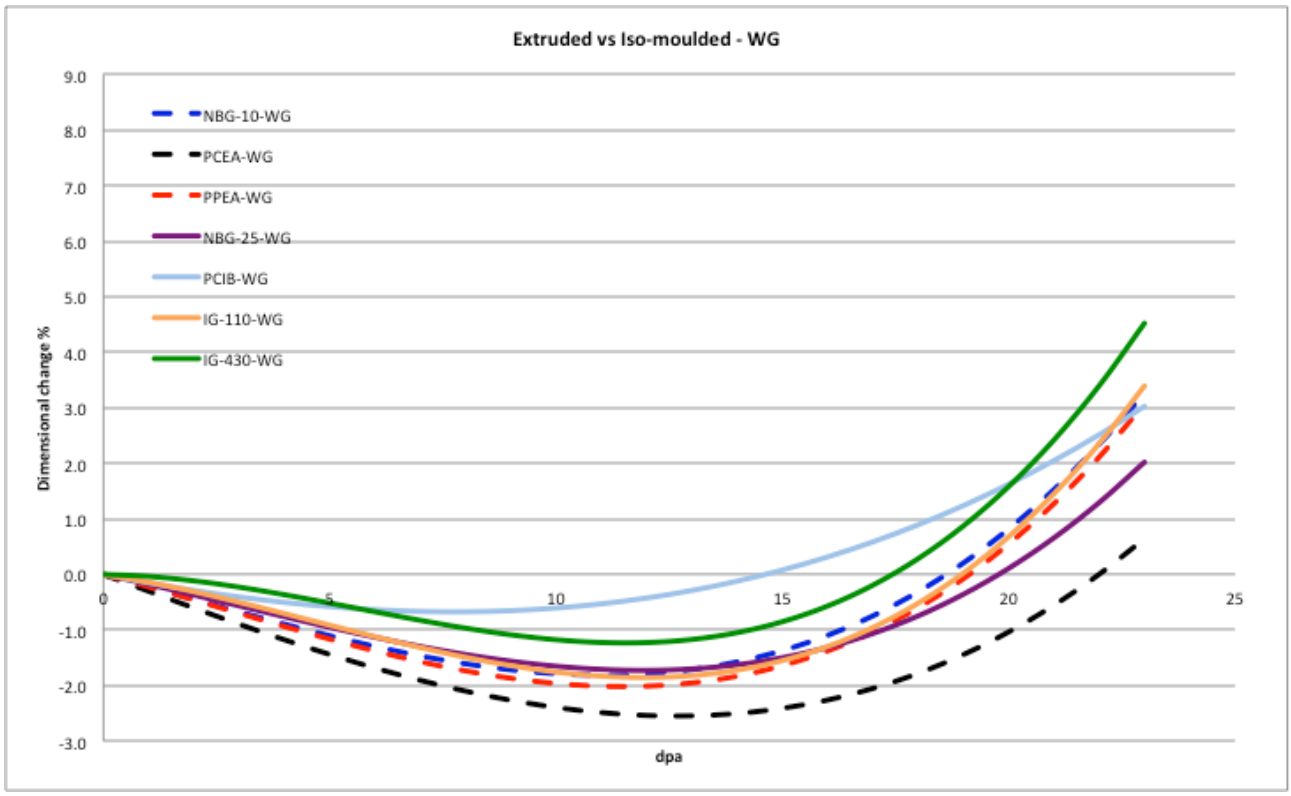

Figure 7- Comparison of extruded and iso-moulded at 750°C - AG

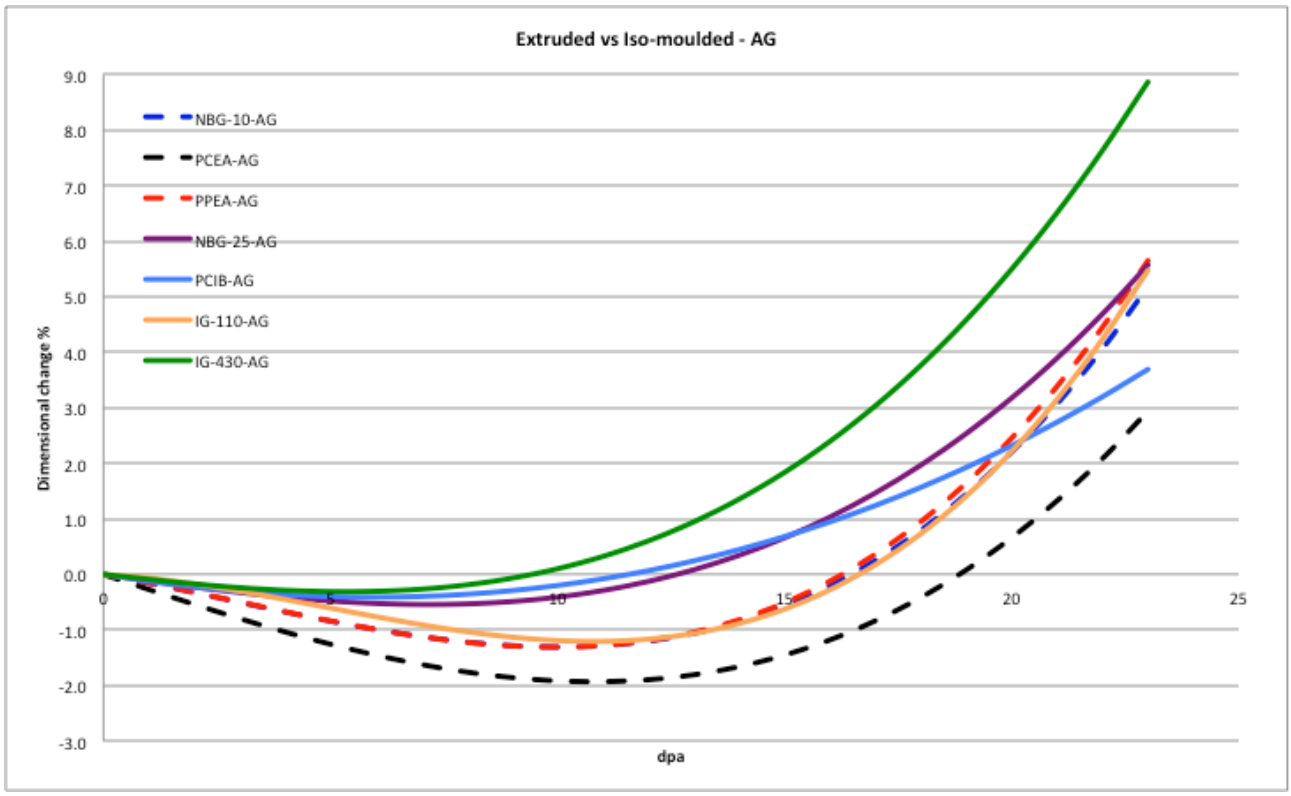

Figure 8- Comparison of extruded and iso-moulded at 750°C - volume

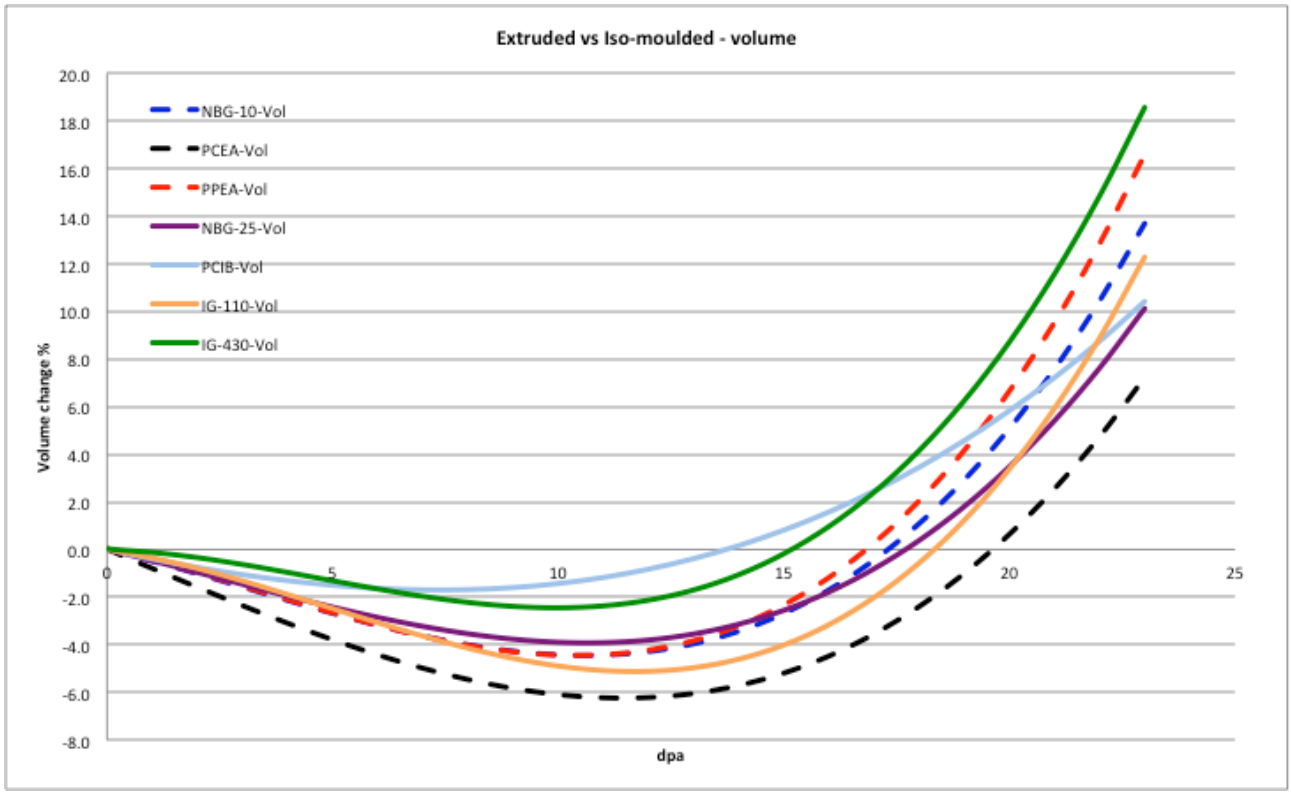

Figure 9- Comparison of dimensional change for PCEA and PPEA at 750°C

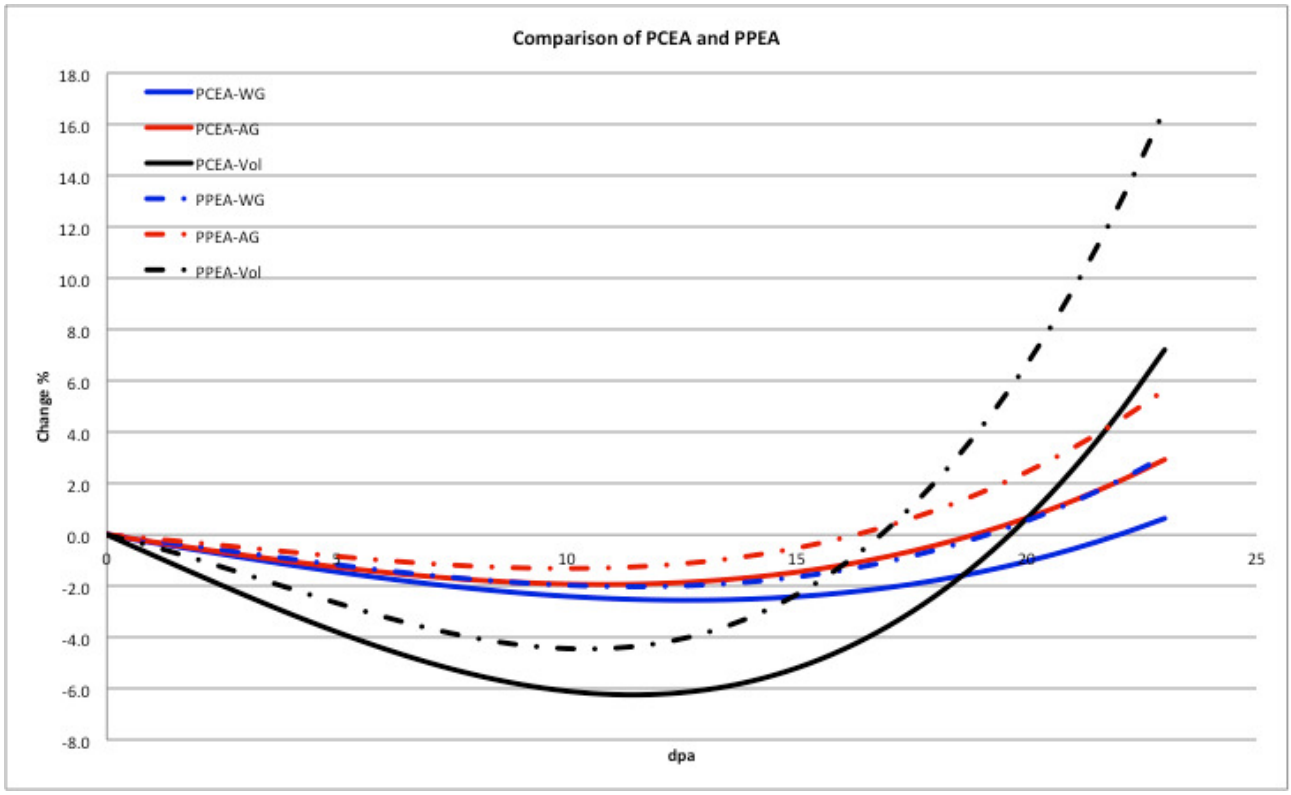

Figure 10- Comparison of dimensional change for IG-110 and IG-430 at 750°C

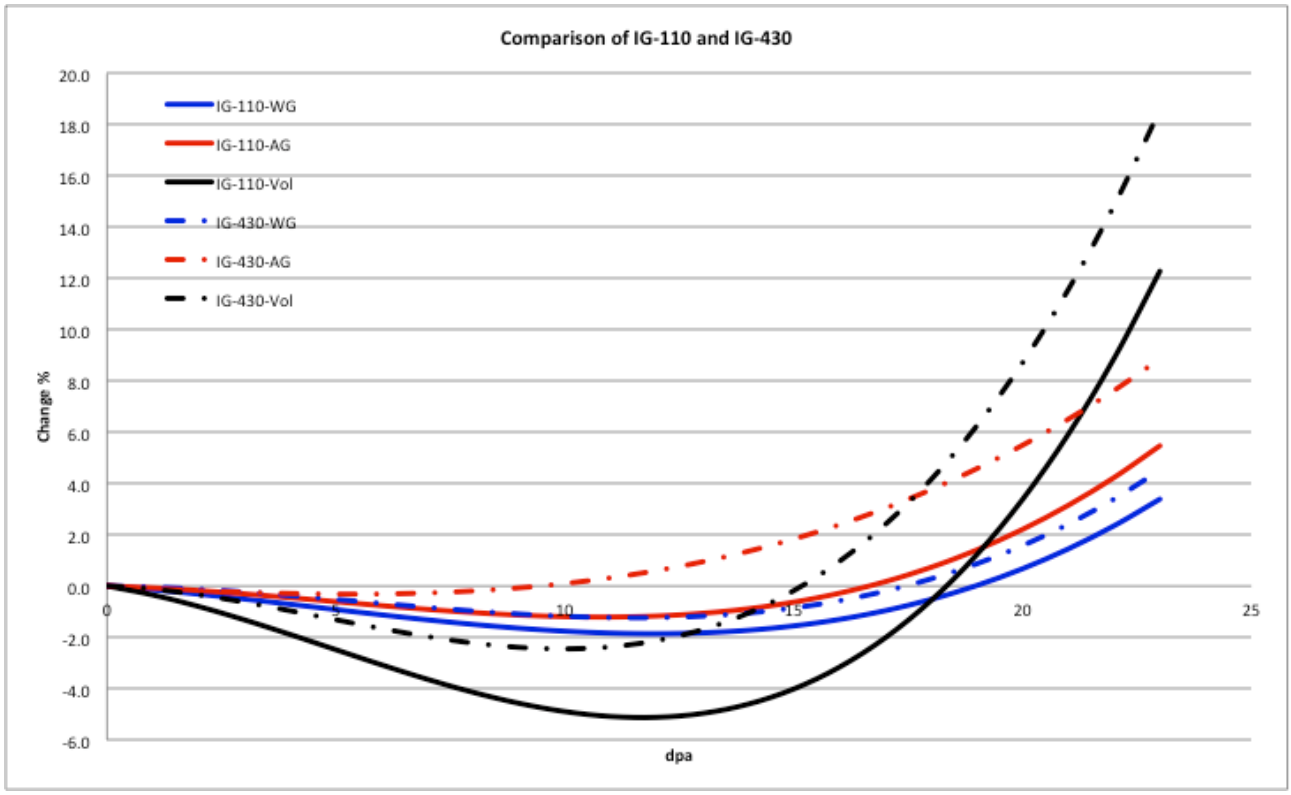

Figure 11- Comparison of dimensional change for NBG-10 and PPEA at 750°C

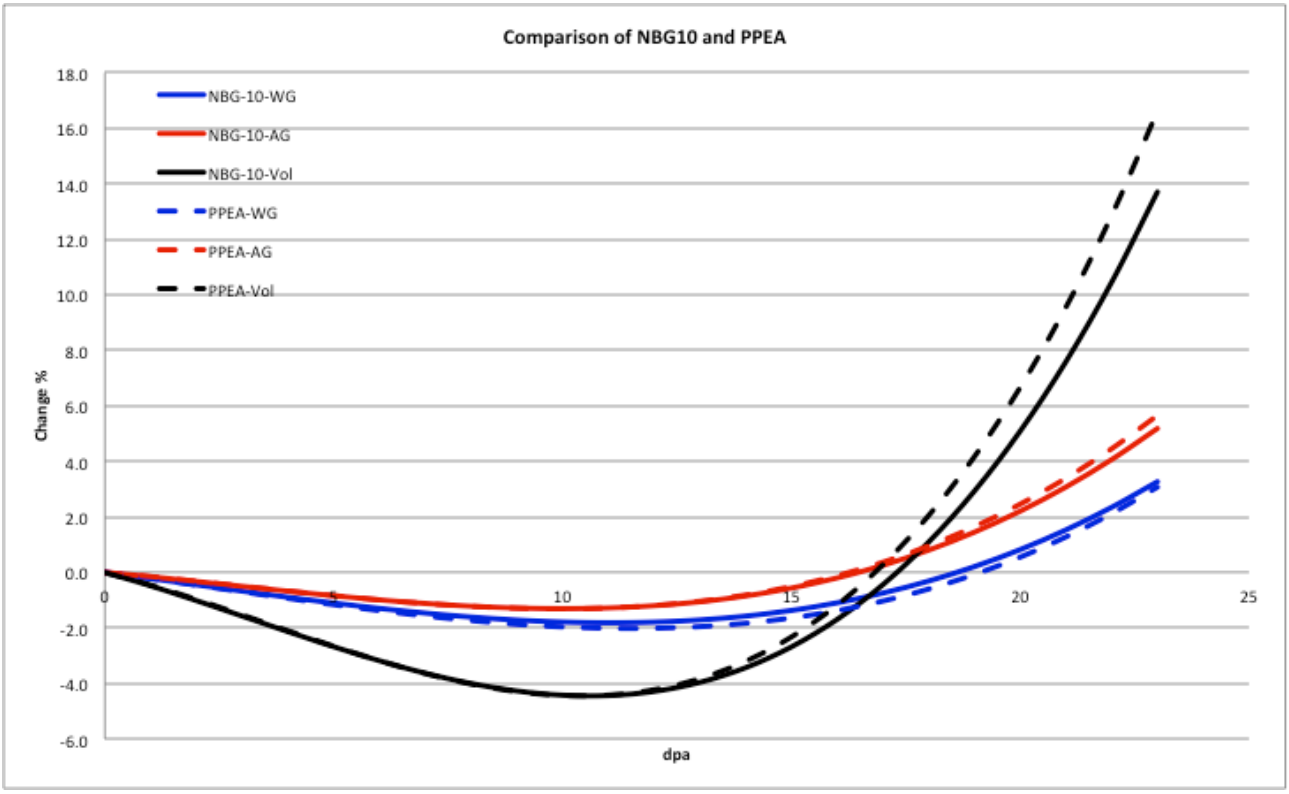

Figure 12 – Comparison of DYM variations for extruded graphites at 750°C

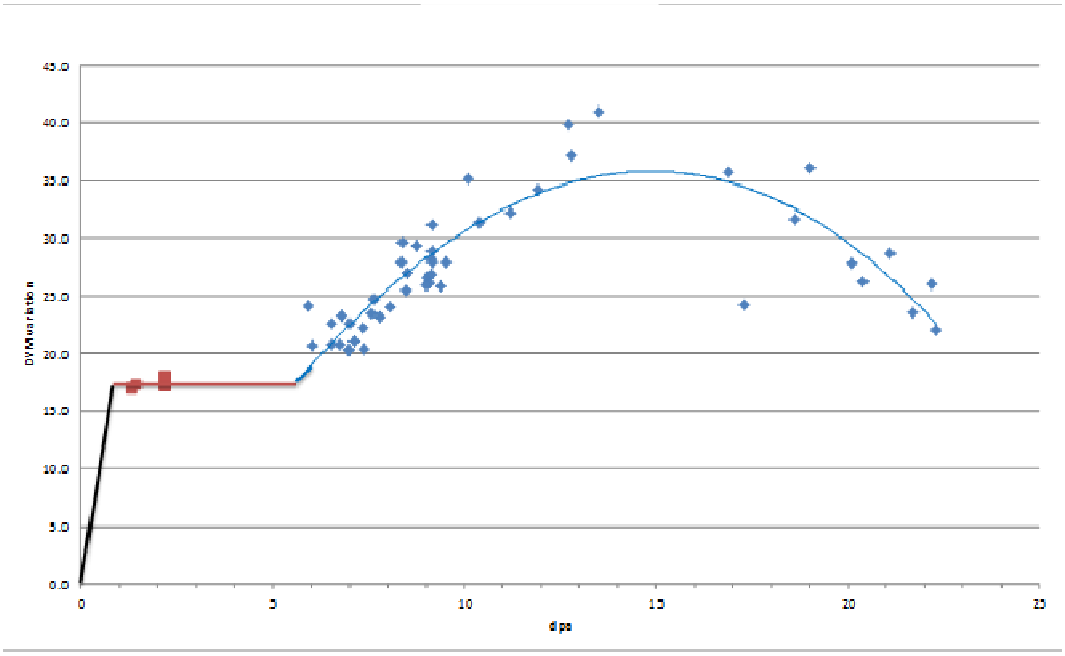

(a) NBG-10

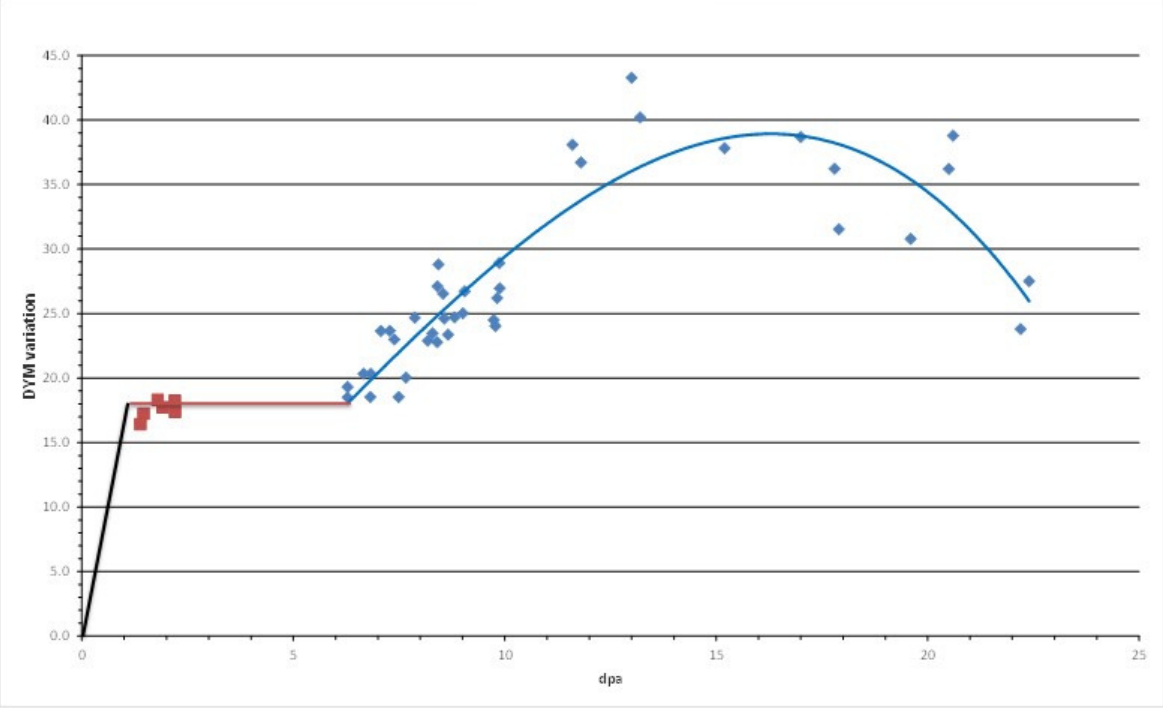

(b) PCEA

Figure 12 – cont'd

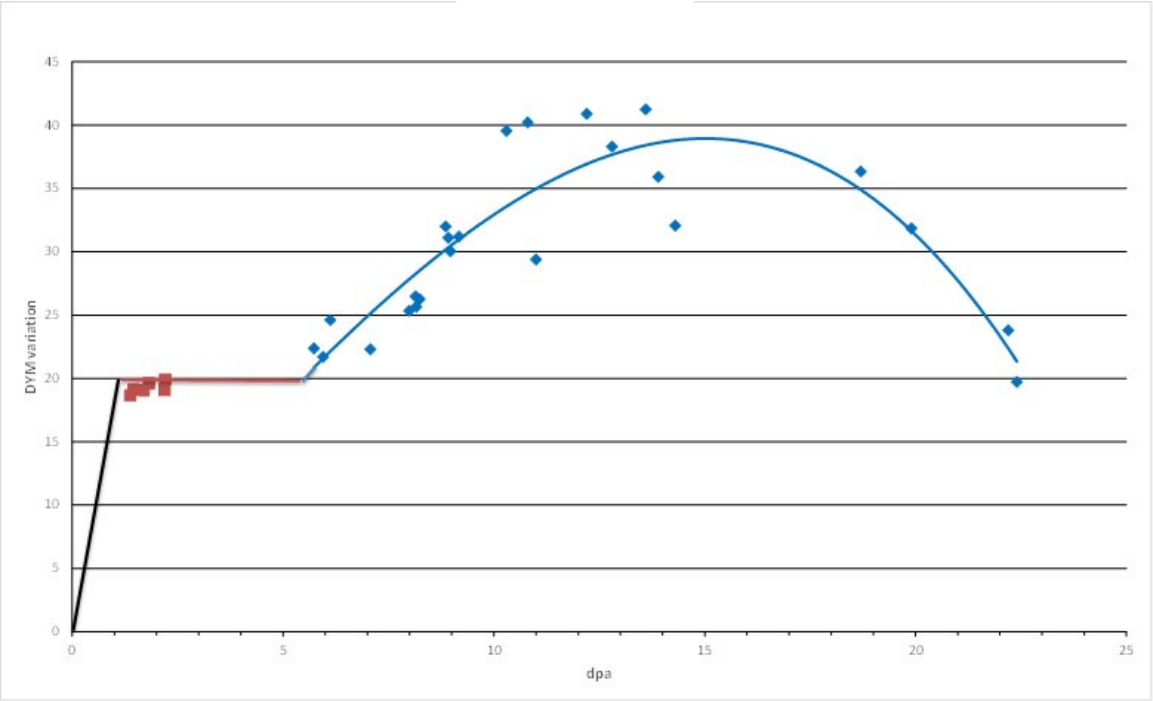

(c) PPEA

Figure 13 – Comparison of DYM fractional changes for extruded graphites at 750°C

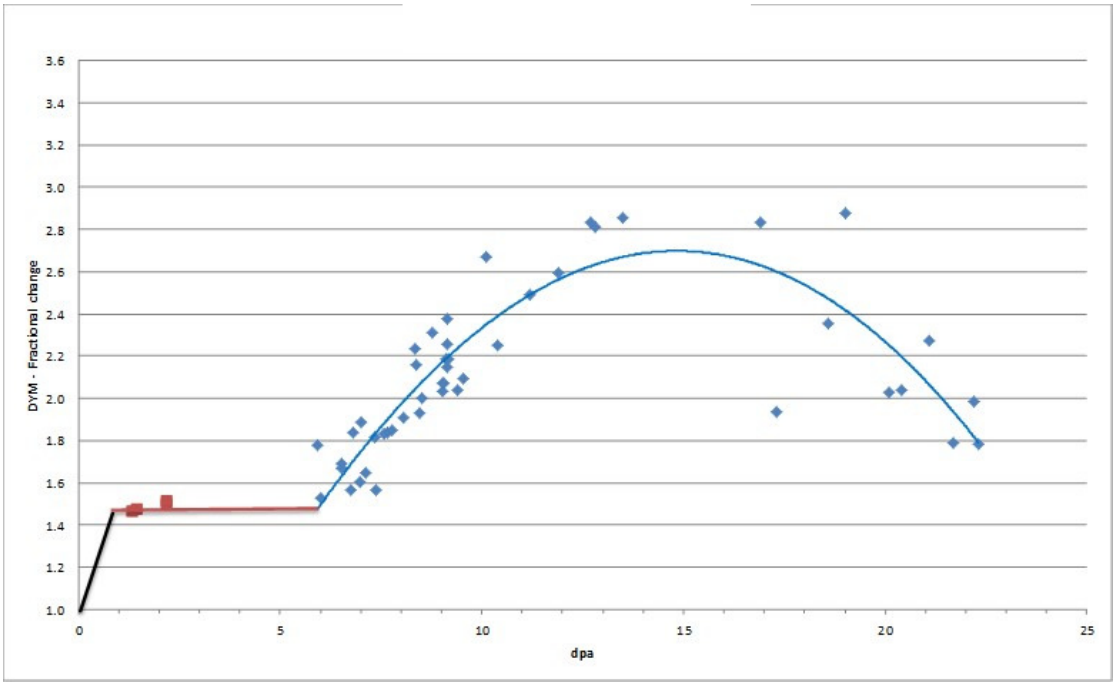

(a) NBG-10

Figure 13 – cont'd

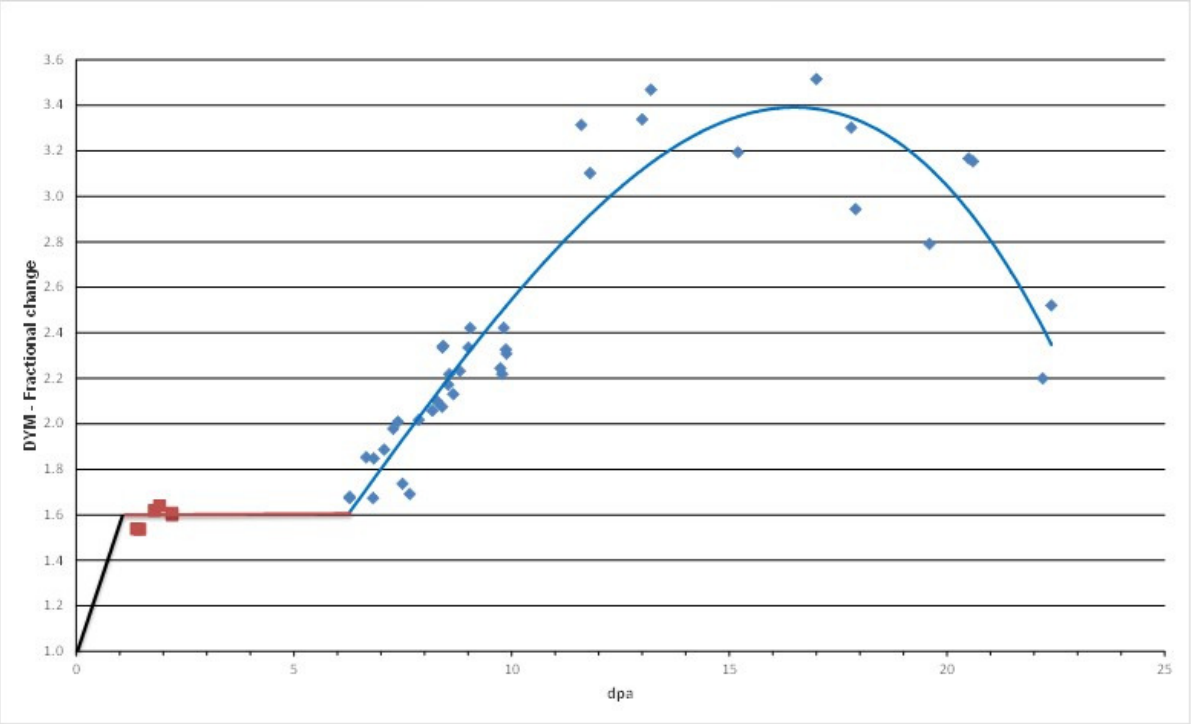

(b) PCEA

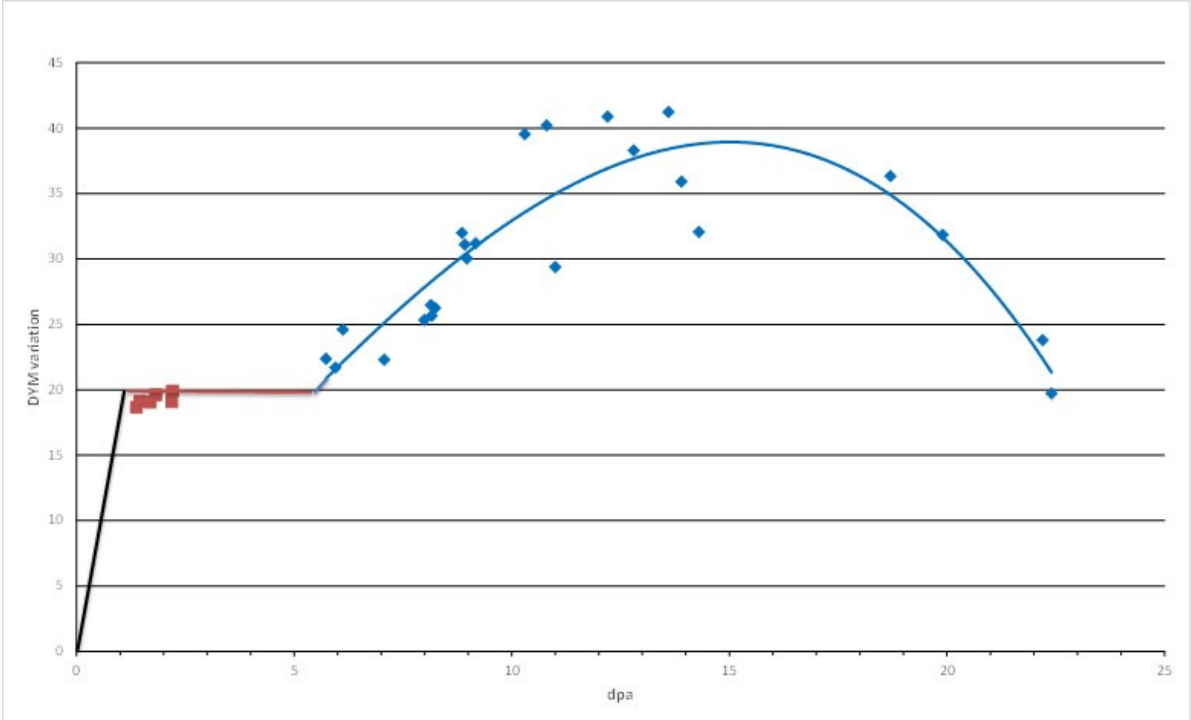

(c) PPEA

Figure 14 – Comparison of DYM variations for iso-moulded graphites at 750°C

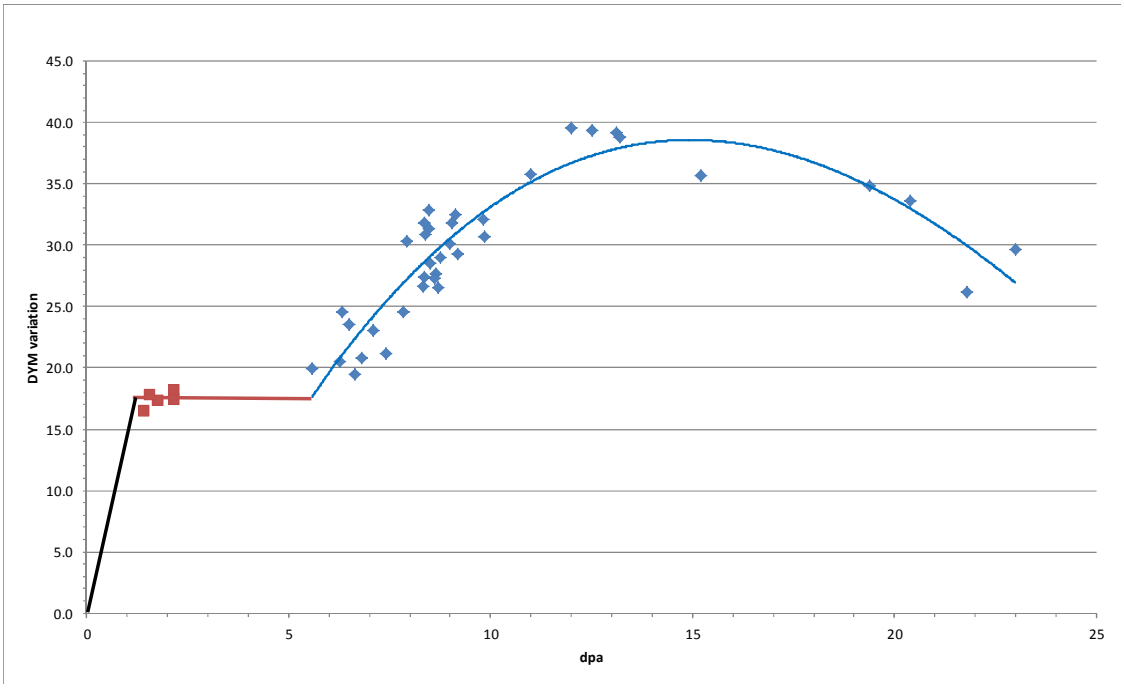

(a) NBG-25

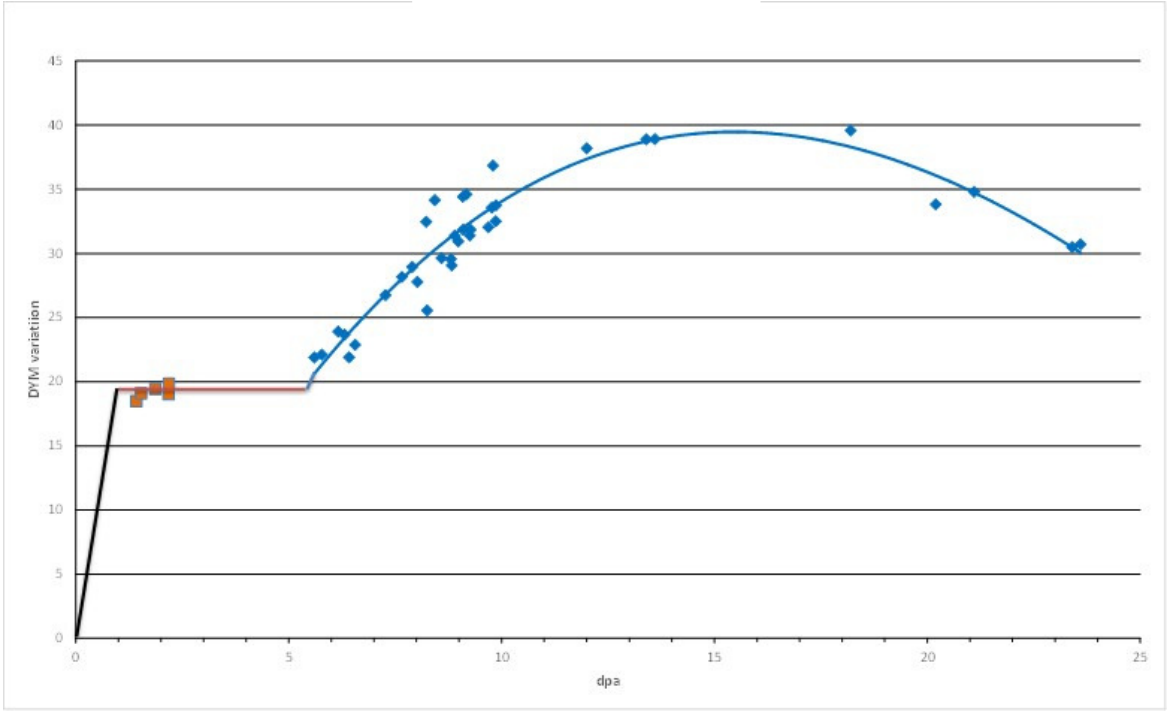

(b) PCIB

Figure 14 – cont'd

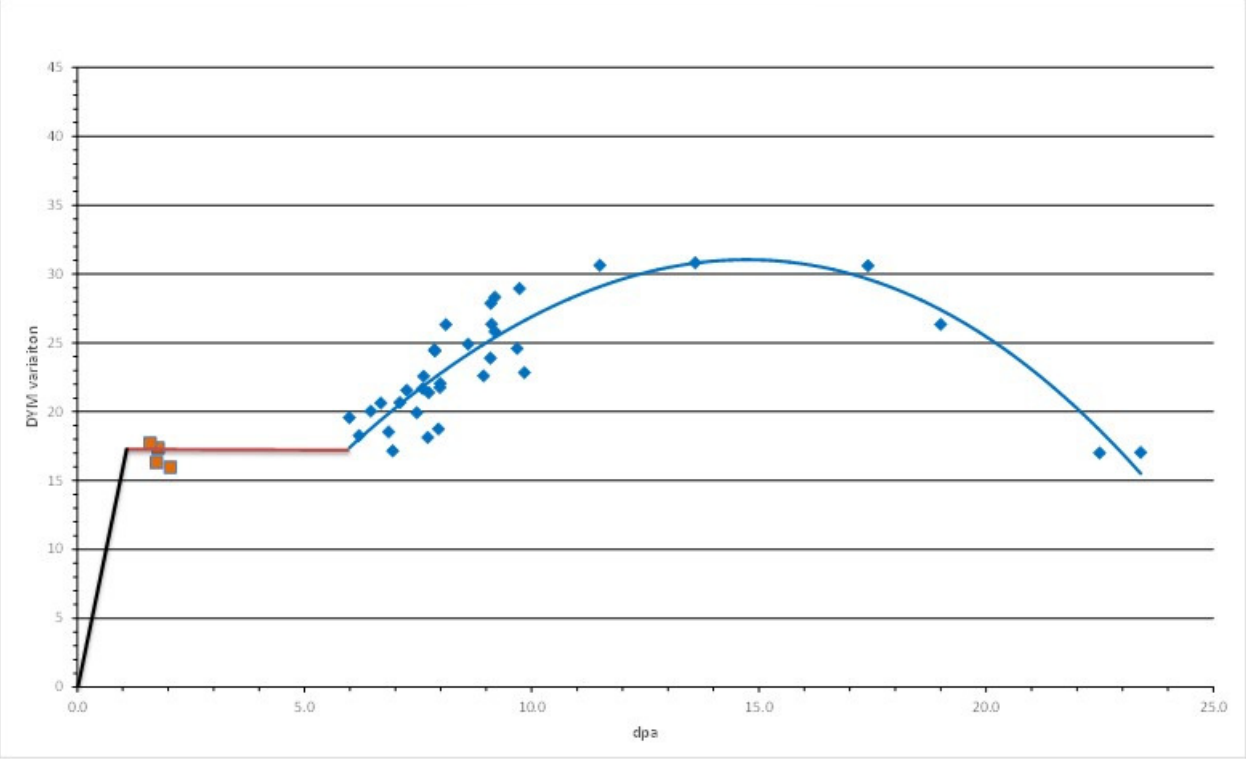

(c) IG-110

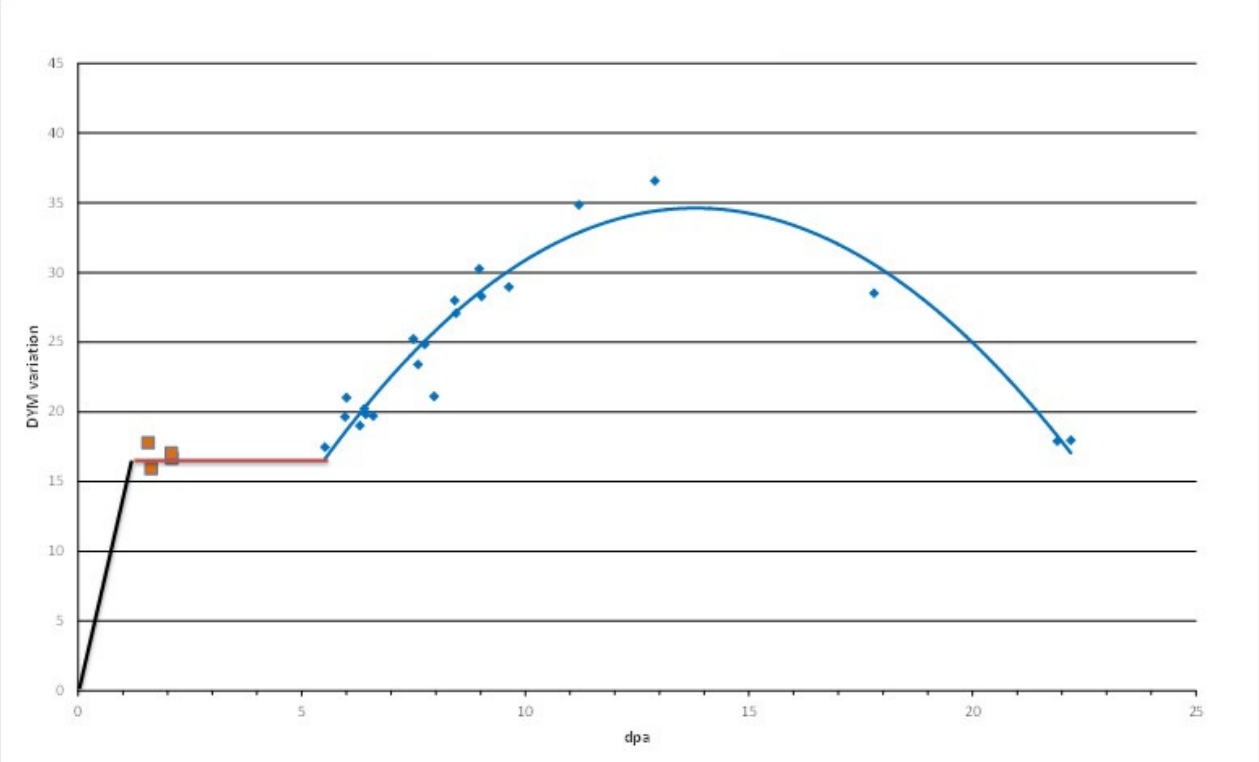

(d) IG-430

Figure 15 – Comparison of DYM fractional changes for iso-moulded graphites at 750ºC

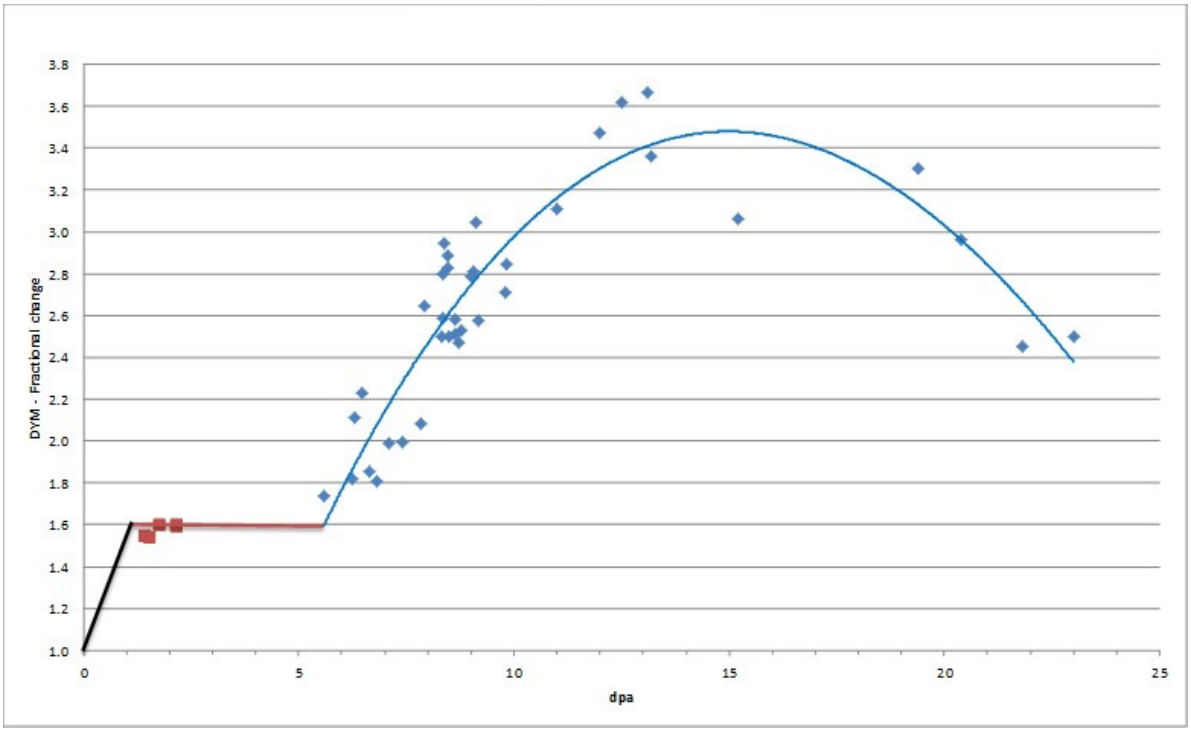

(a) NBG-25

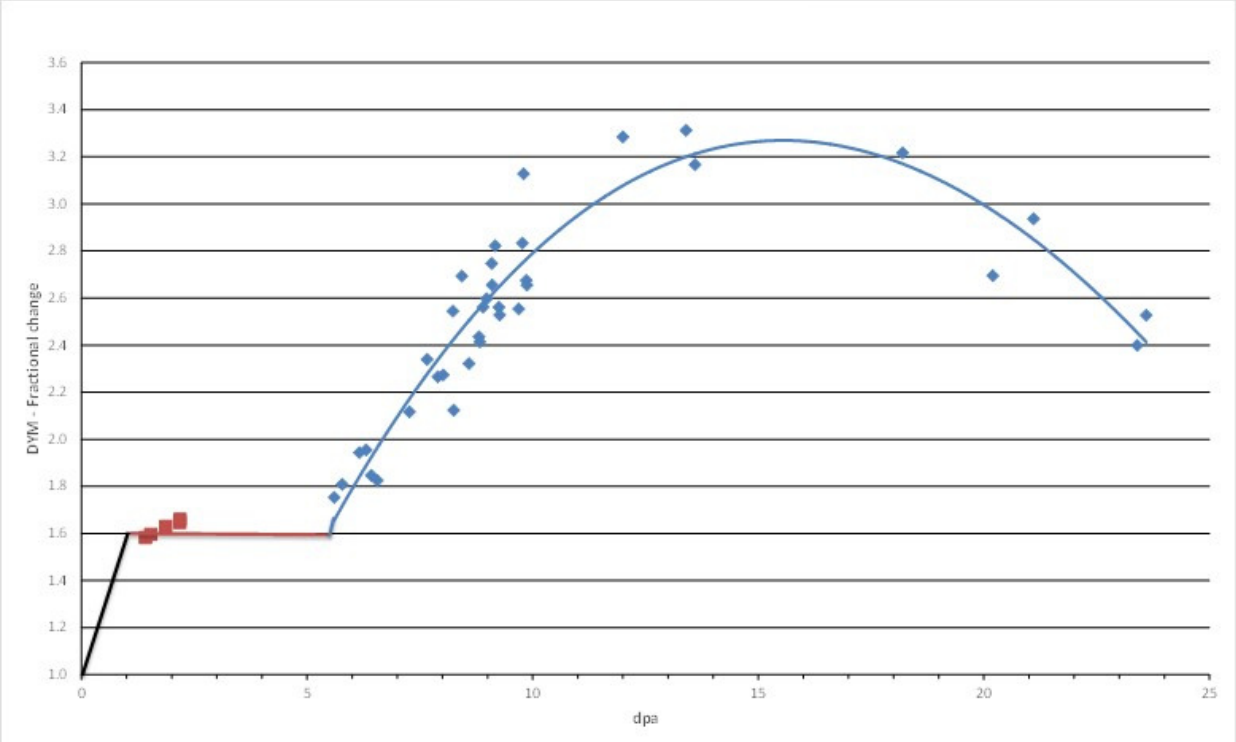

(b) PCIB

Figure 15 – cont'd

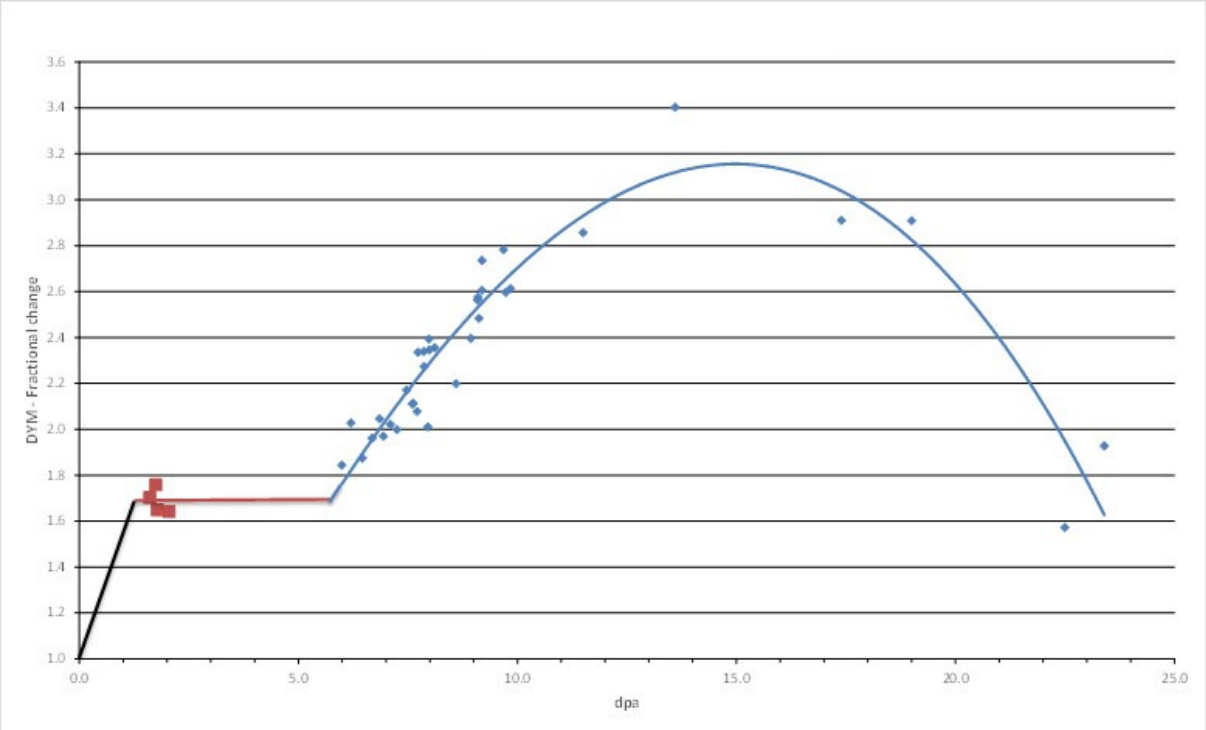

(c) IG-110

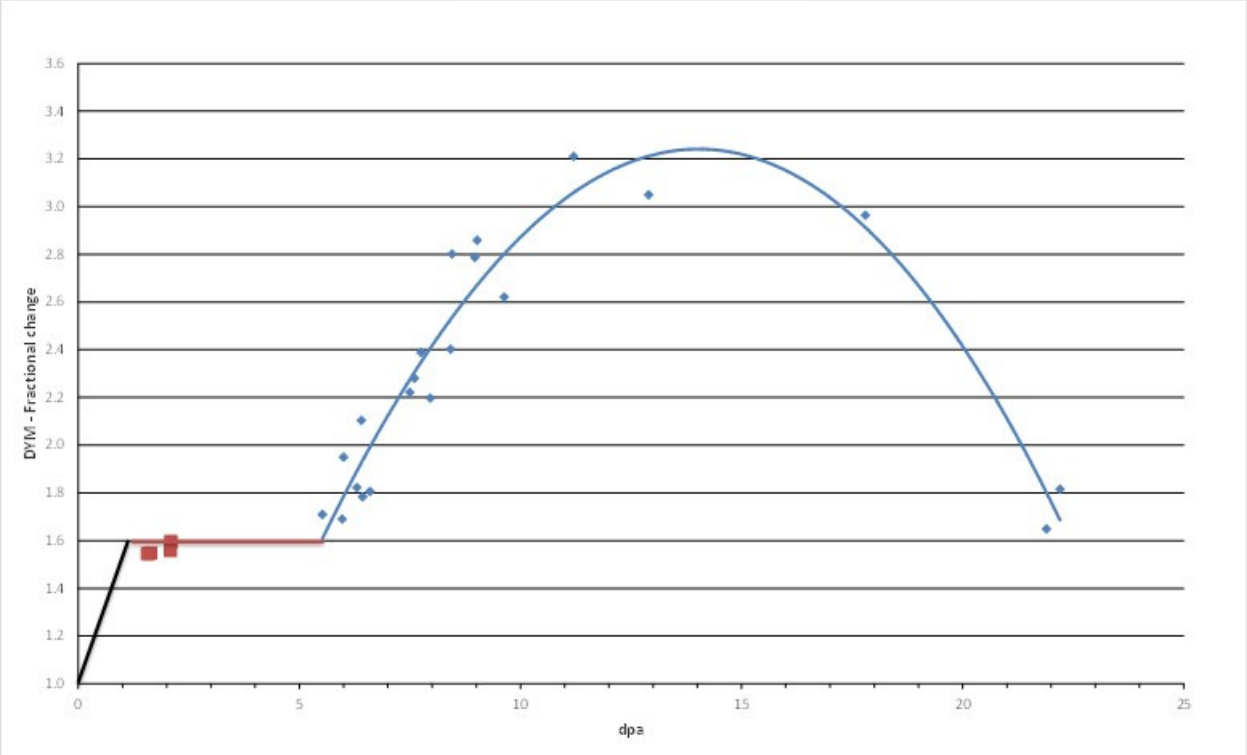

(d) IG-430

Figure 16 – Comparison of CTE variations for extruded graphites at 750°C

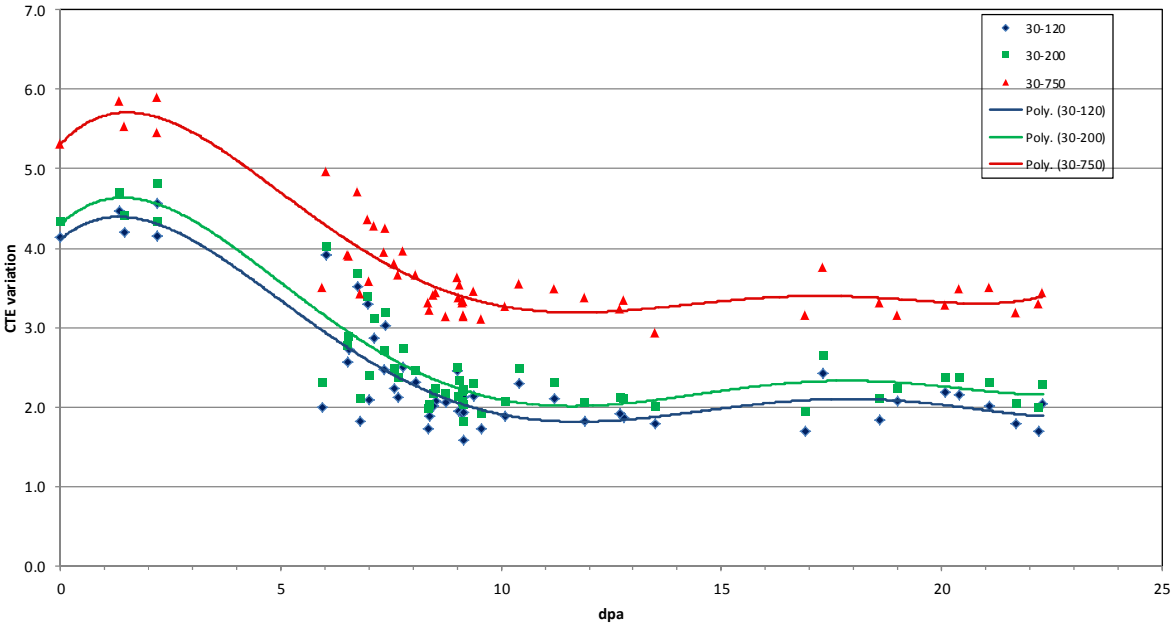

(a) NBG-10

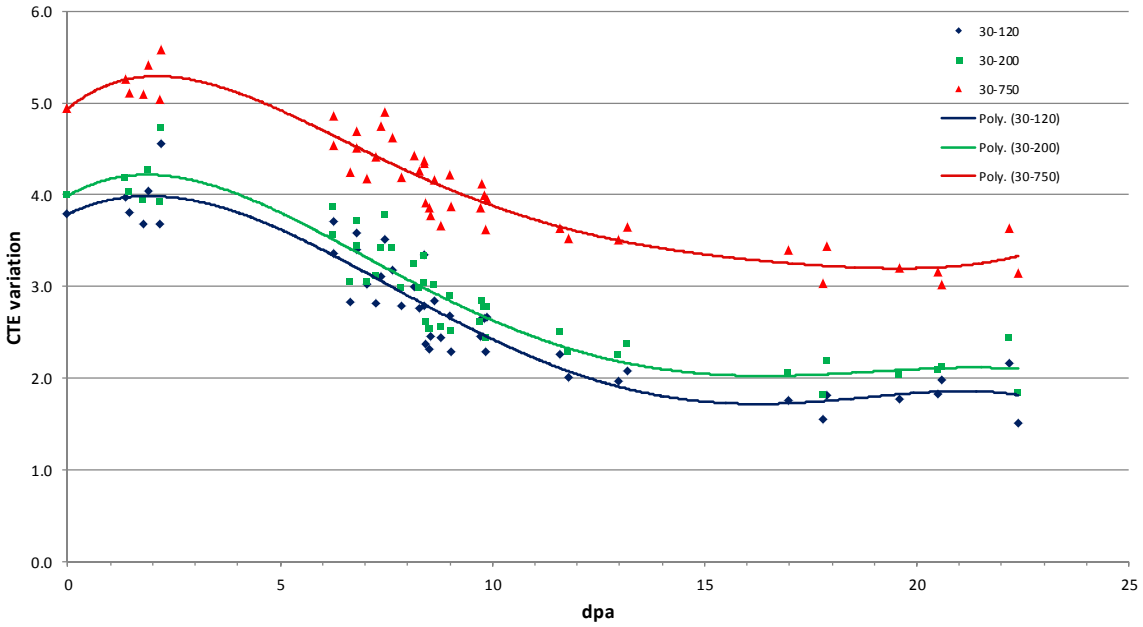

(b) PCEA

Figure 16 – cont'd

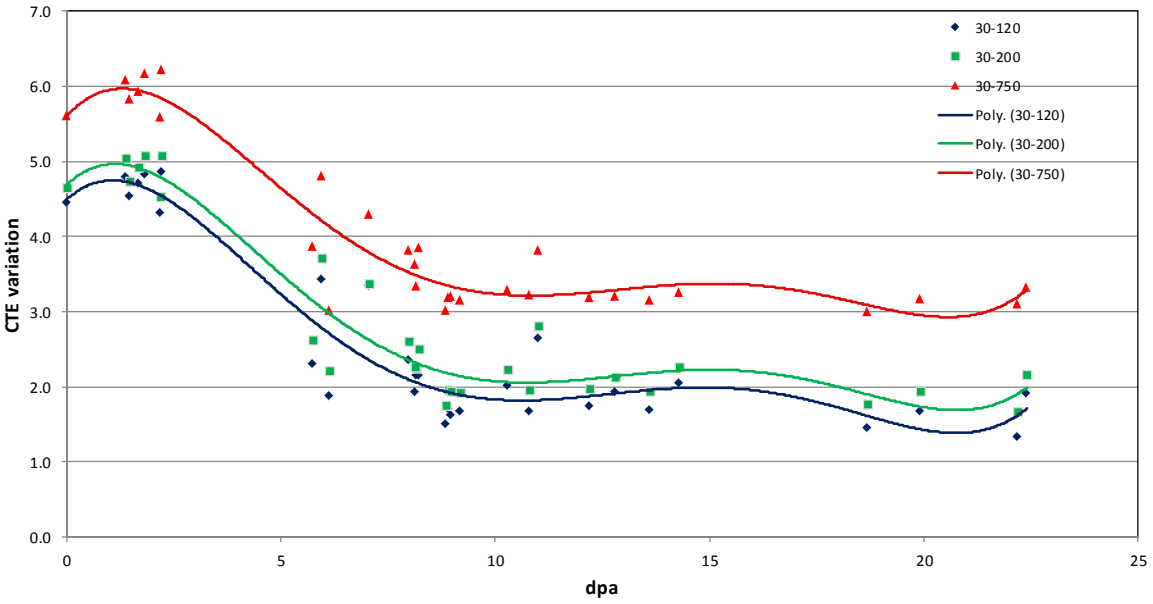

(c) PPEA

Figure 17 – Comparison of CTE fractional changes for extruded graphites at 750°C

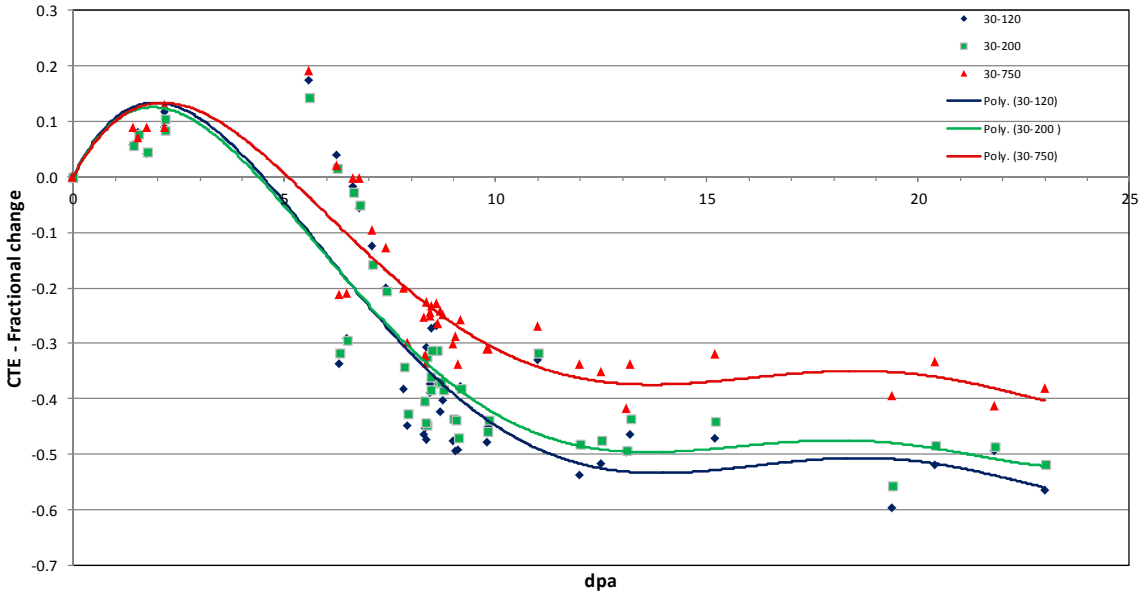

(a) NBG-10

Figure 17 – cont'd

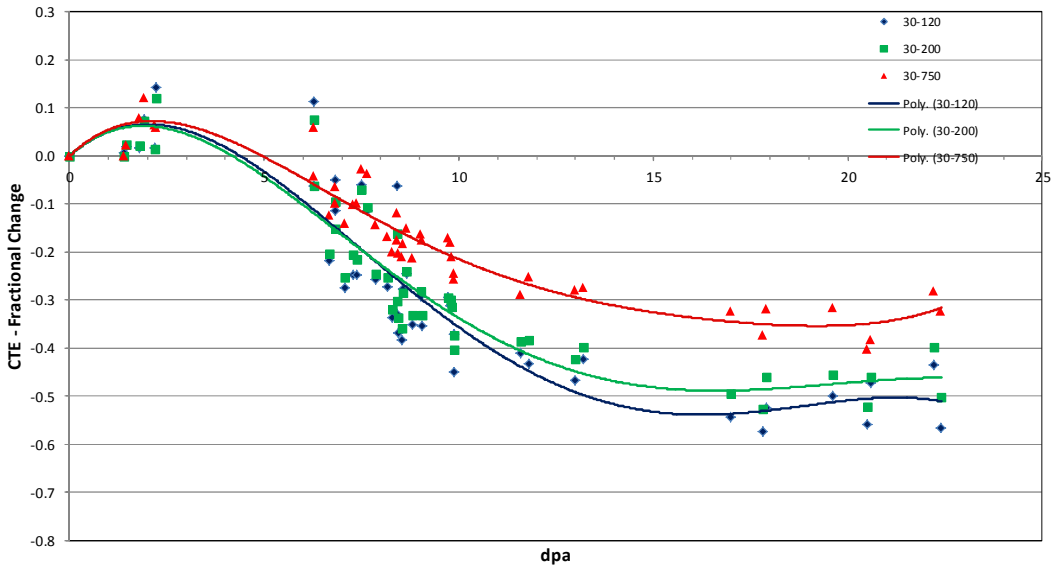

(b) PCEA

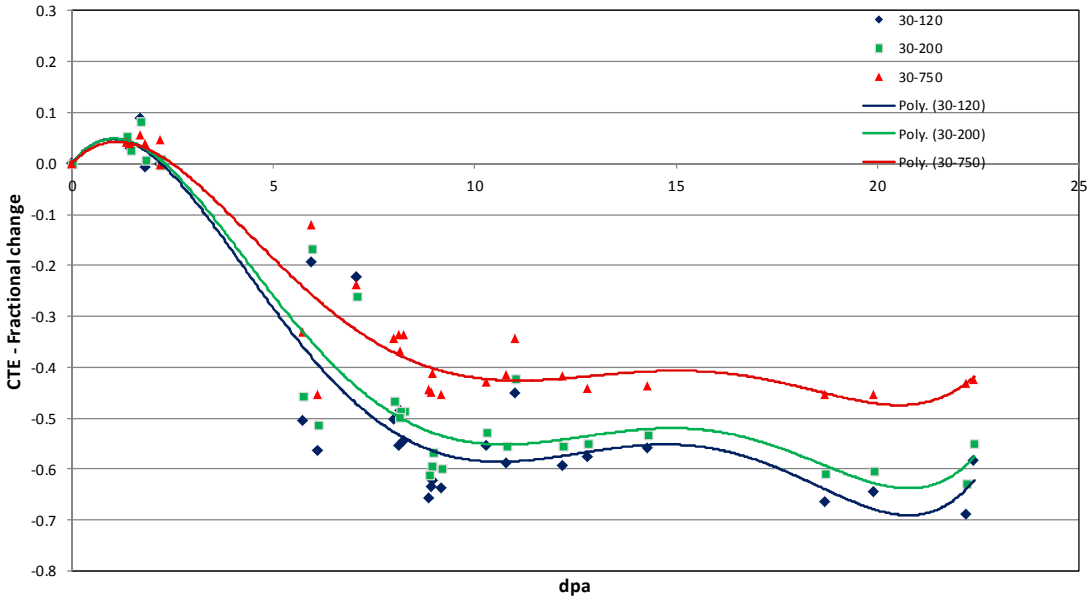

(c) PPEA

Figure 18 – Comparison of CTE variations for iso-moulded graphites at 750°C

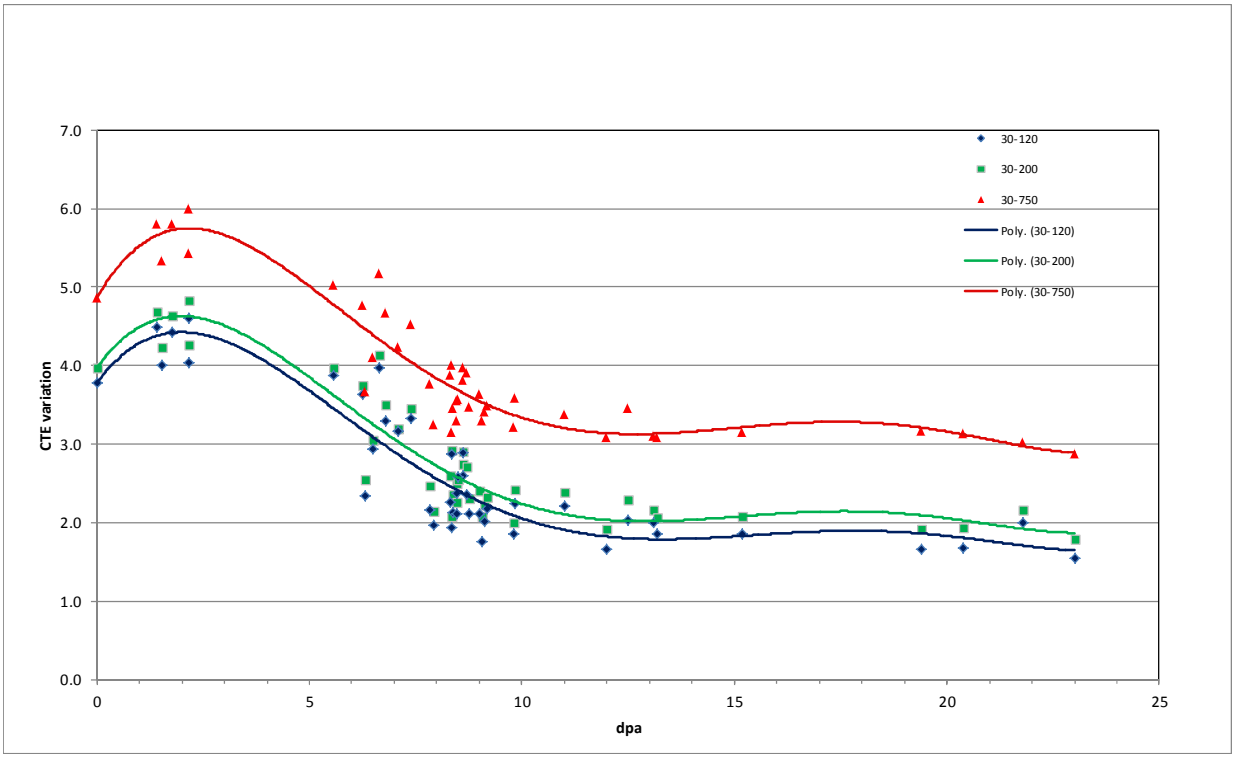

(a) NBG-25

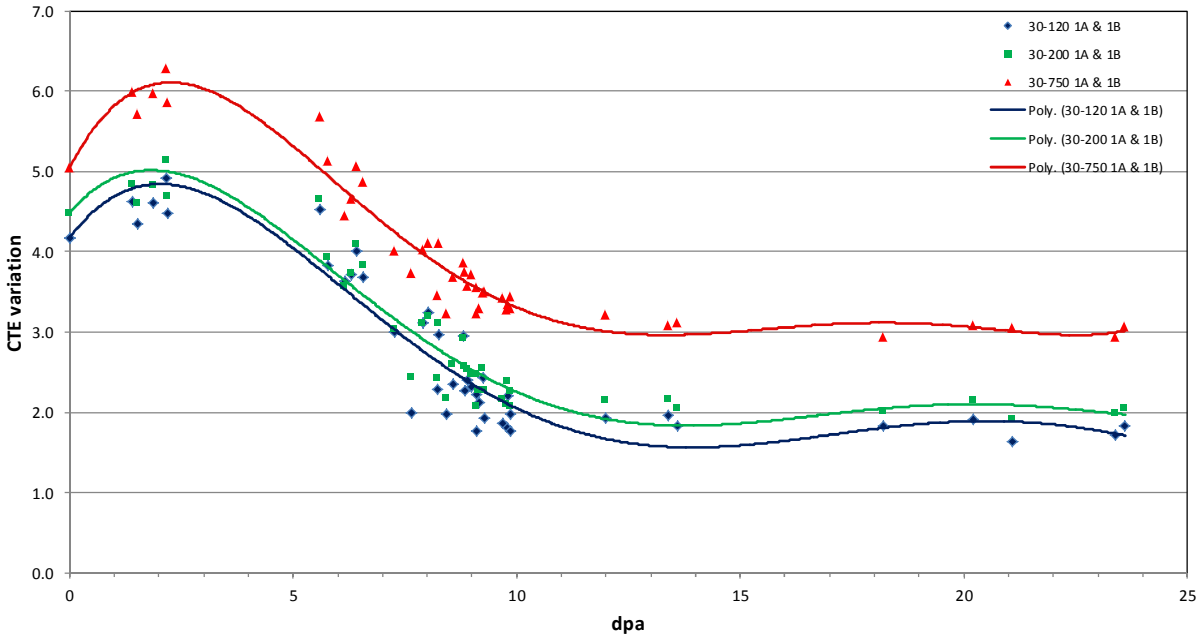

(b) PCIB

Figure 18 – cont'd

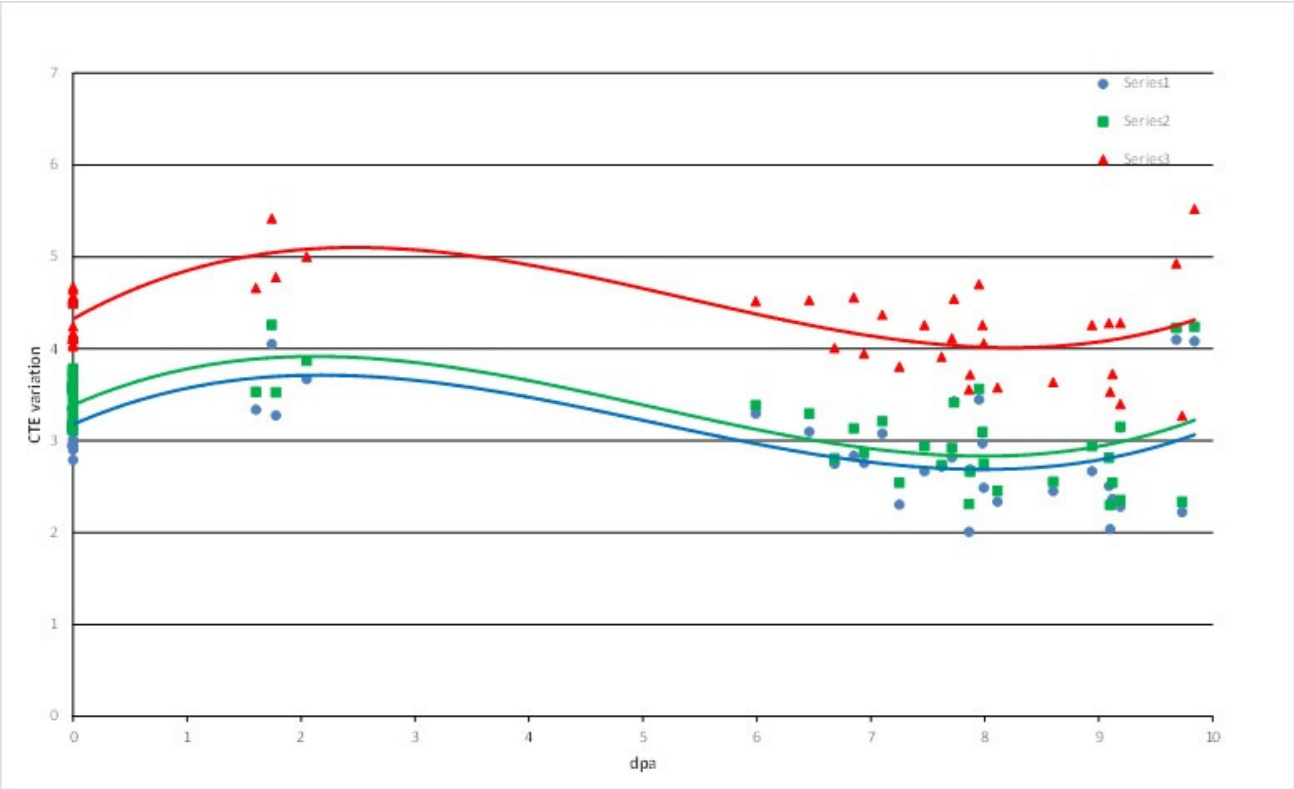

(c) IG-110

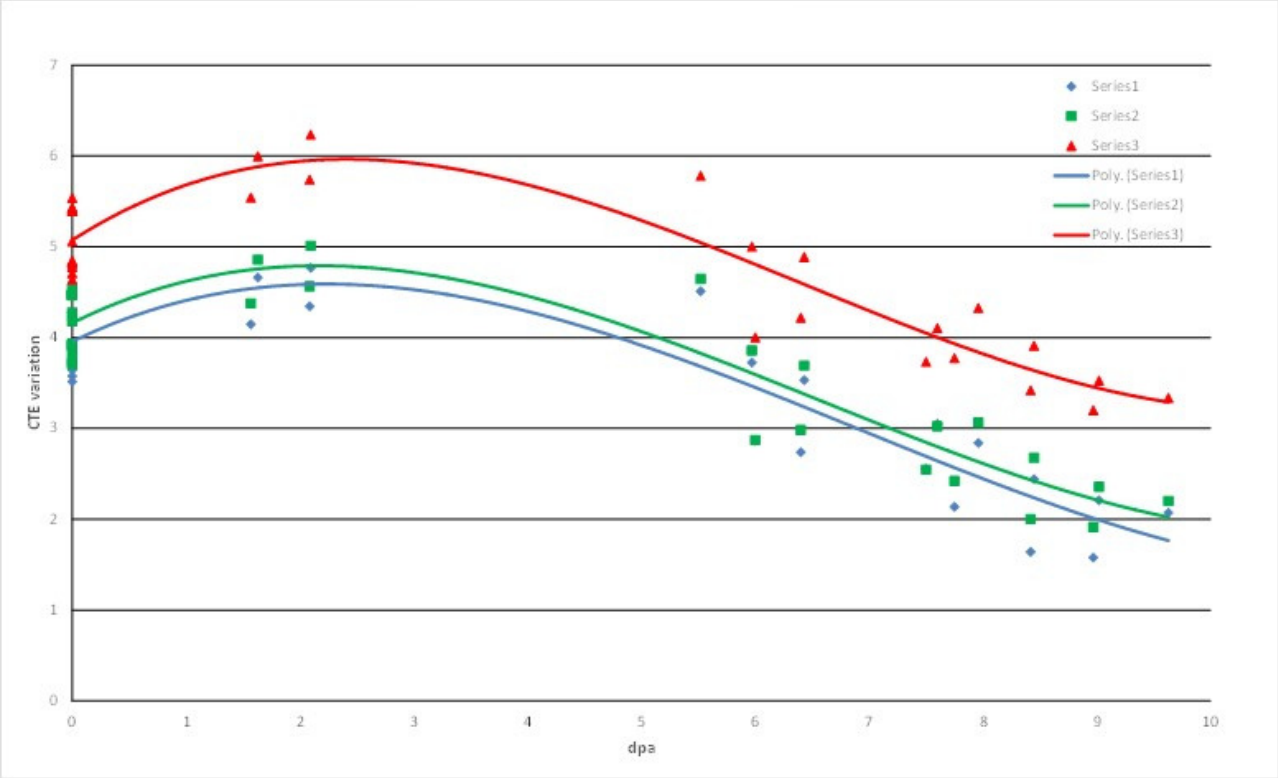

(d) IG-430

Figure 19 – Comparison of CTE fractional changes for iso-moulded graphites at 750ºC

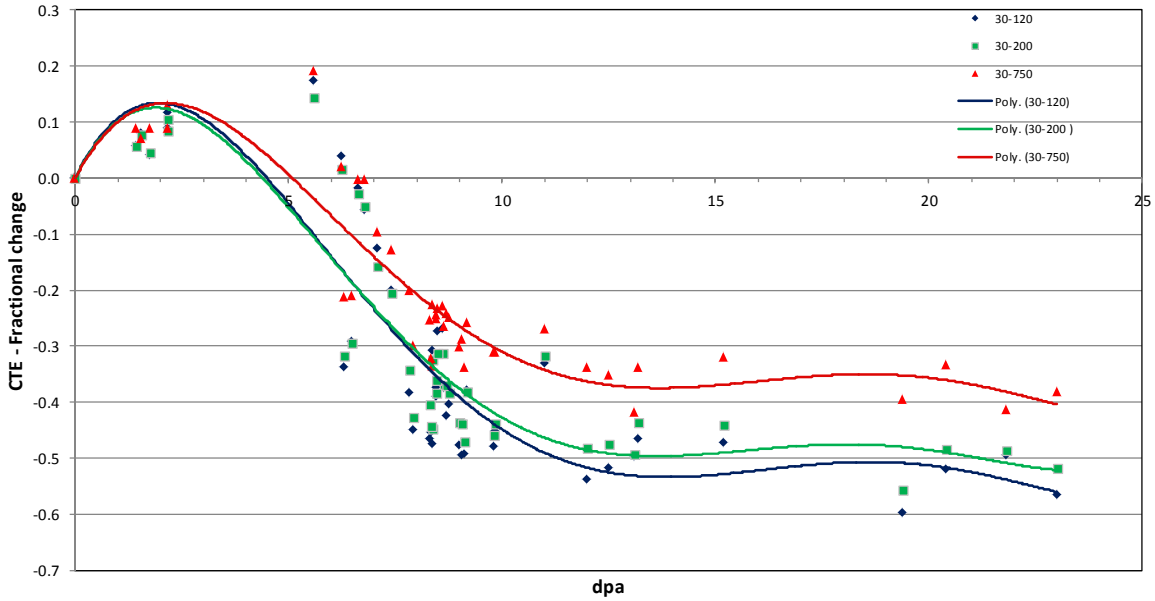

(a) NBG-25

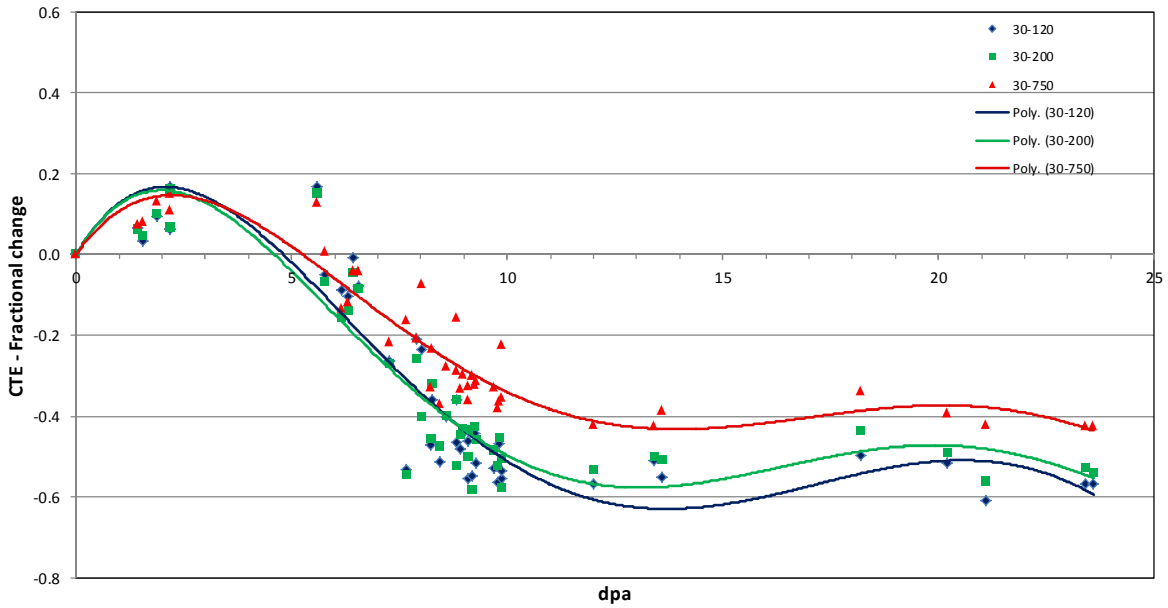

(b) PCIB

Figure 19 – cont'd

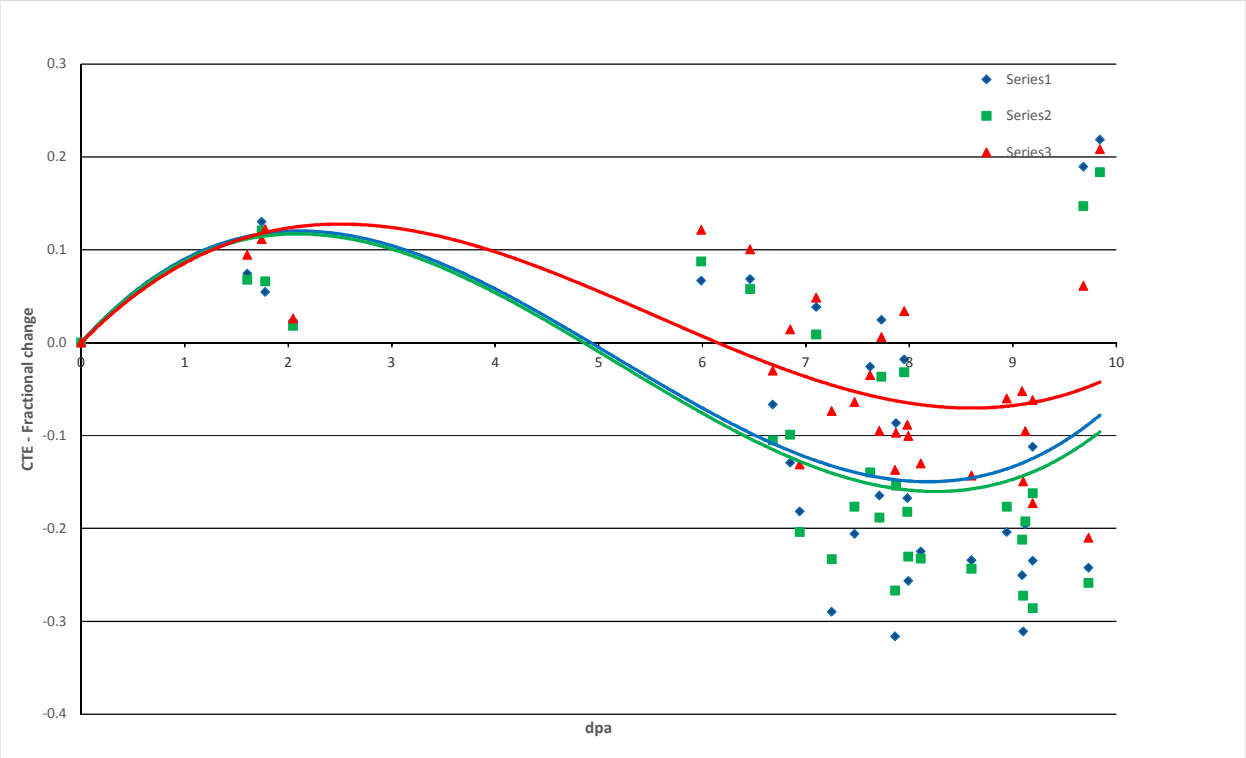

(c) IG-110

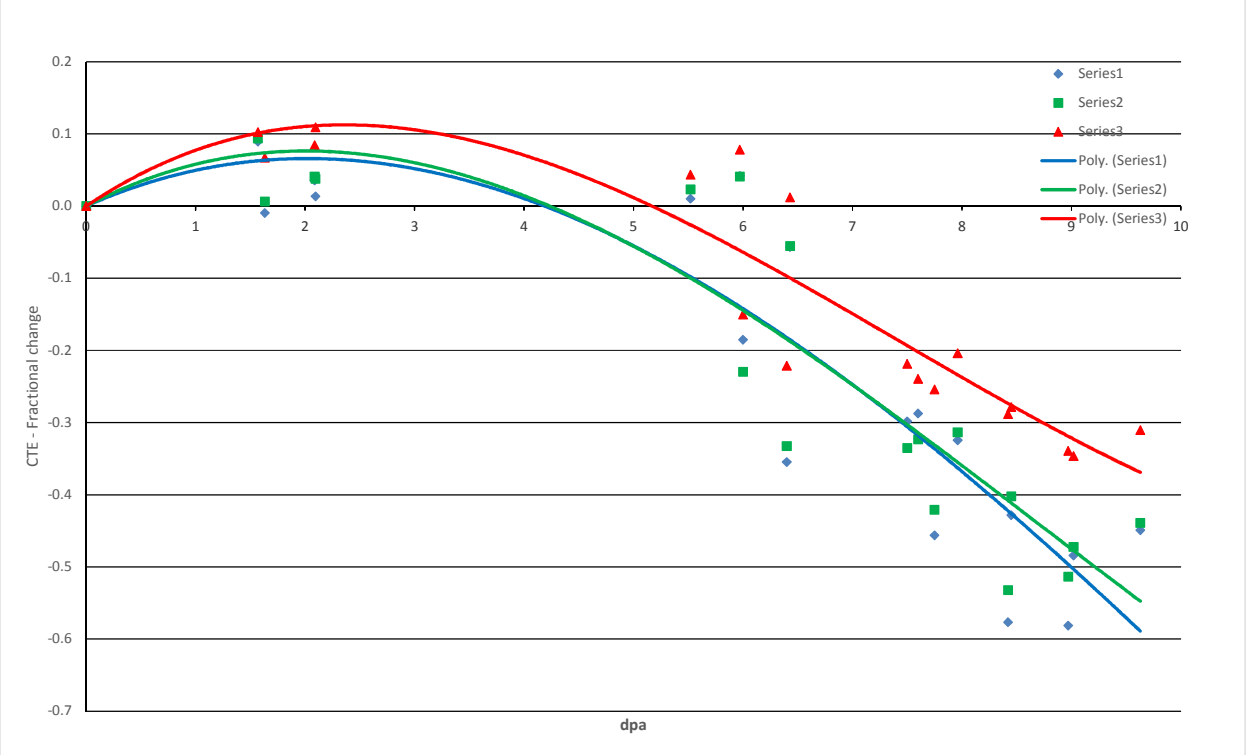

(d) IG-430

Figure 20 – Comparison of thermal conductivity variations for extruded graphites at 750°C

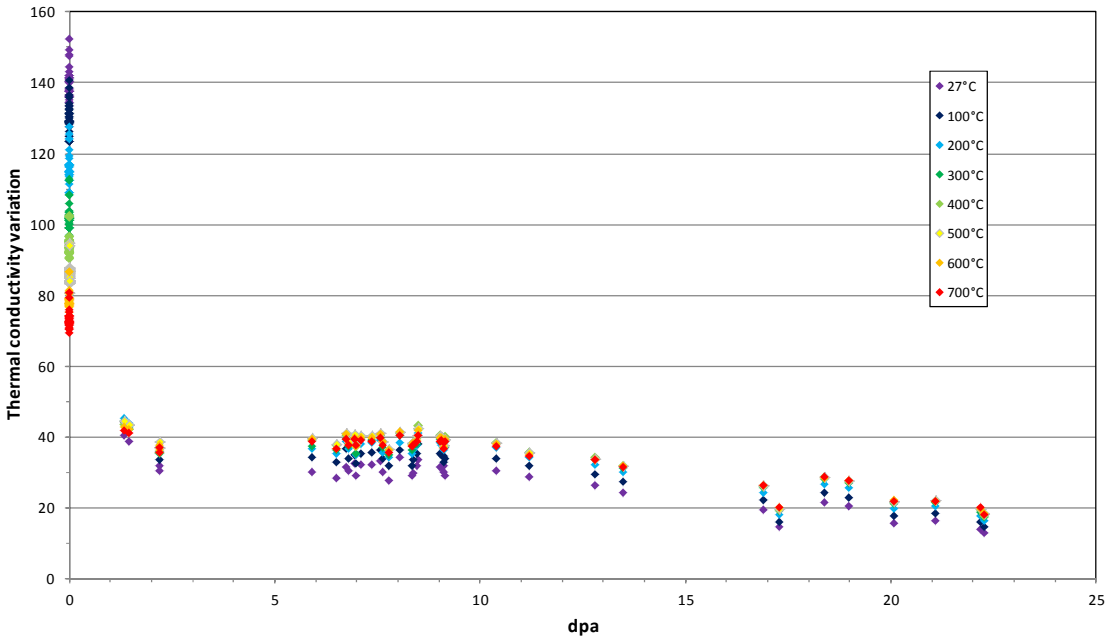

(a) NBG-10

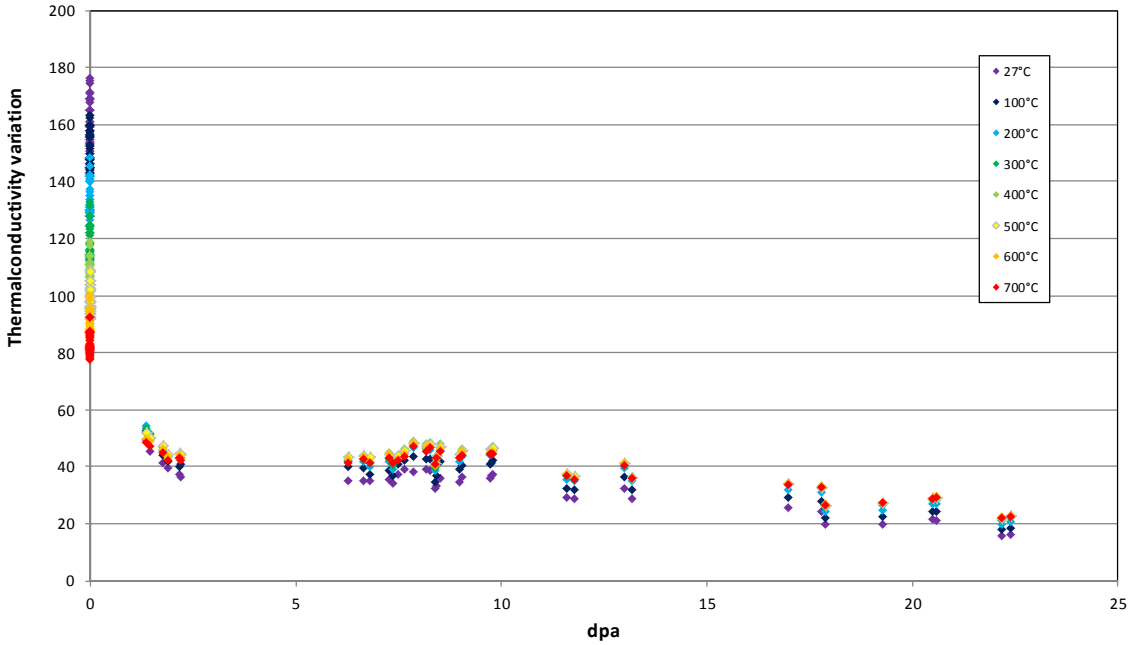

(b) PCEA

Figure 20 – cont'd

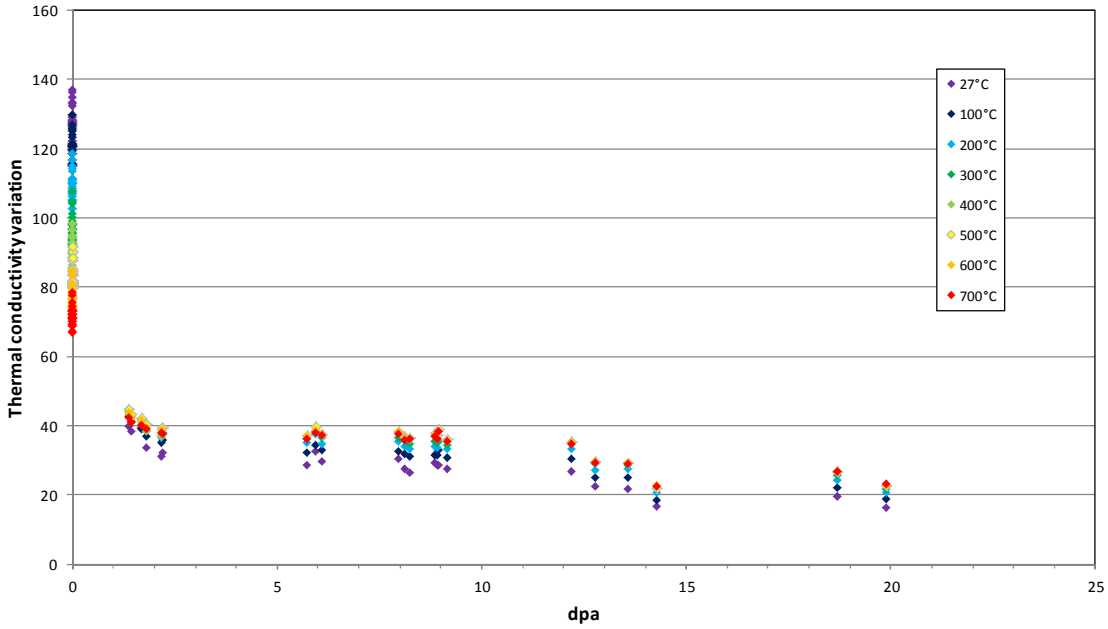

(c) PPEA

Figure 21 – Comparison of thermal conductivity fractional changes for extruded graphites at 750°C

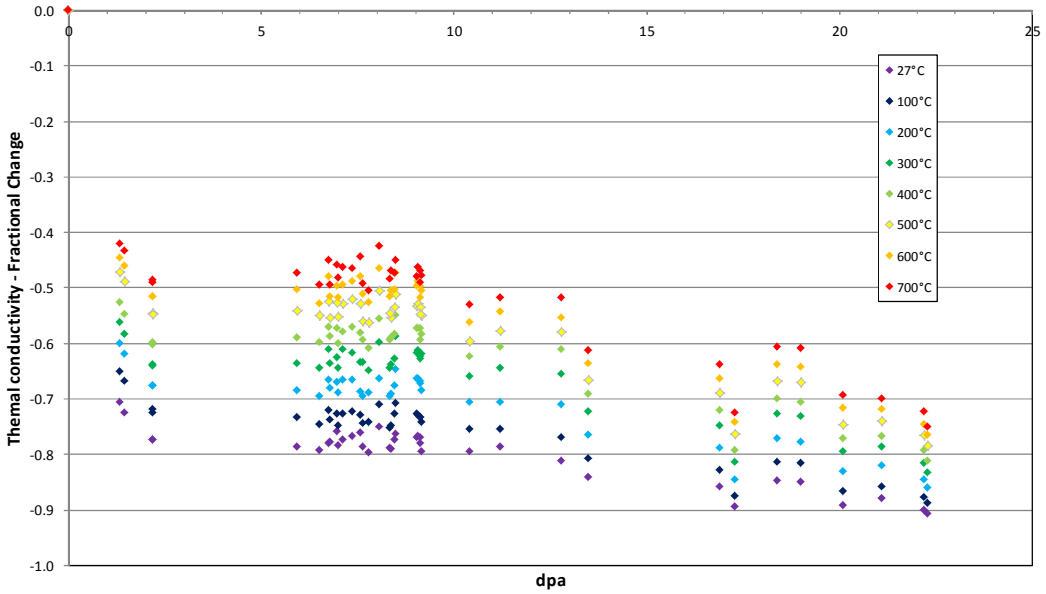

(a) NBG-10

Figure 21 – cont'd

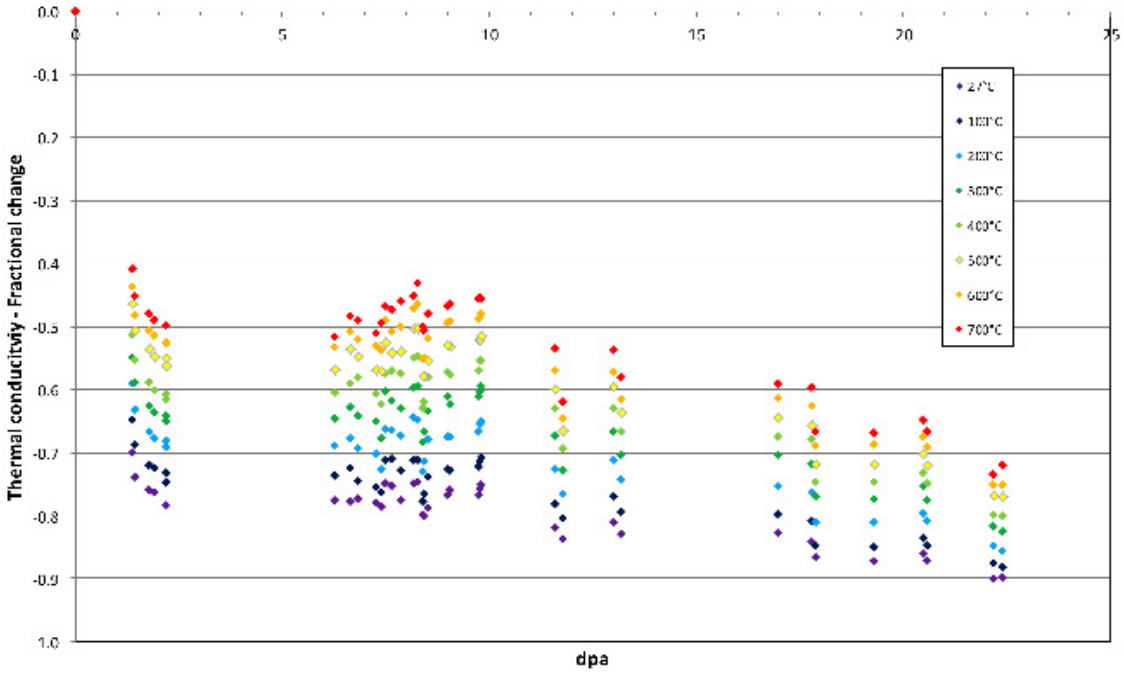

(b) PCEA

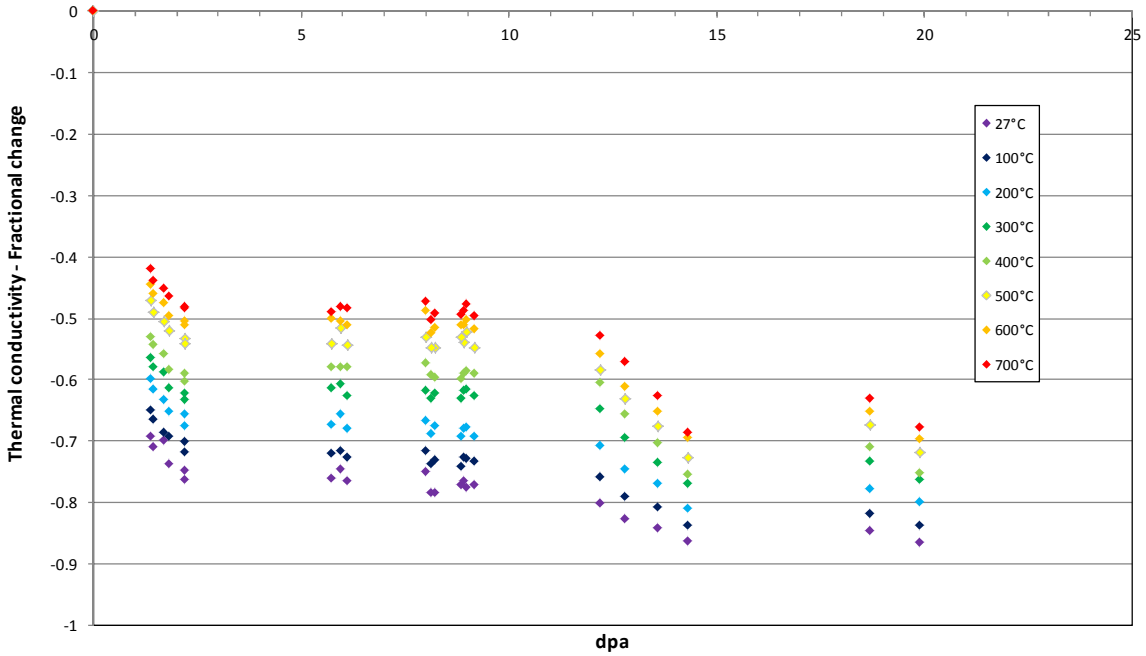

(c) PPEA

Figure 22 – Comparison of thermal conductivity variations for iso-moulded graphites at 750°C

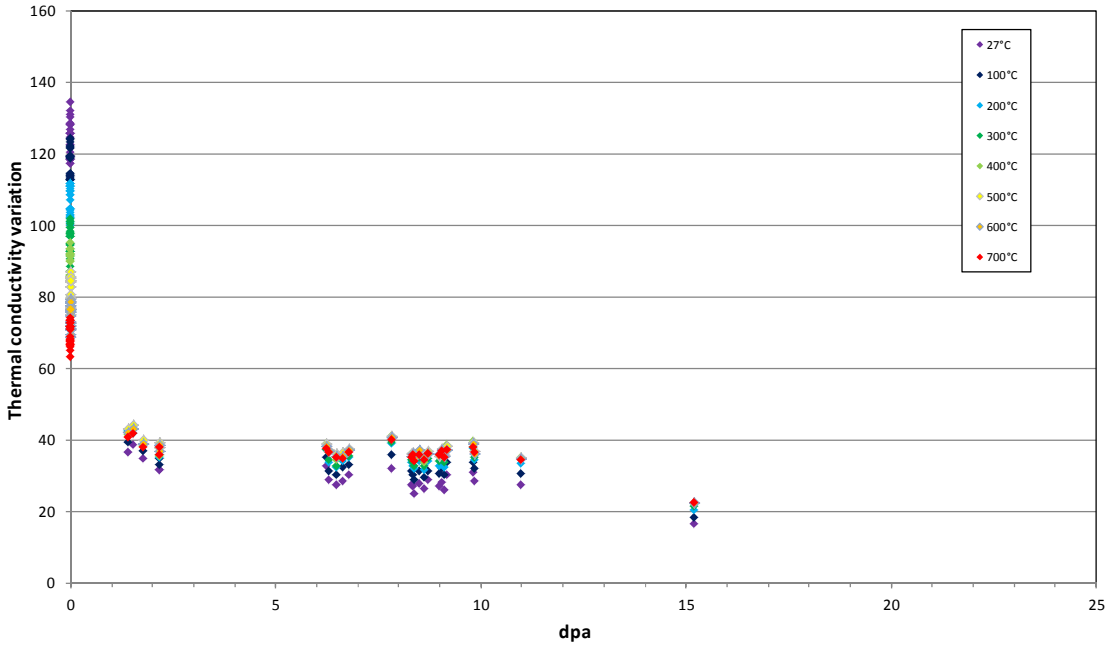

(a) NBG-25

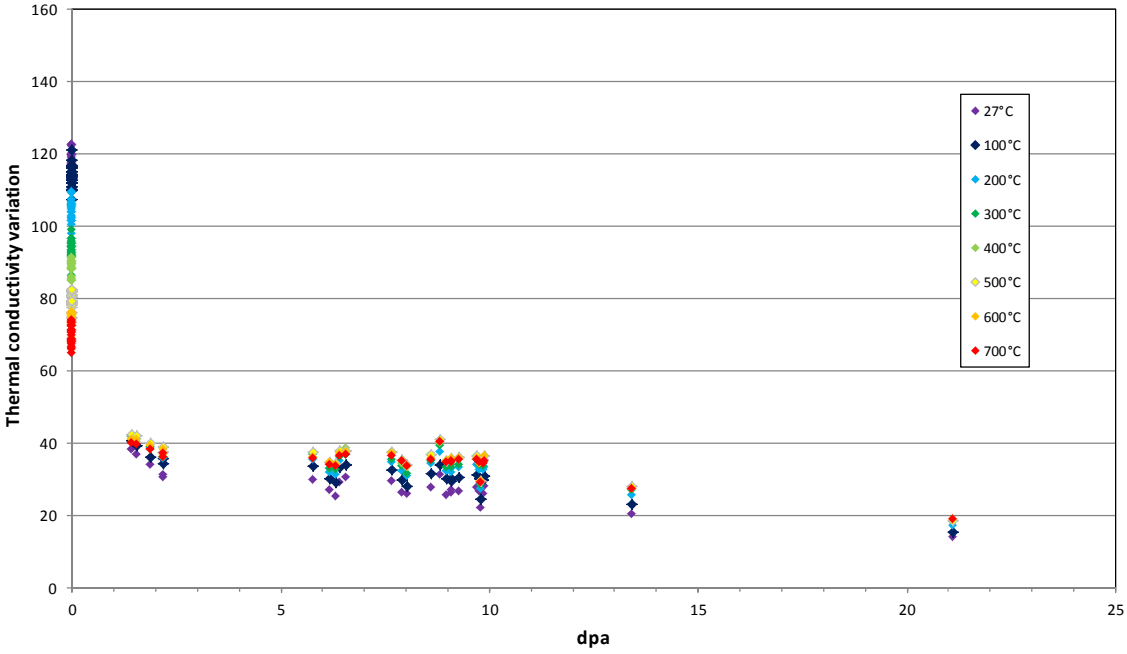

(b) PCIB

Figure 22 – cont'd

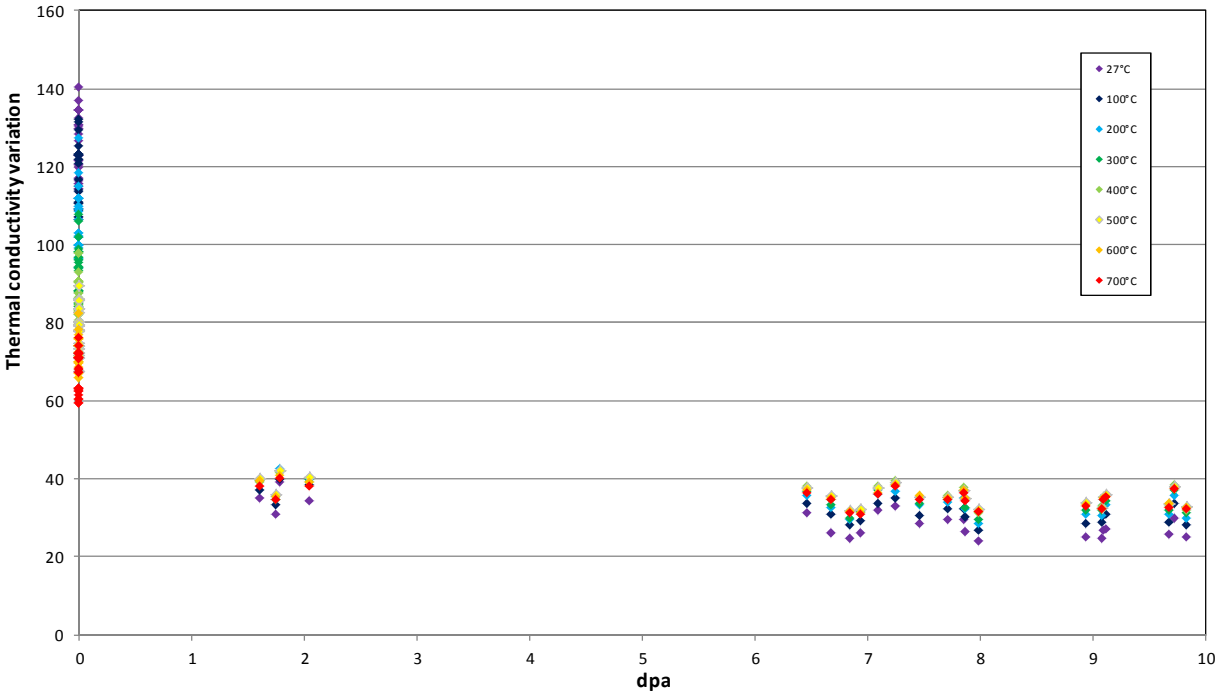

(c) IG-110

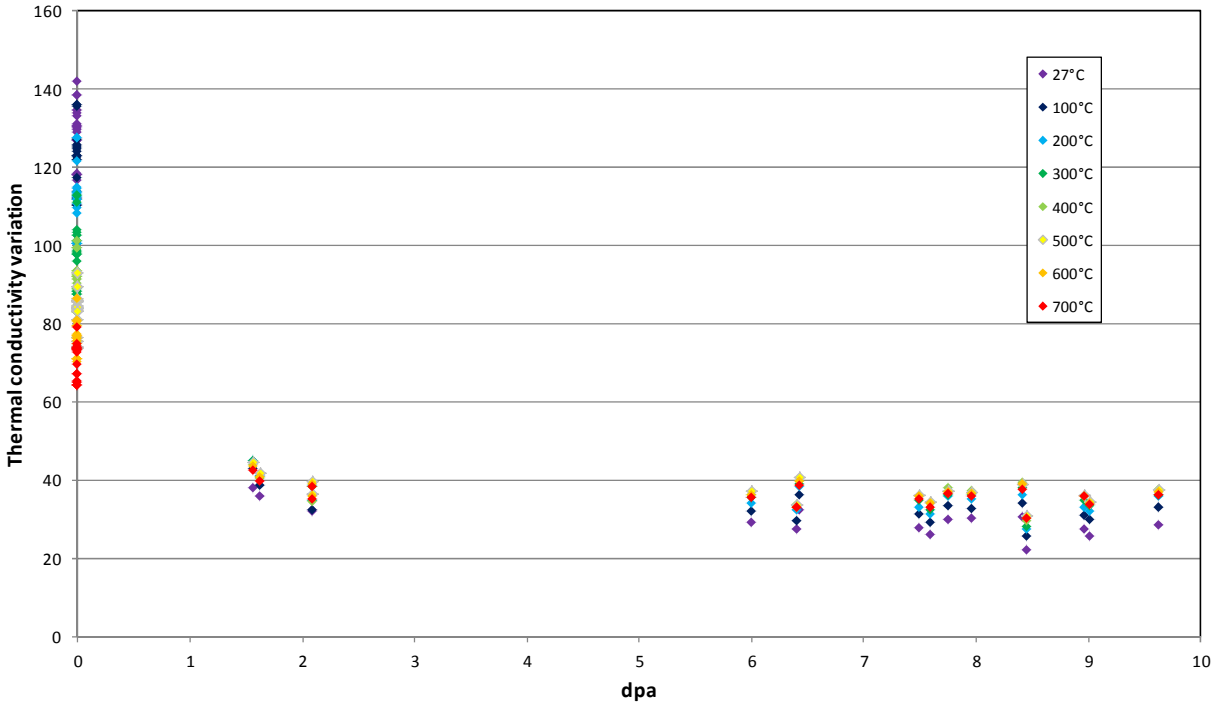

(d) IG-430

Figure 23 – Comparison of thermal conductivity fractional changes for iso-moulded graphites at 750°C

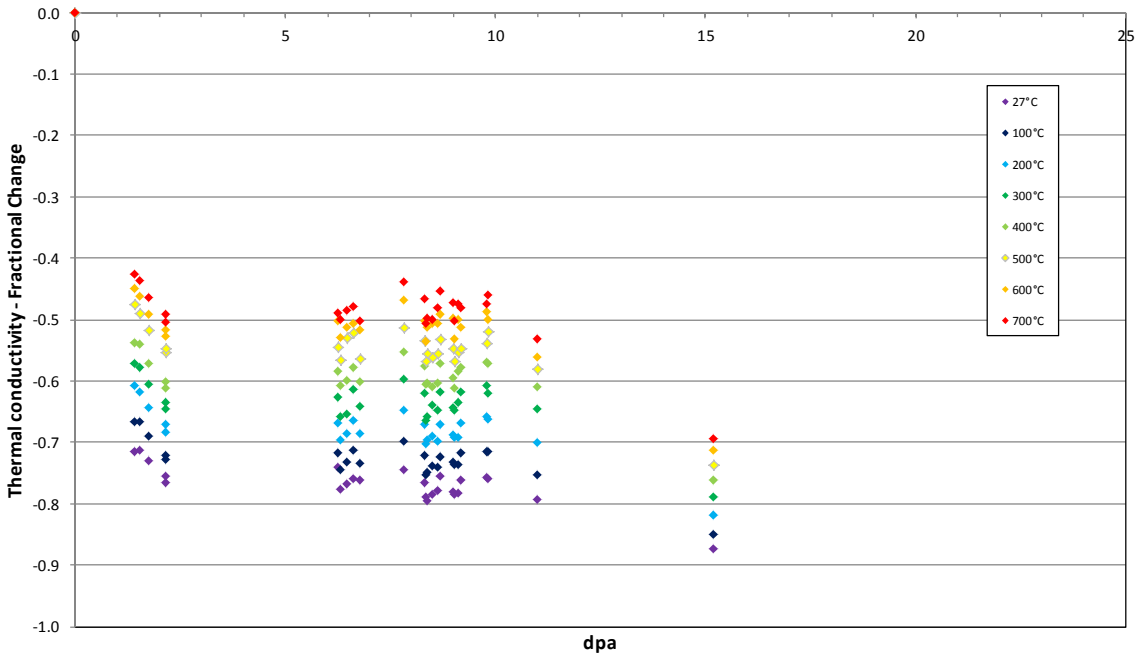

(a) NBG-25

(b) Thermal conductivity - Fractional change

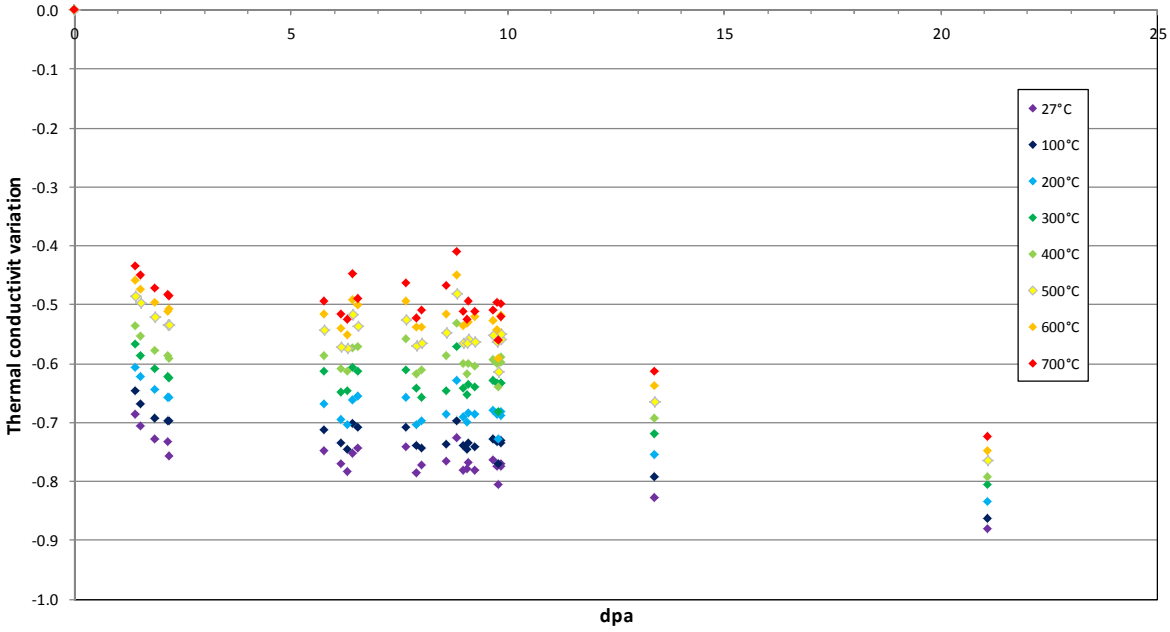

(b) PCIB

Figure 23 – cont'd

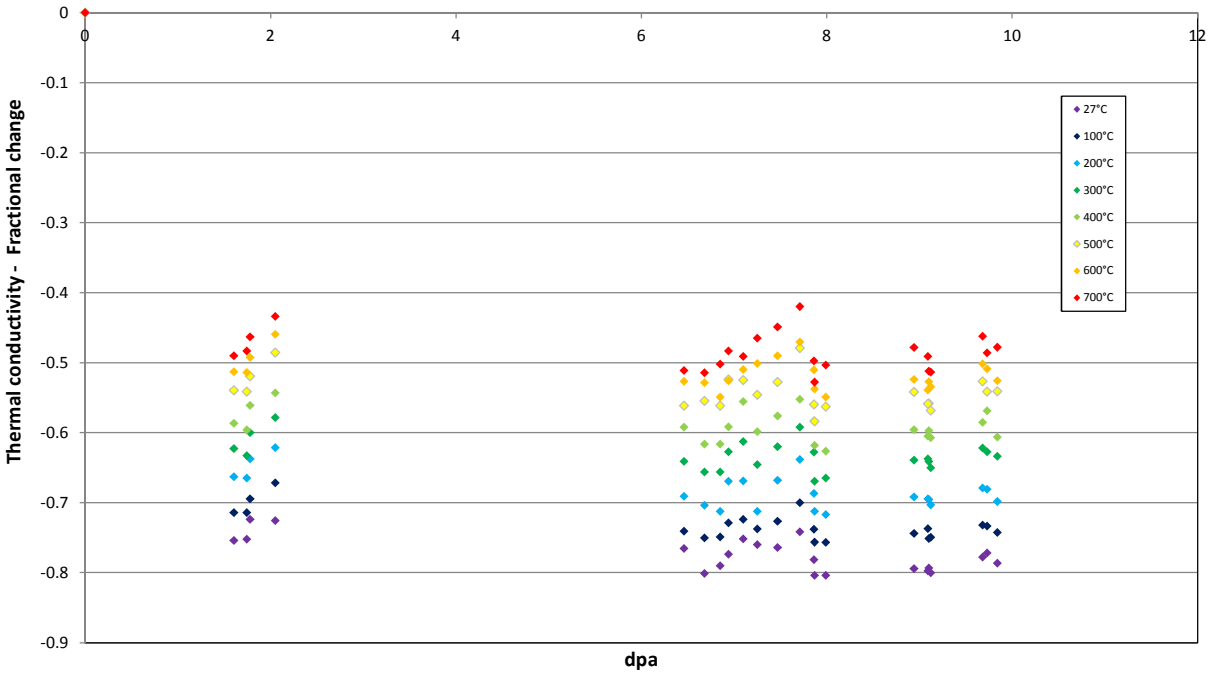

(c) IG-110

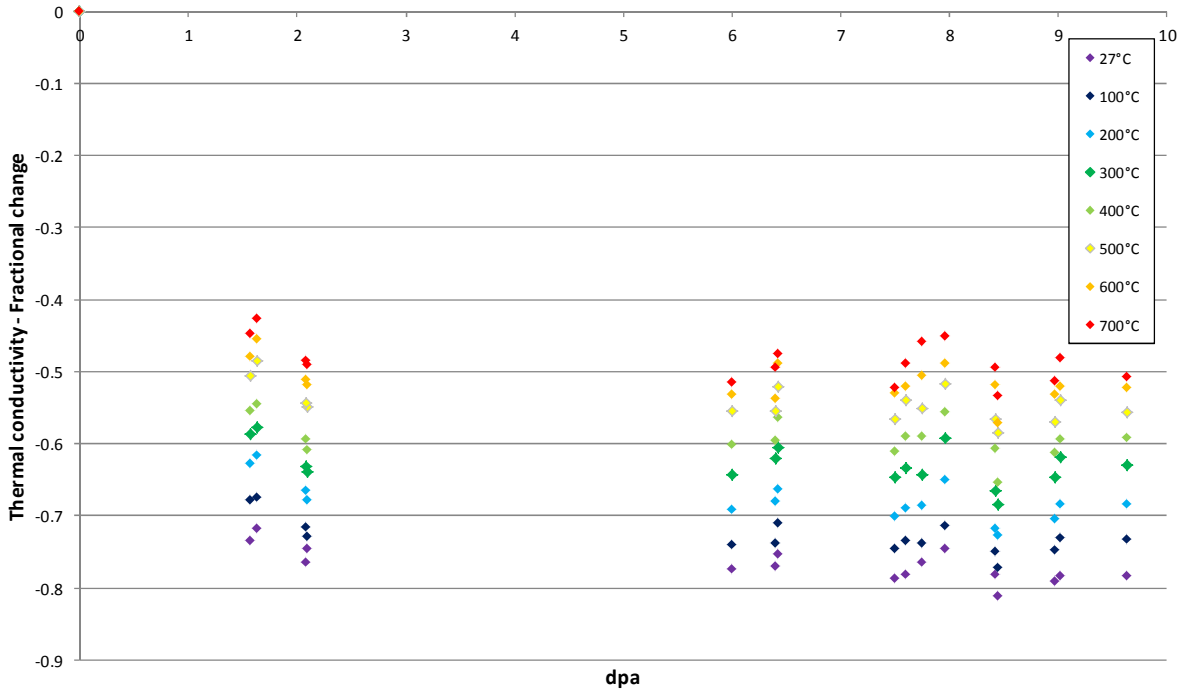

(d) IG-430

Figure 24 - Dimensional change behaviour at 950ºC - WG

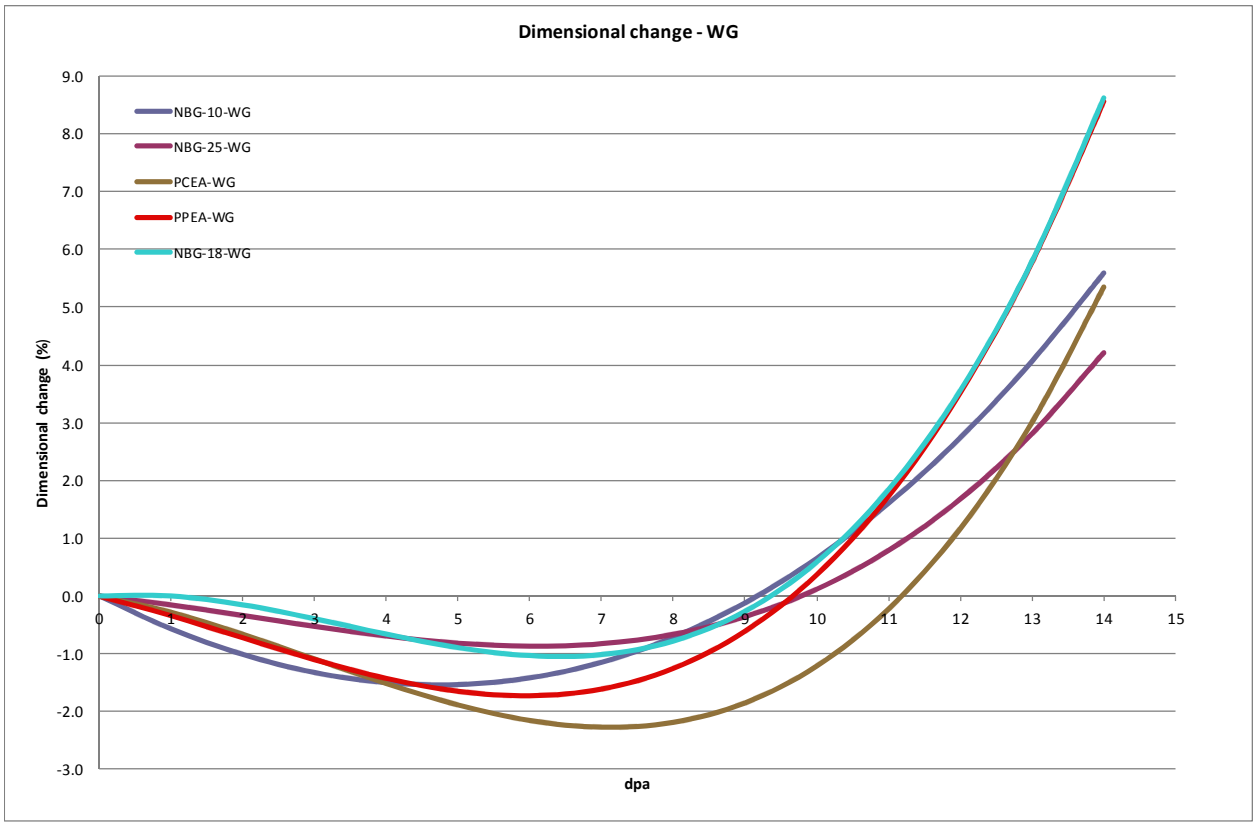

Figure 25- Dimensional change behaviour at 950ºC - AG

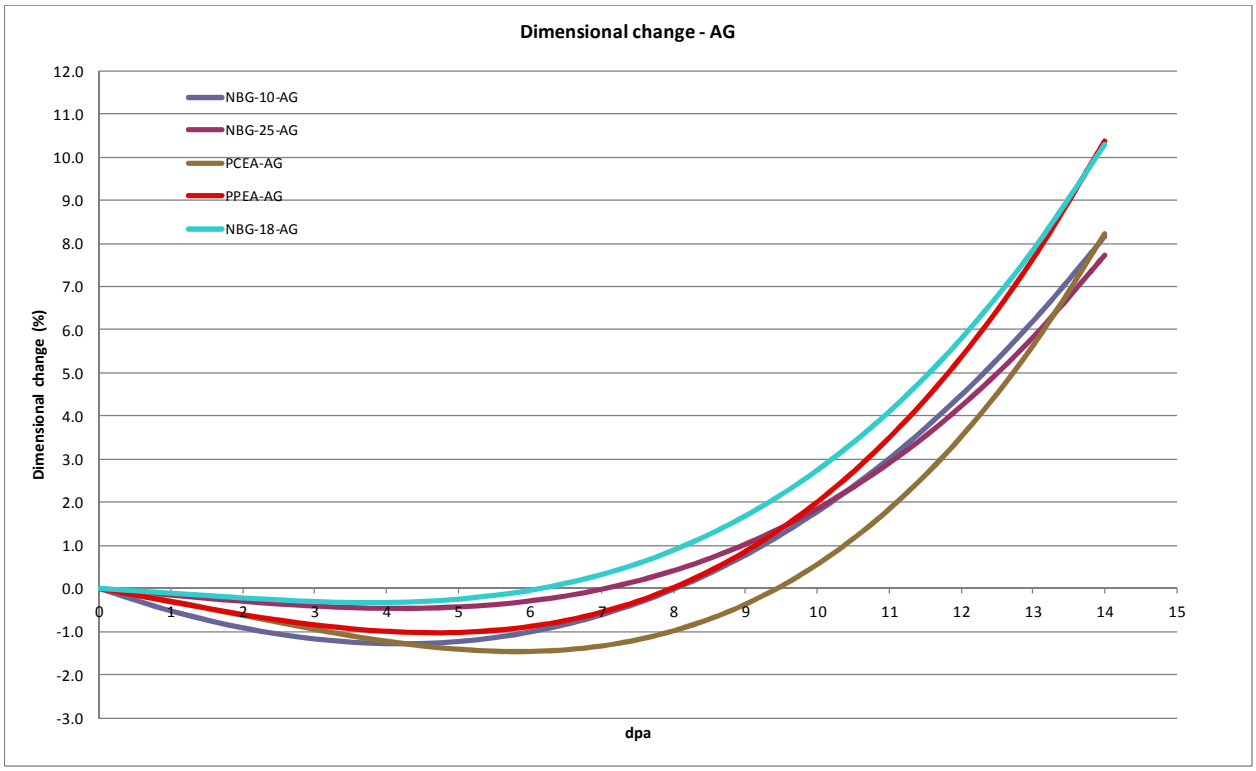

Figure 26- Volume change behaviour at 950ºC

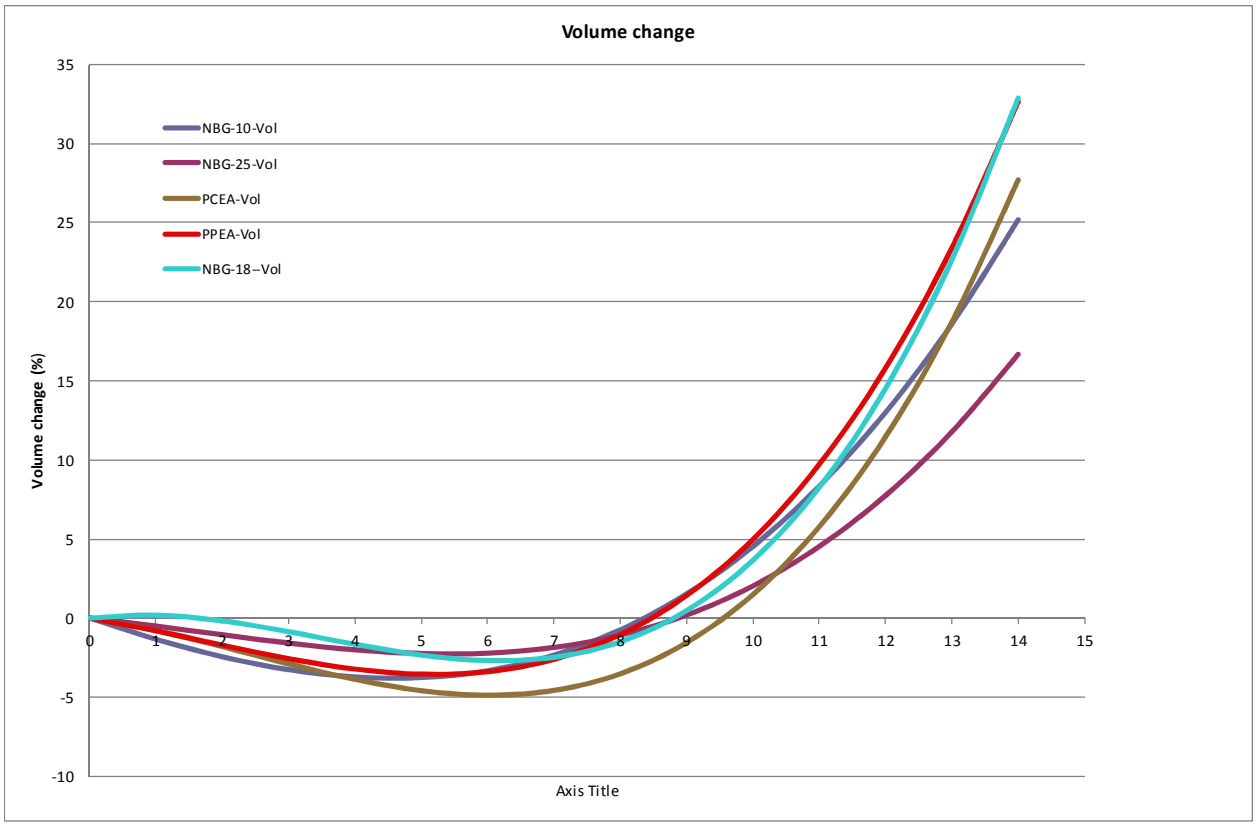

Figure 27- Comparison of extruded and moulded at 950ºC - WG

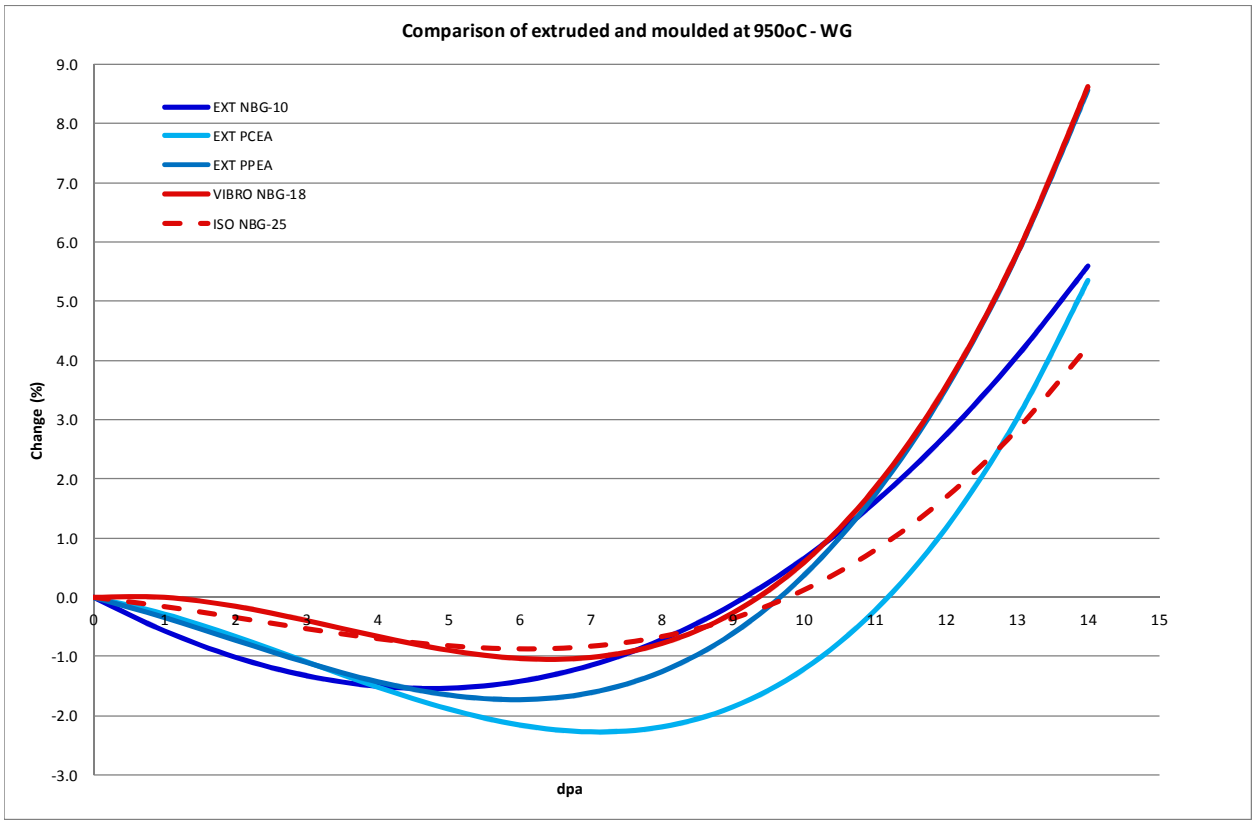

Figure 28- Comparison of extruded and iso-moulded at 950ºC - AG

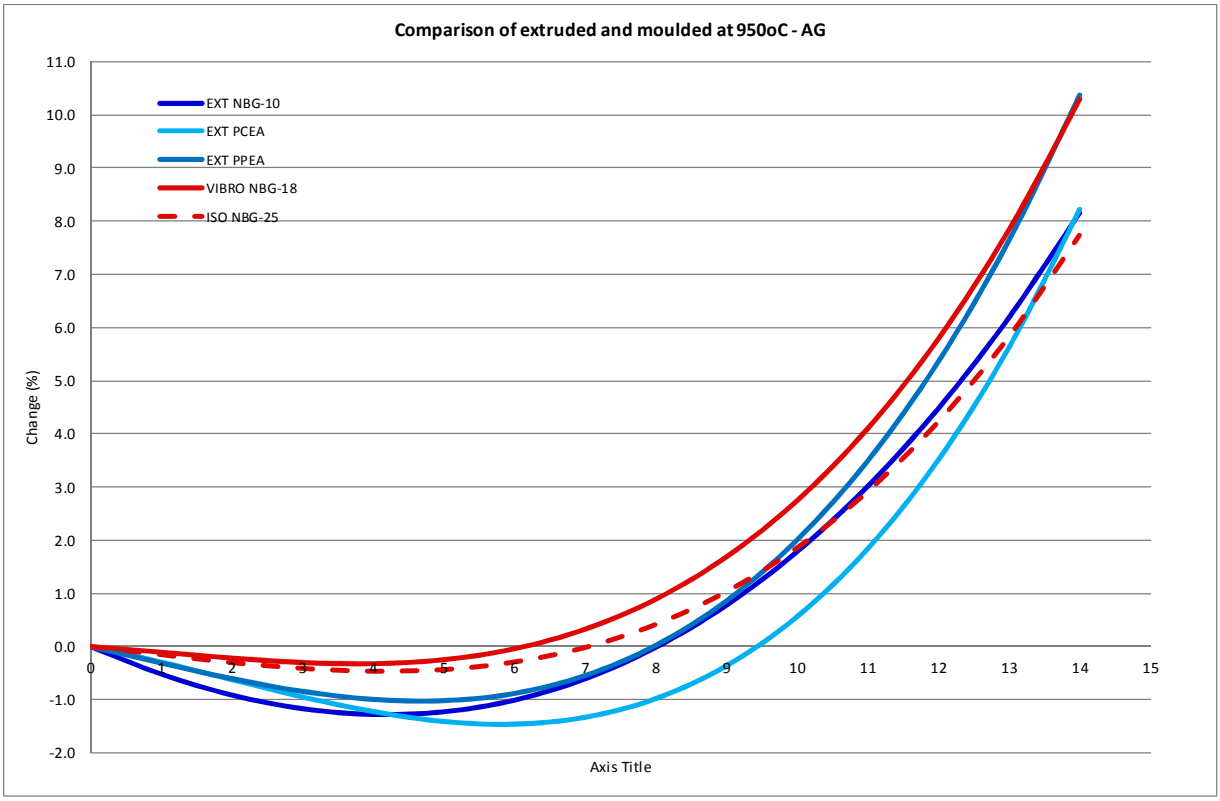

Figure 29- Comparison of extruded and moulded at 950ºC - volume

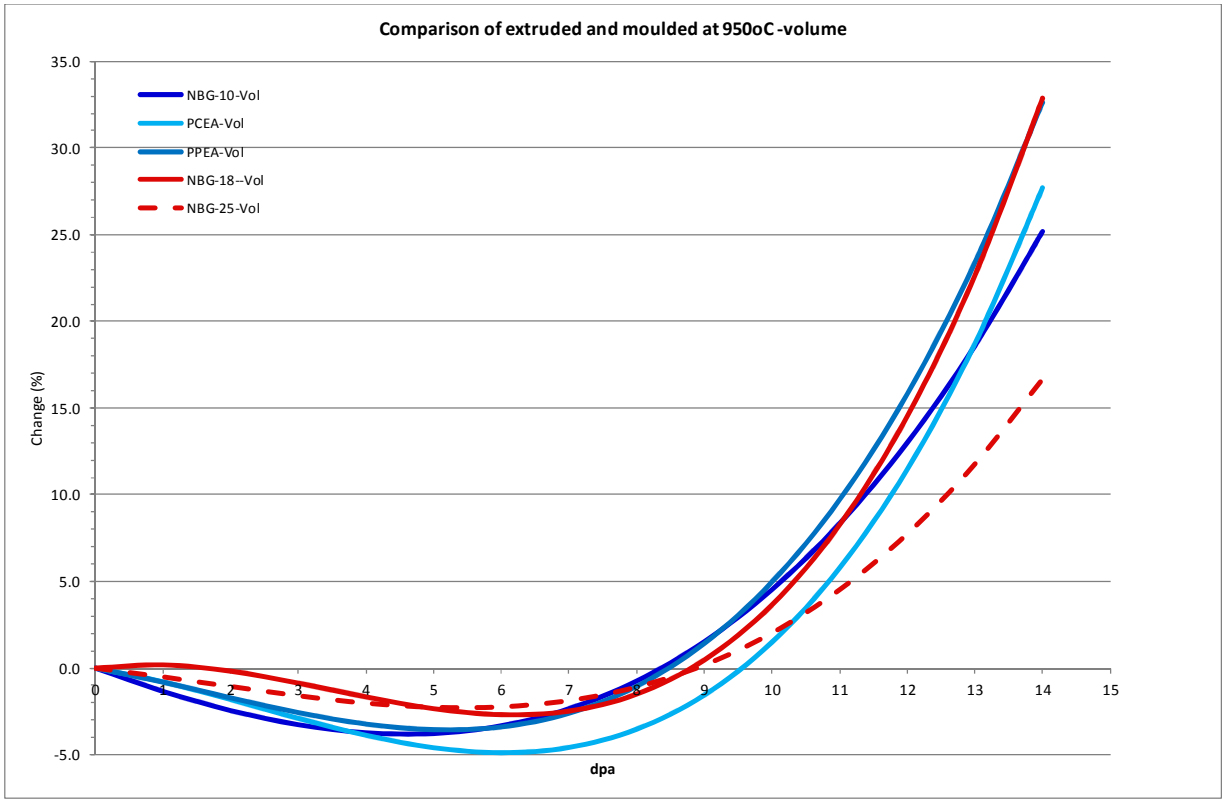

Figure 30- Comparison of dimensional change for PCEA and PPEA at 950°C

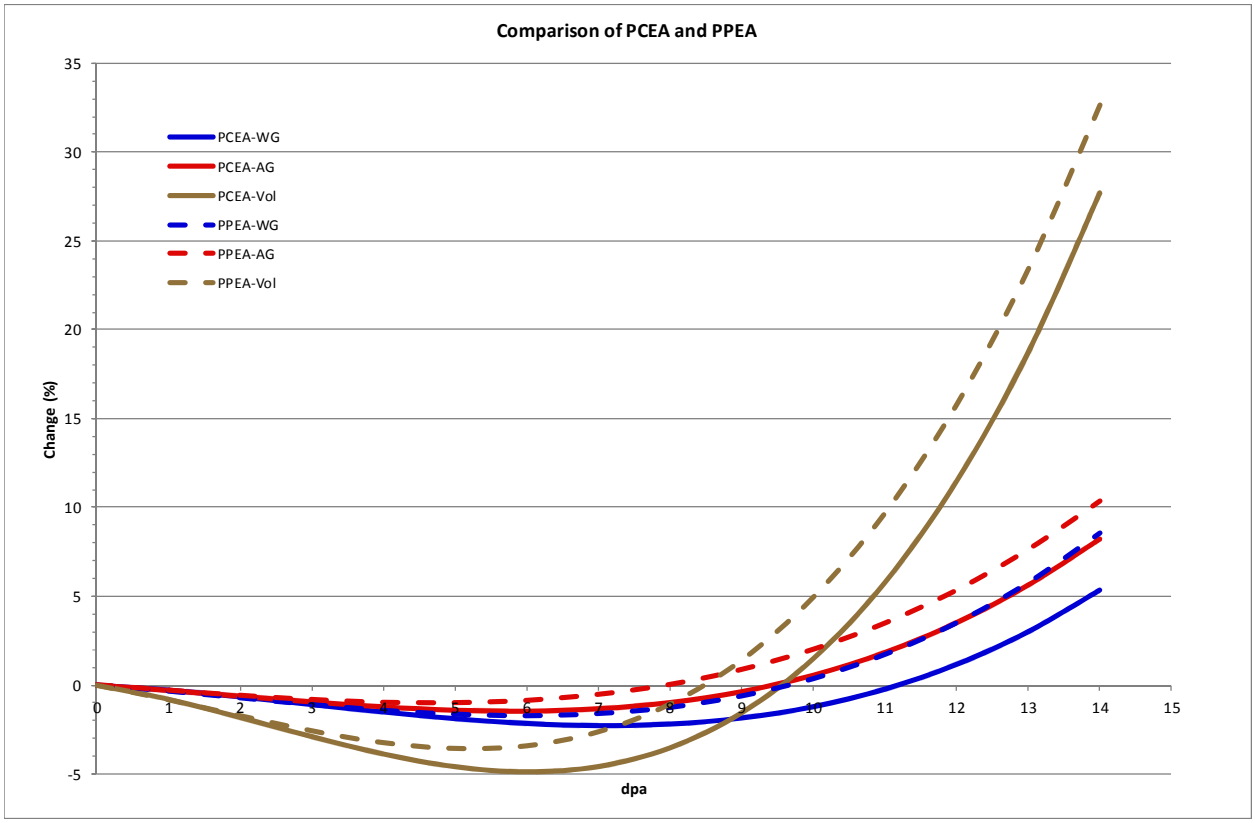

Figure 31- Comparison of dimensional/volume change for NBG-10 and PPEA at 950°C

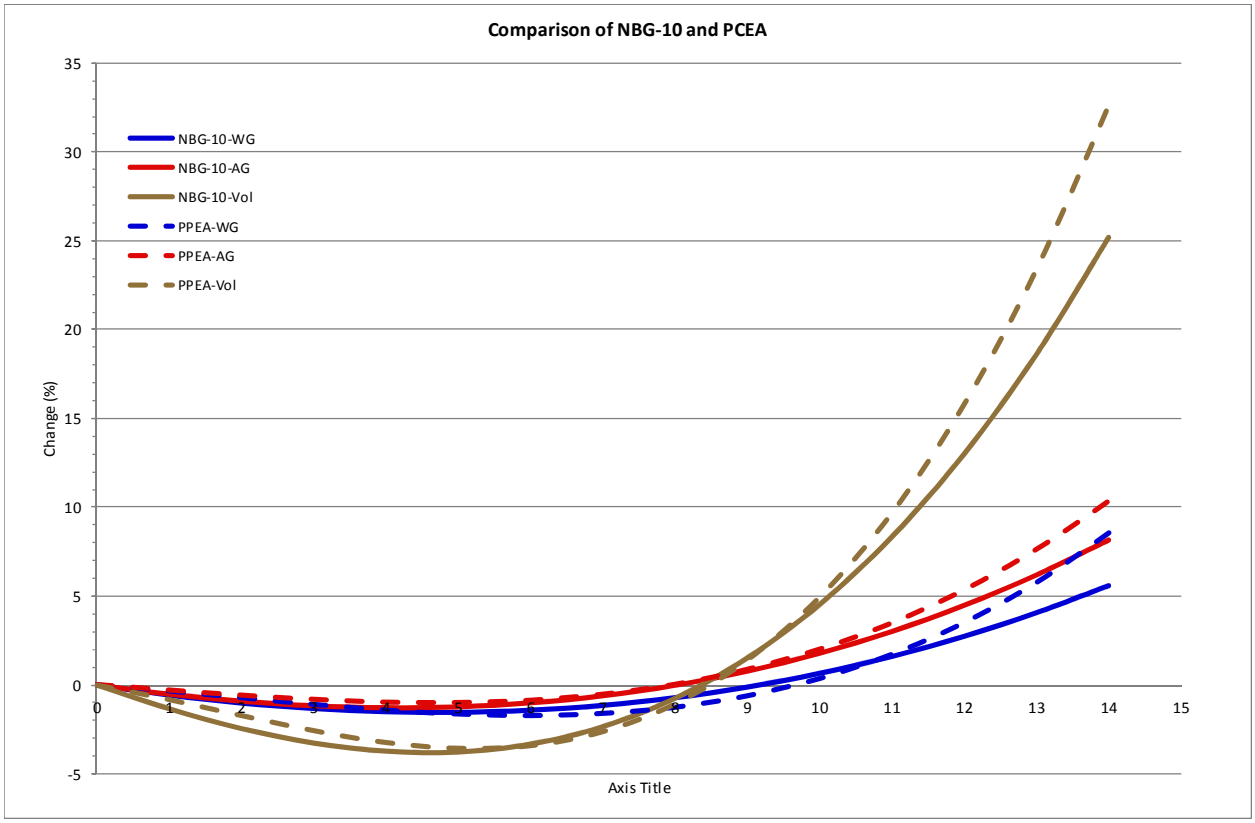

Figure 32 – Comparison of DYM variations for graphites at 950°C

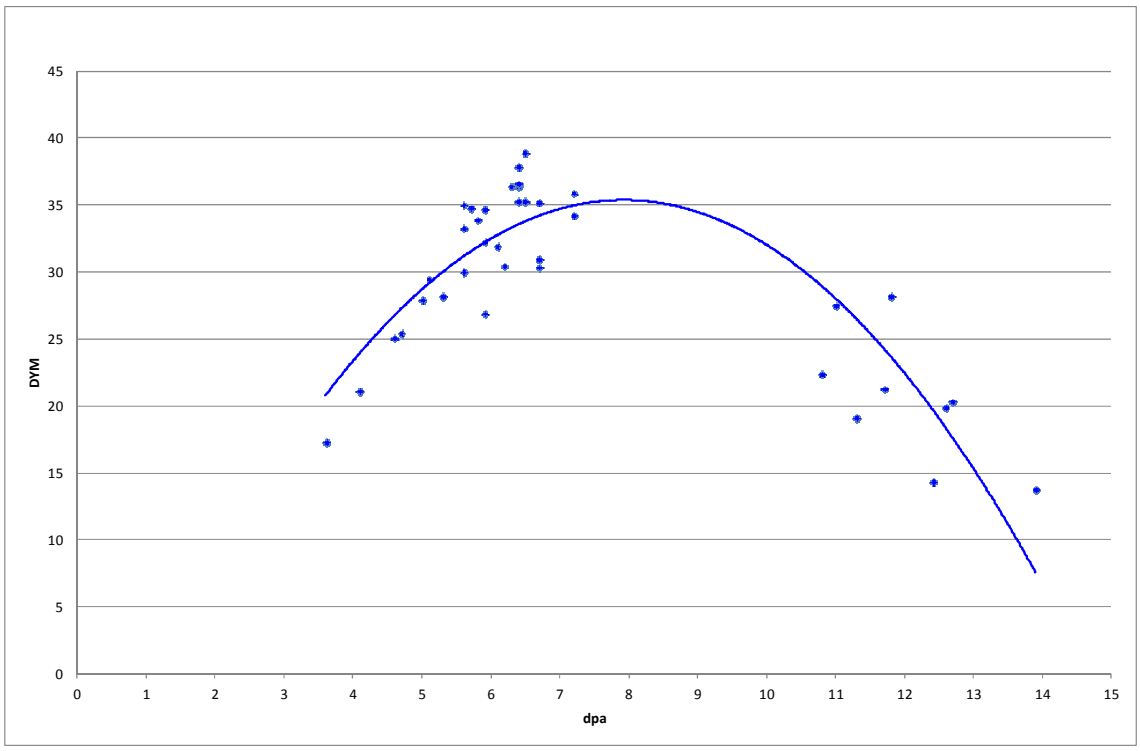

(a) NBG-10

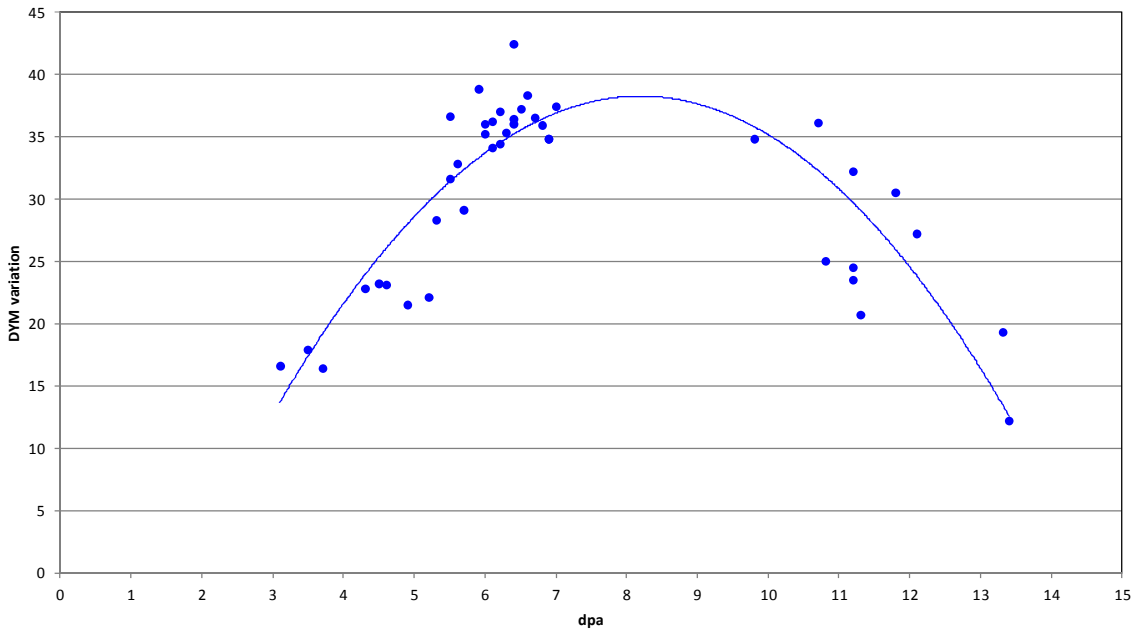

(b) PCEA

Figure 32 – cont'd

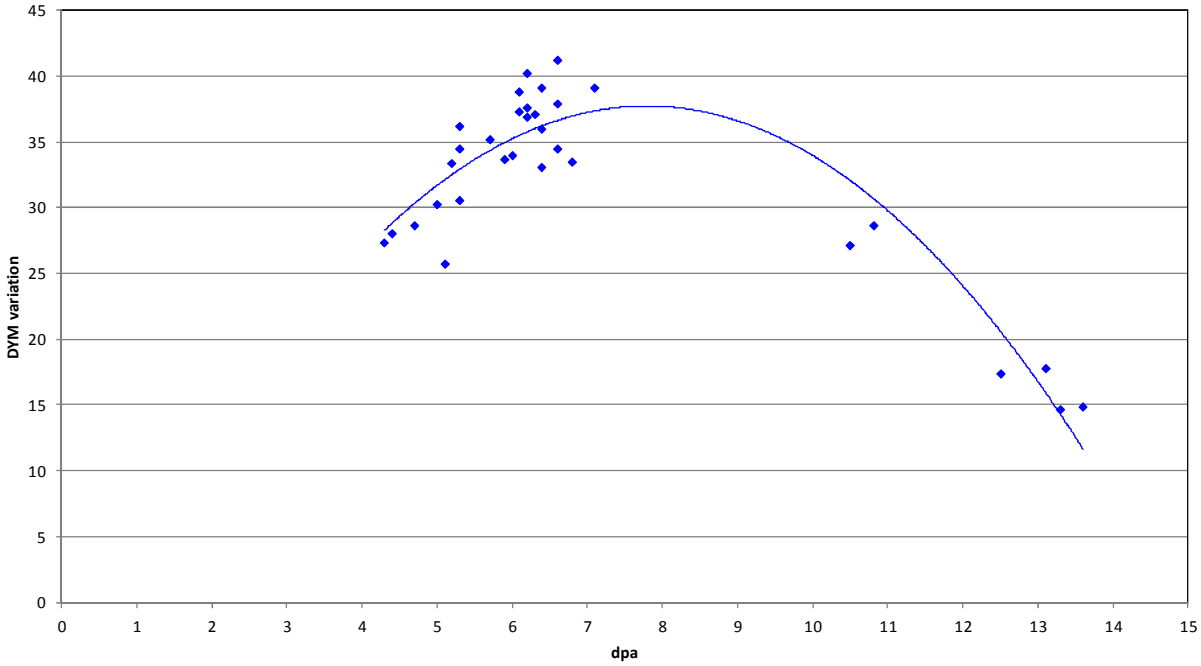

(c) PPEA

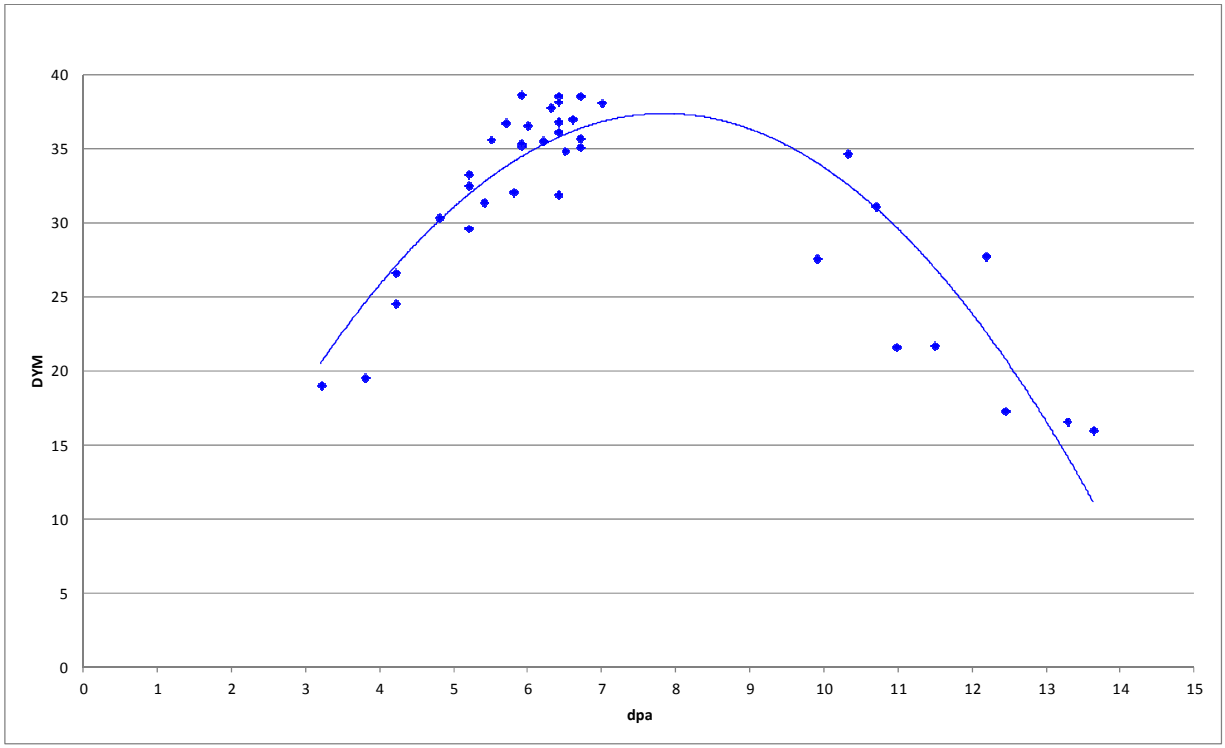

(d) NBG-18

Figure 32 – cont'd

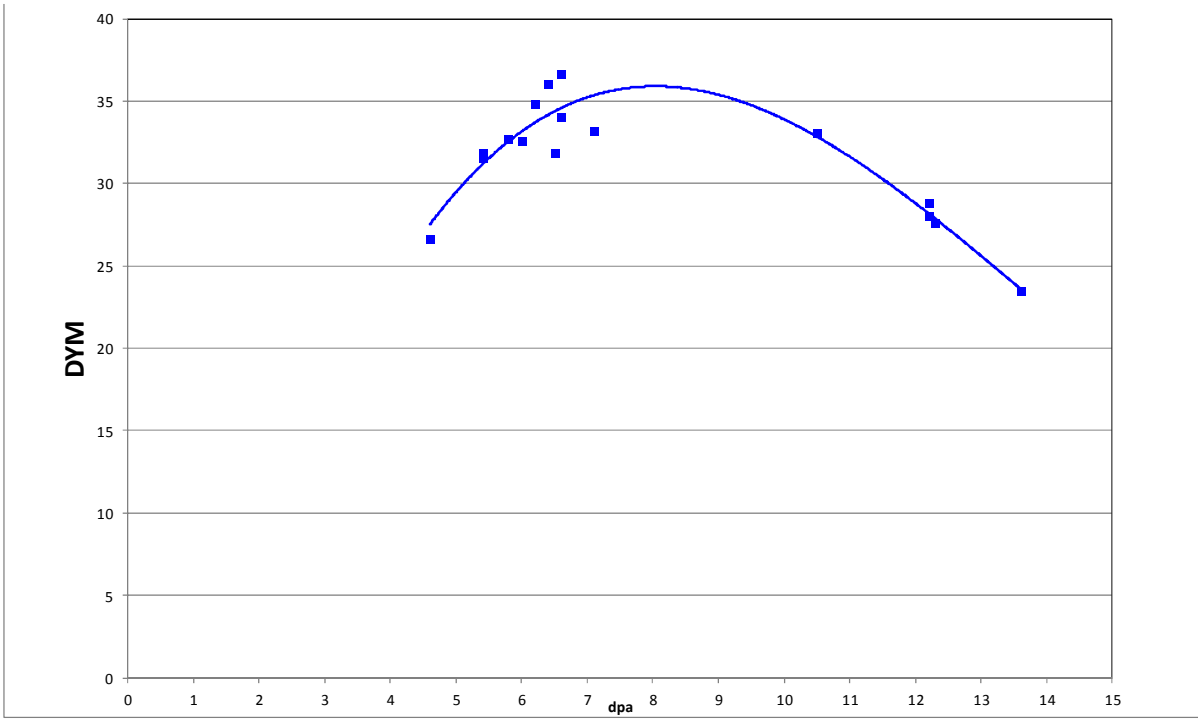

(e) NBG-25

Figure 33 – Comparison of DYM fractional changes for graphites at 950°C

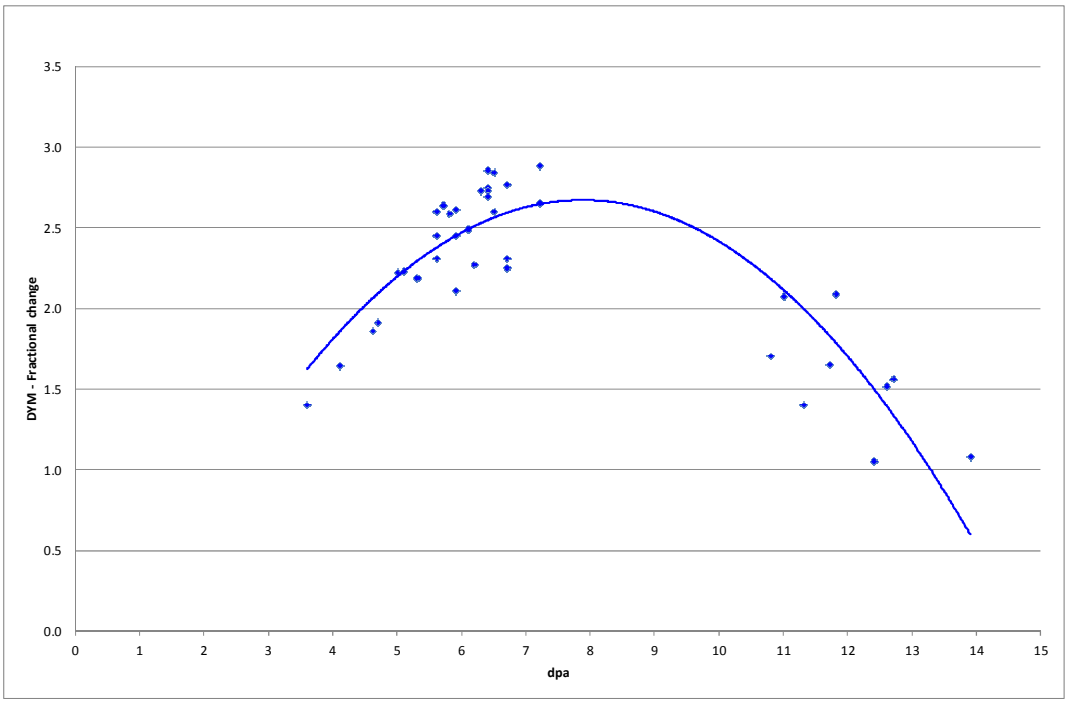

(a) NBG-10

Figure 33 – cont'd

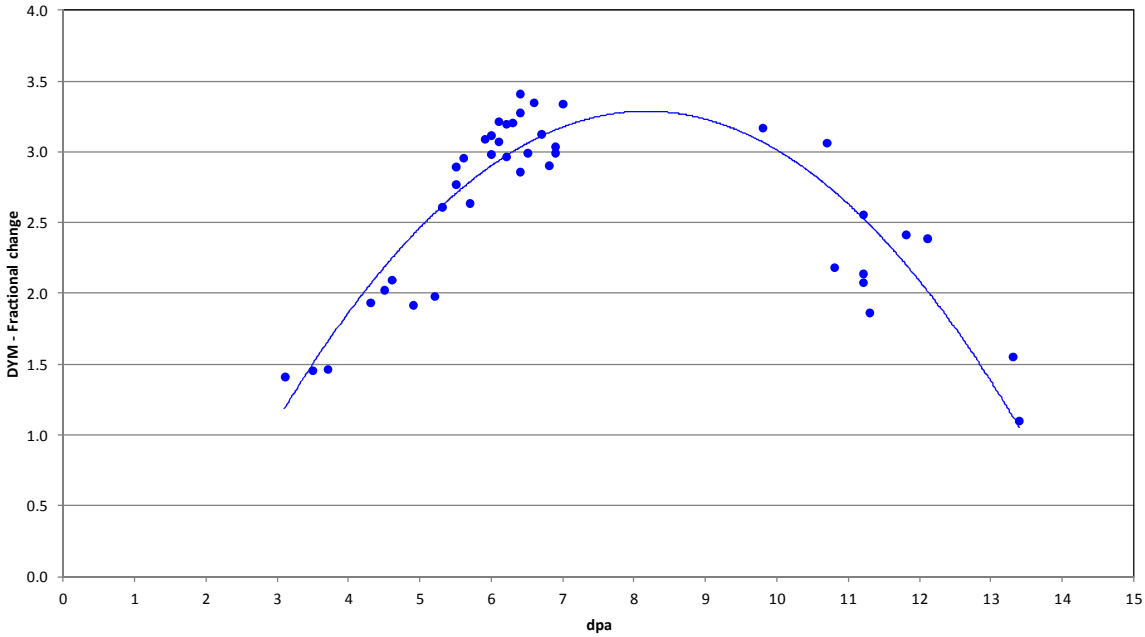

(b) PCEA

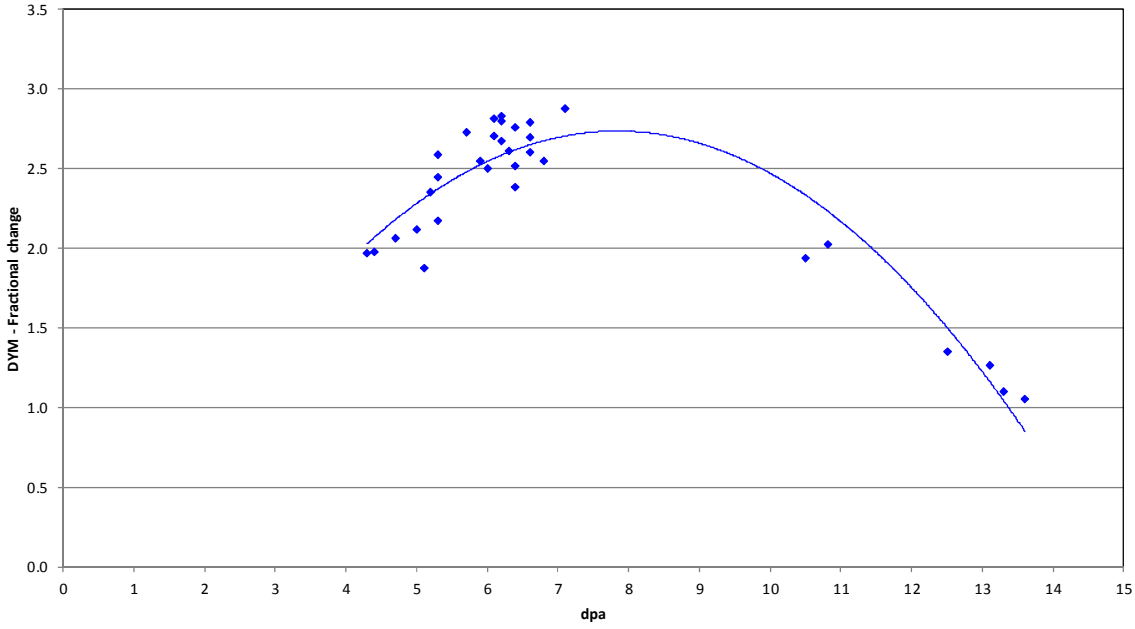

(c) PPEA

Figure 33 – cont'd

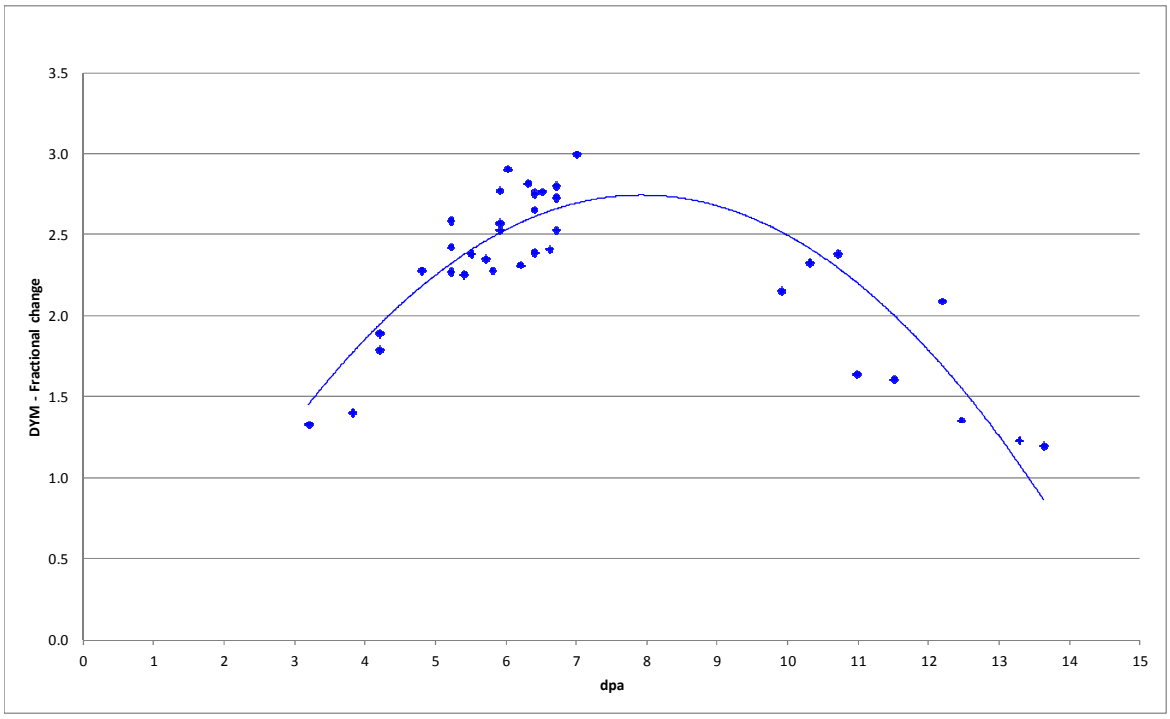

(d) NBG-18

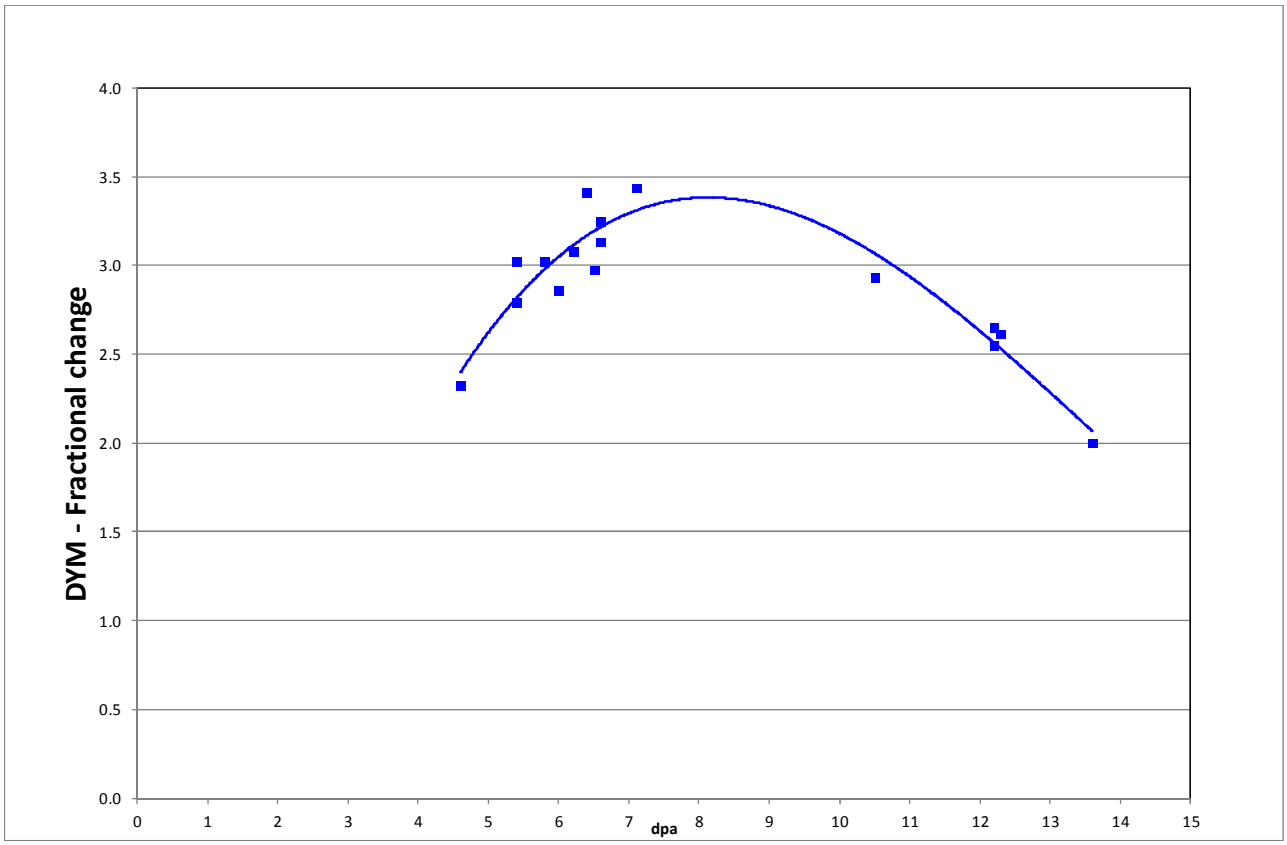

(e) NBG-25

Figure 34 – Comparison of CTE variations for graphites at 950°C

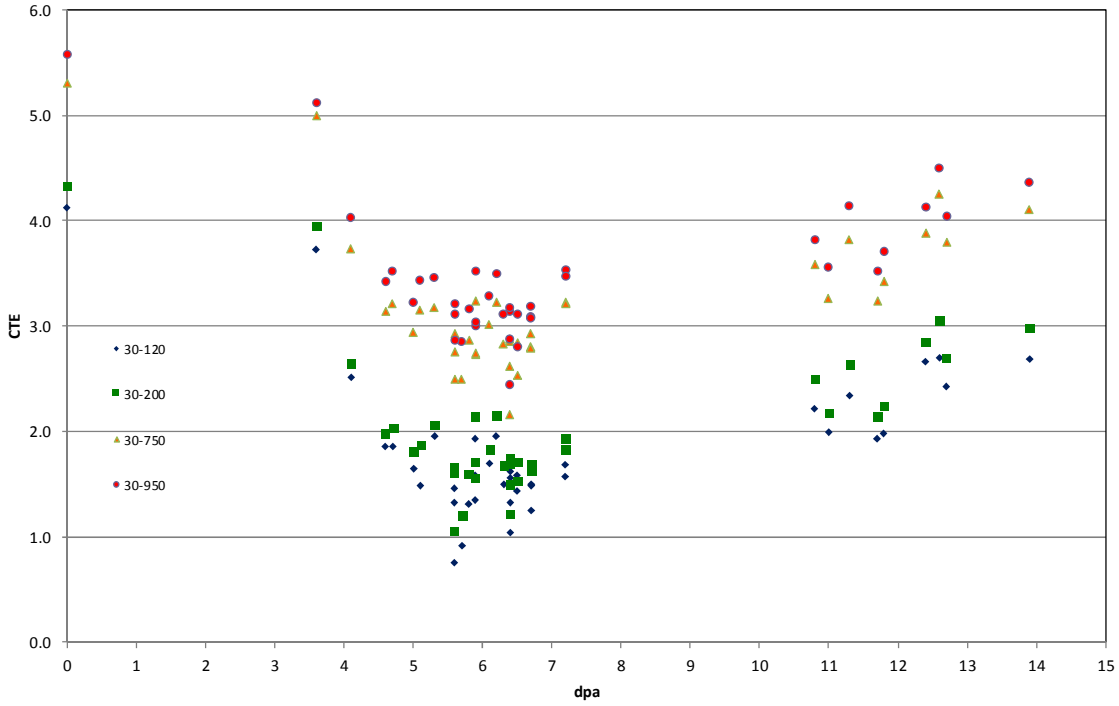

(a) NBG-10

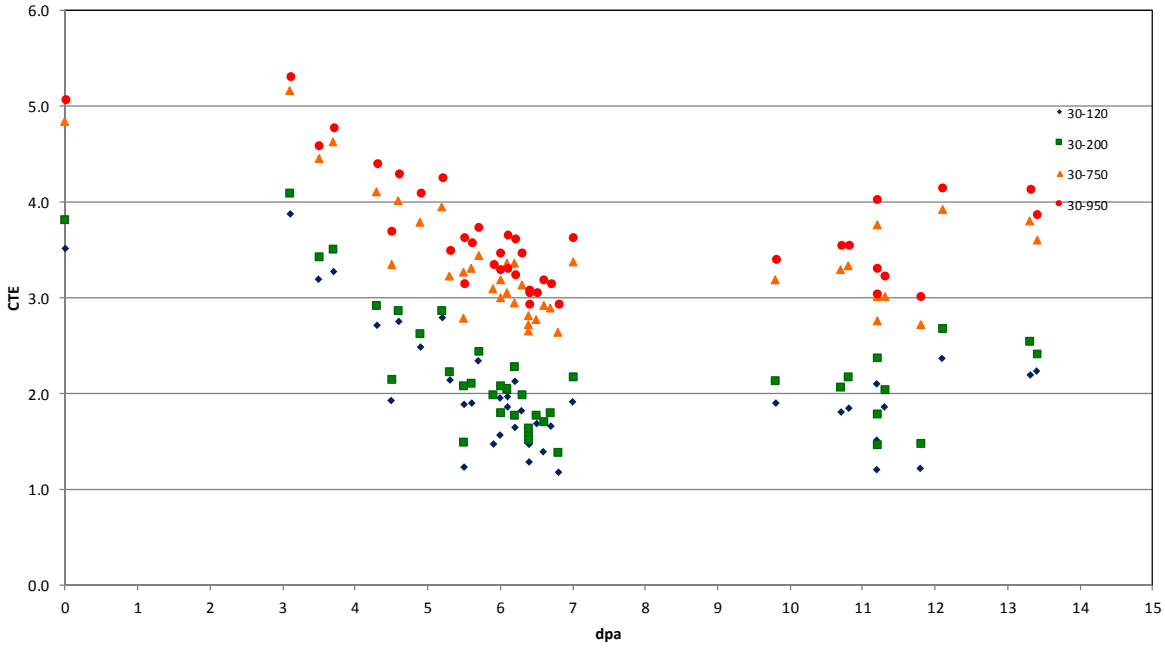

(b) PCEA

Figure 34 – cont'd

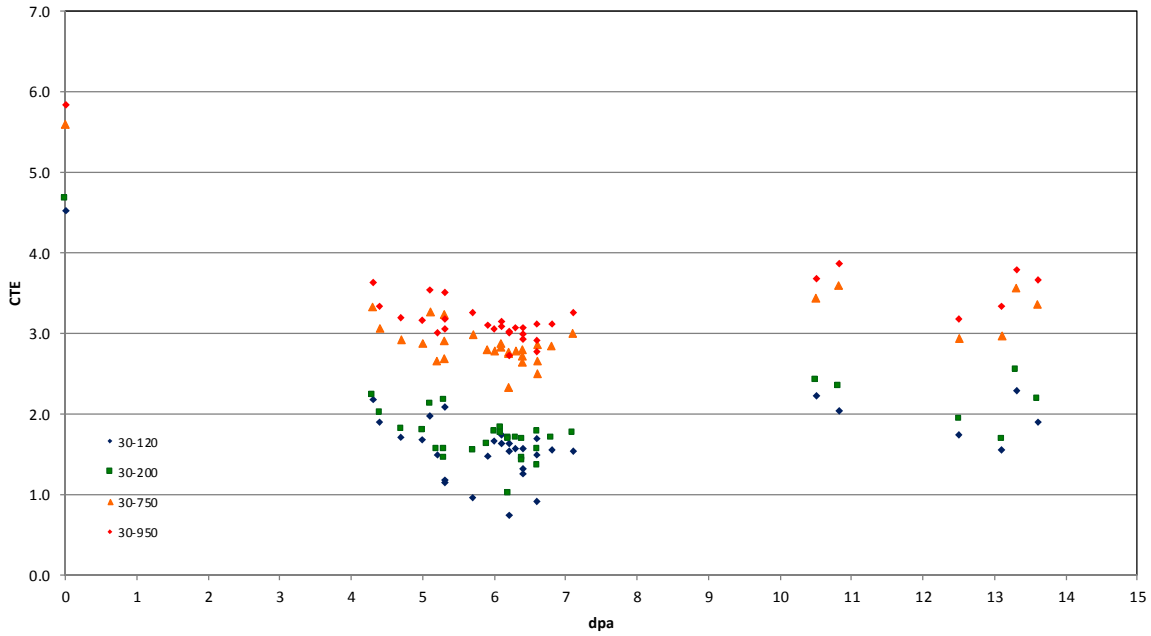

(c) PPEA

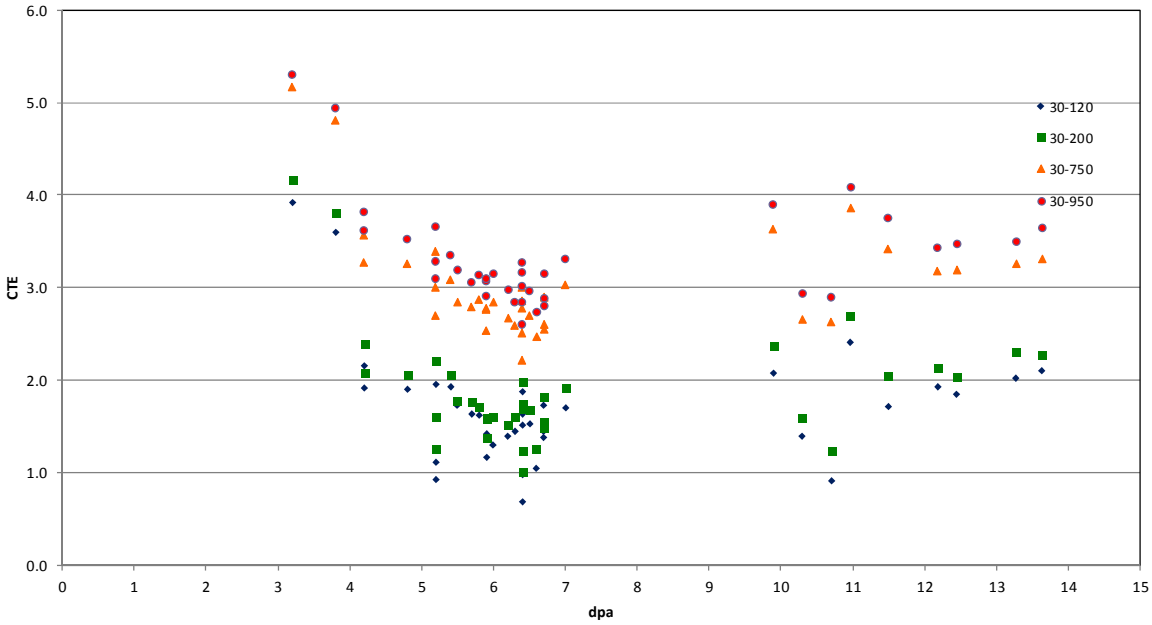

(d) NBG-18

Figure 34 – cont'd

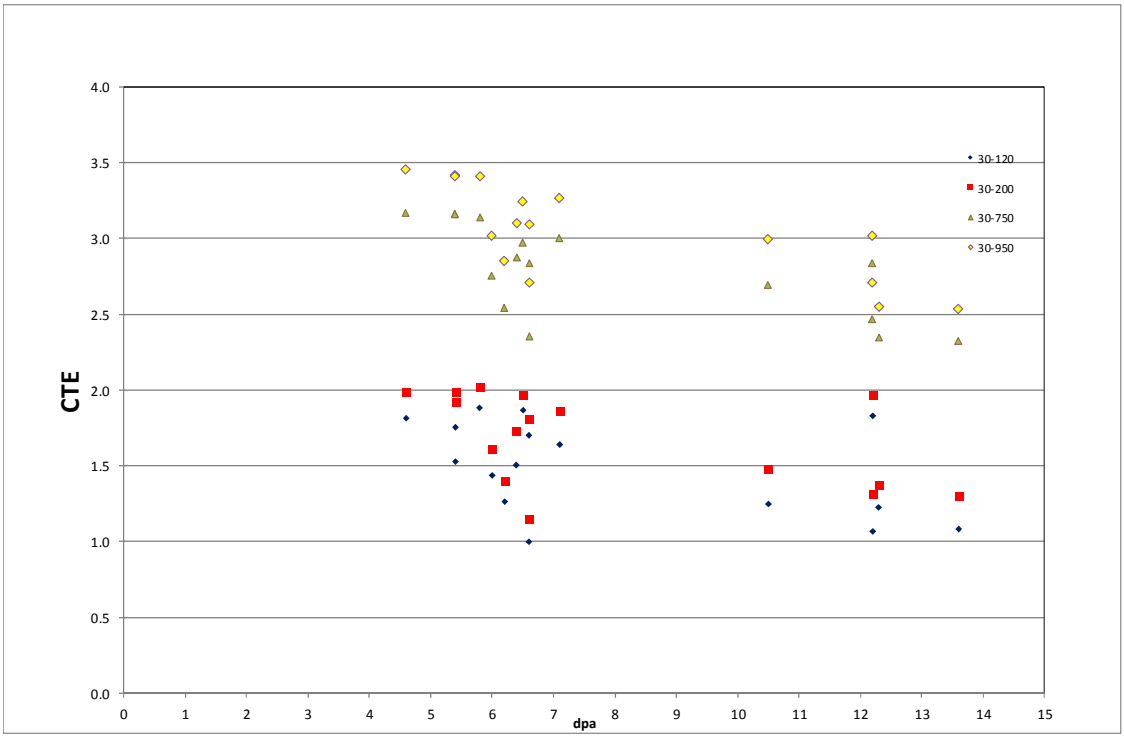

(e) NBG-25

Figure 35 – Comparison of CTE fractional changes graphites at 950°C

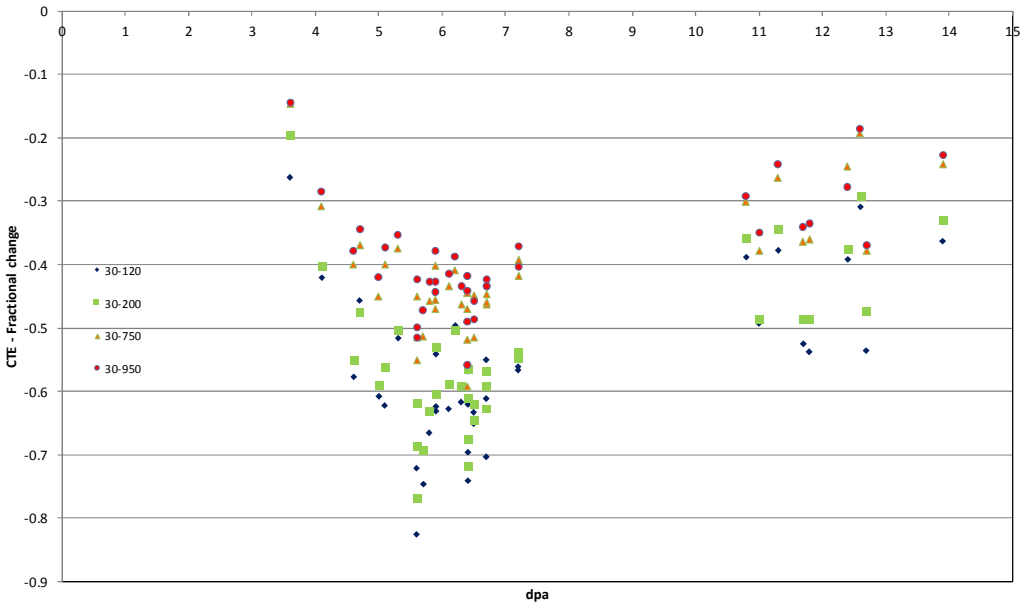

(a) NBG-10

Figure 35 – cont'd

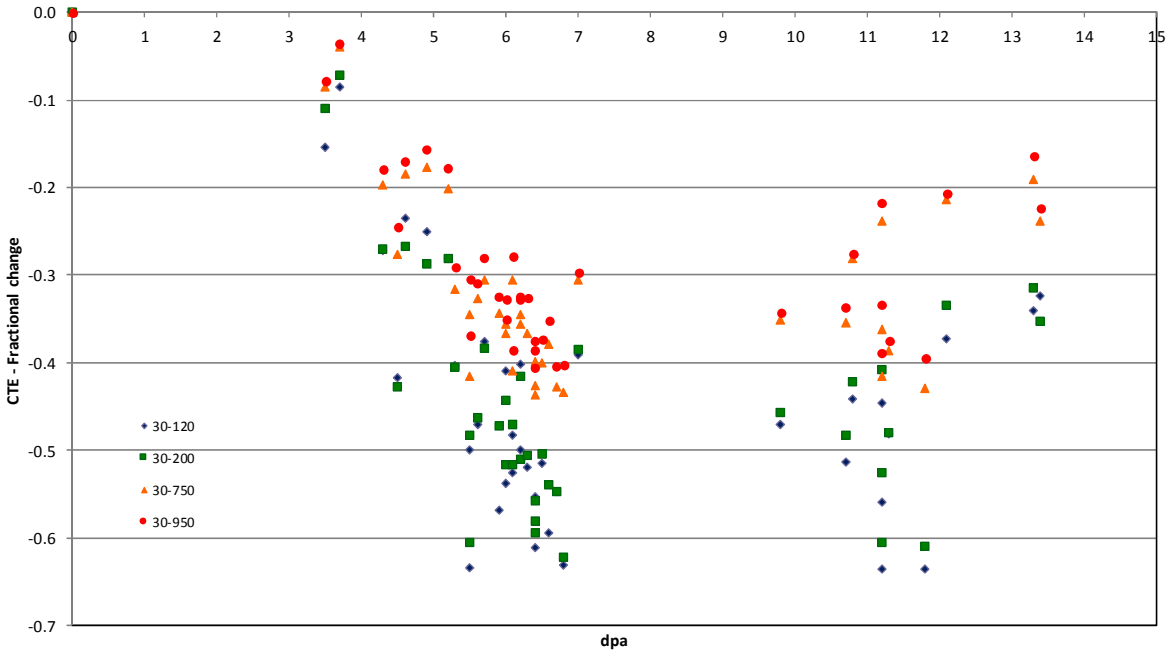

(b) PCEA

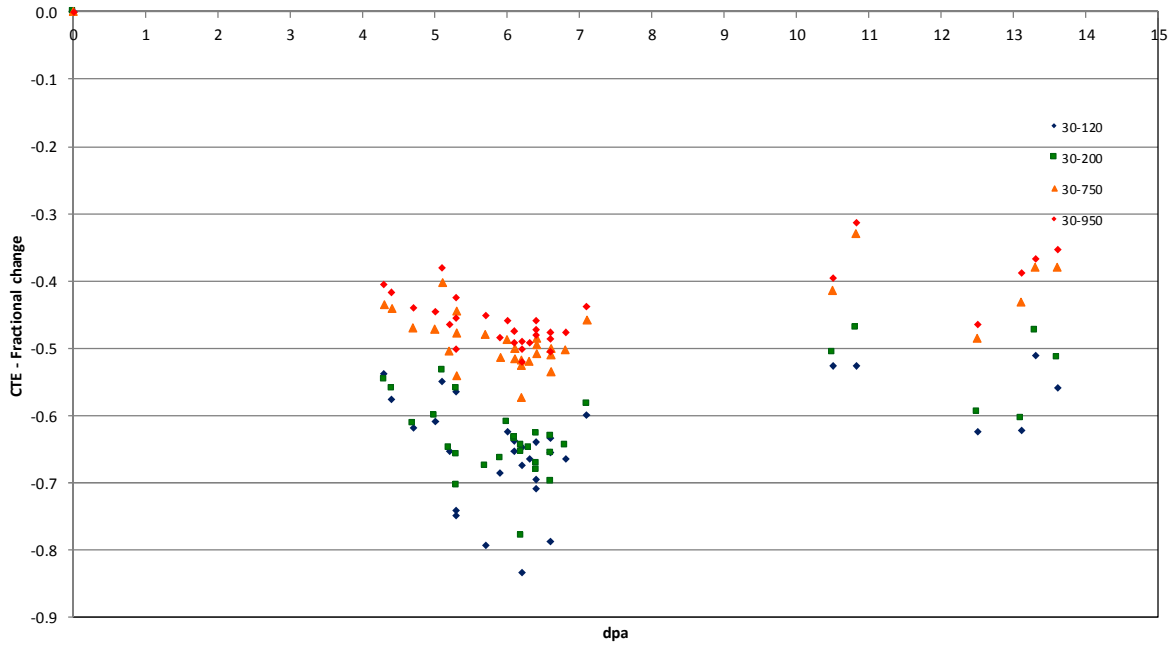

(c) PPEA

Figure 35 – cont'd

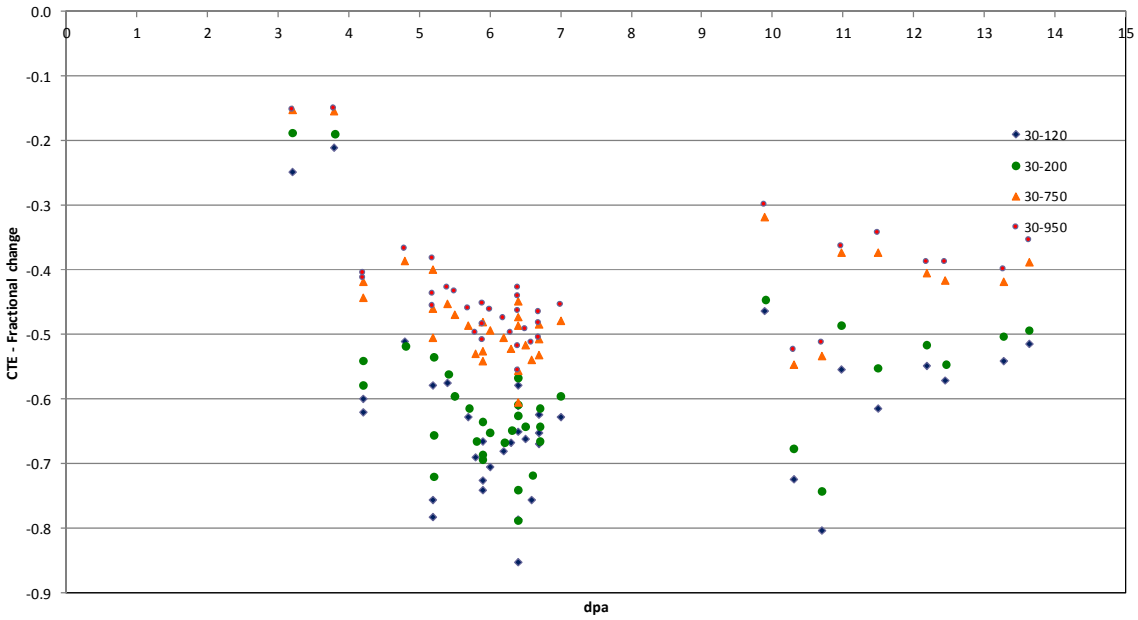

(d) NBG-18

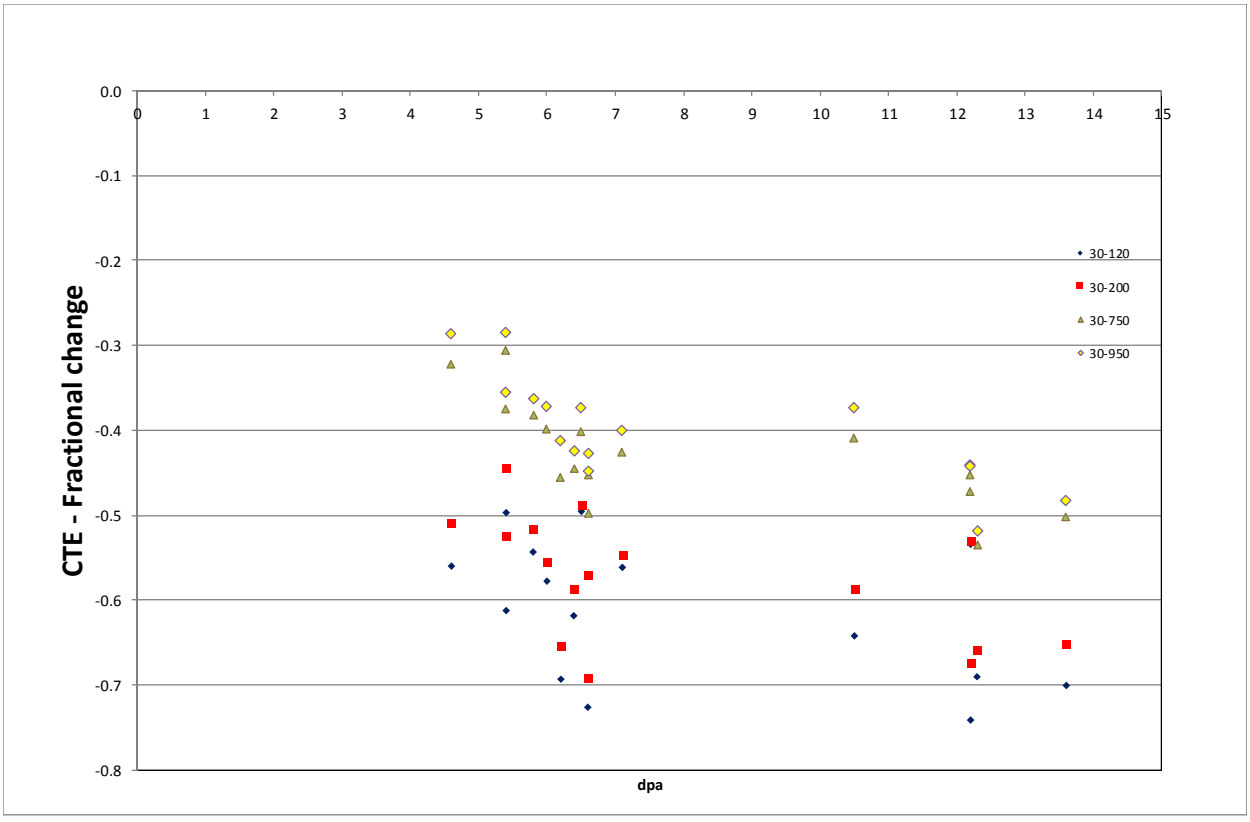

(e) NBG-25

Figure 36 – Comparison of thermal conductivity variations for graphites at 950°C

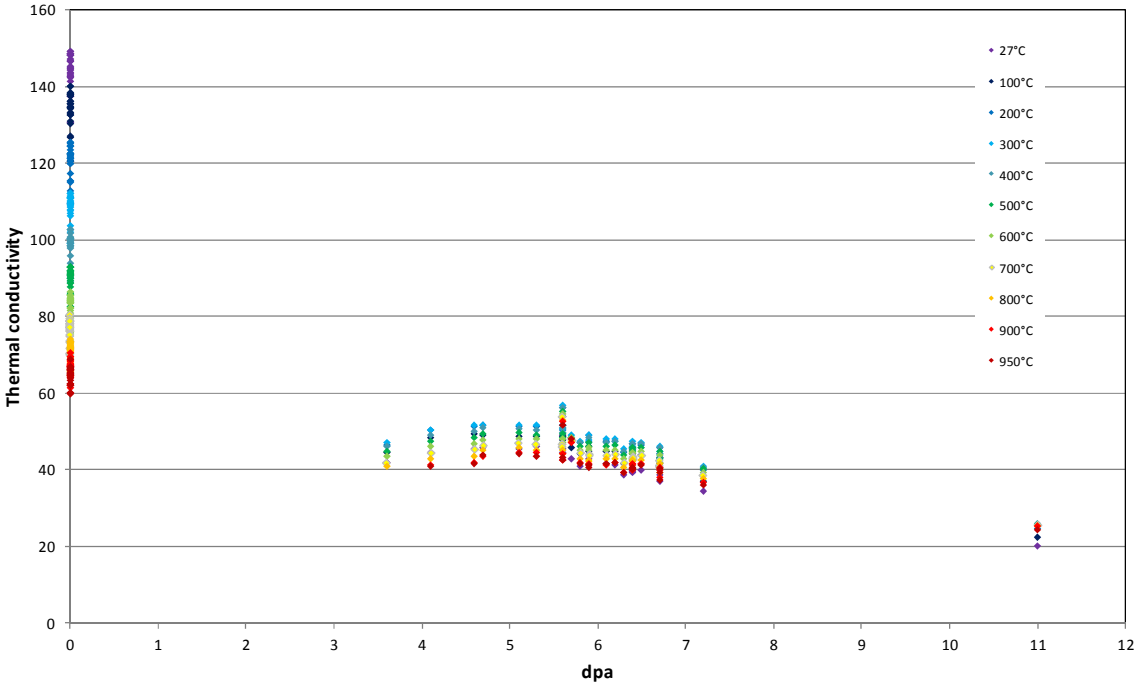

(a) NBG-10

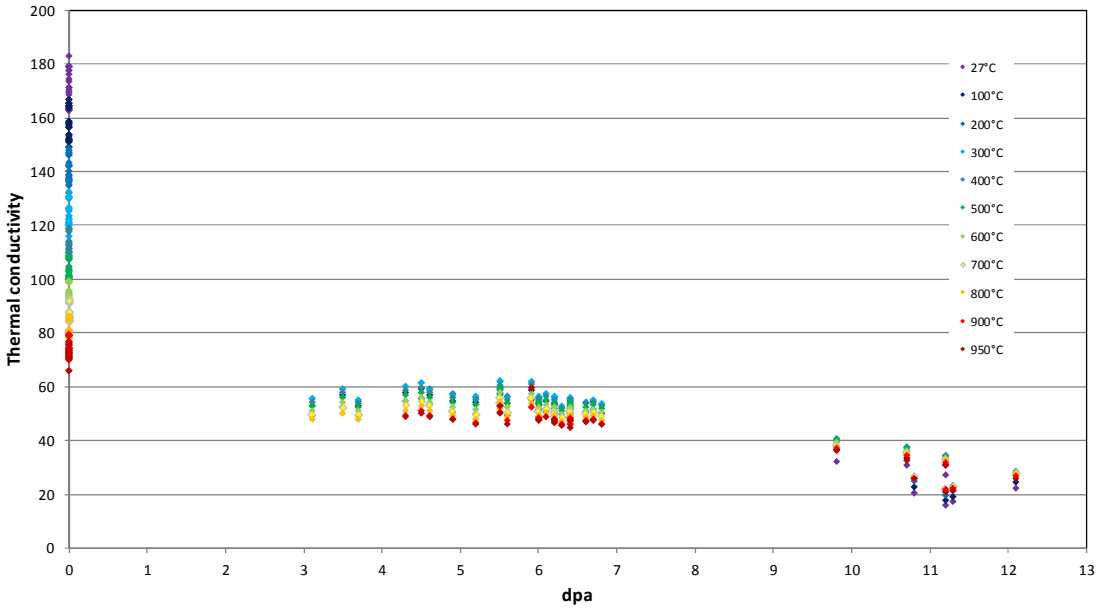

(b) PCEA

Figure 36 – cont'd

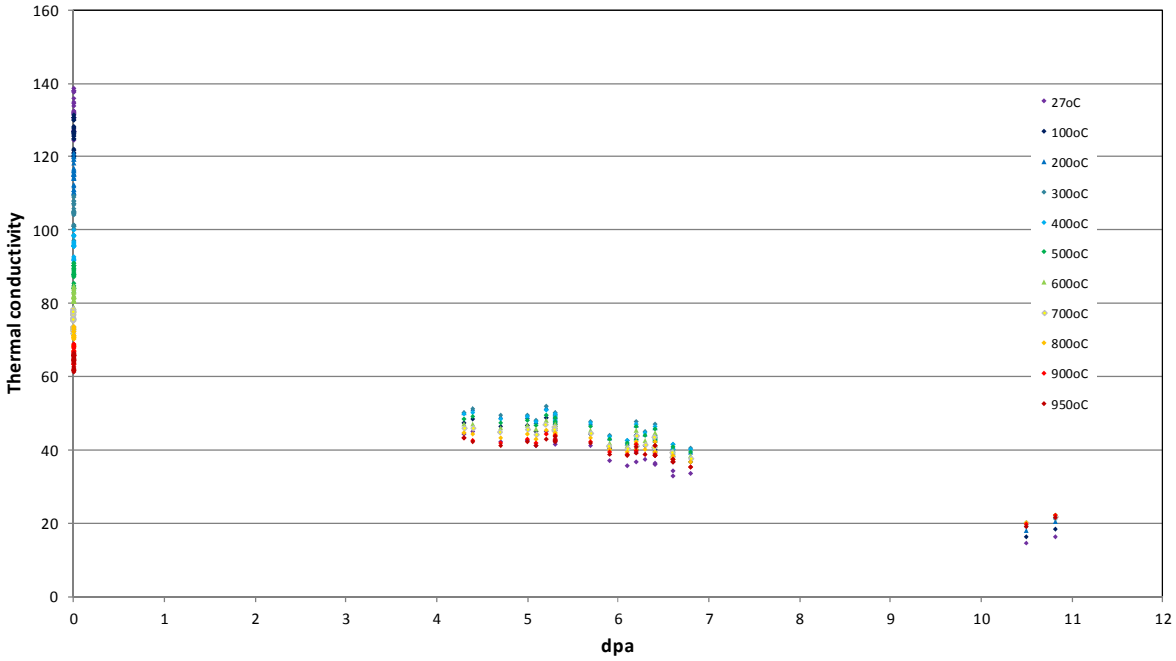

(c) PPEA

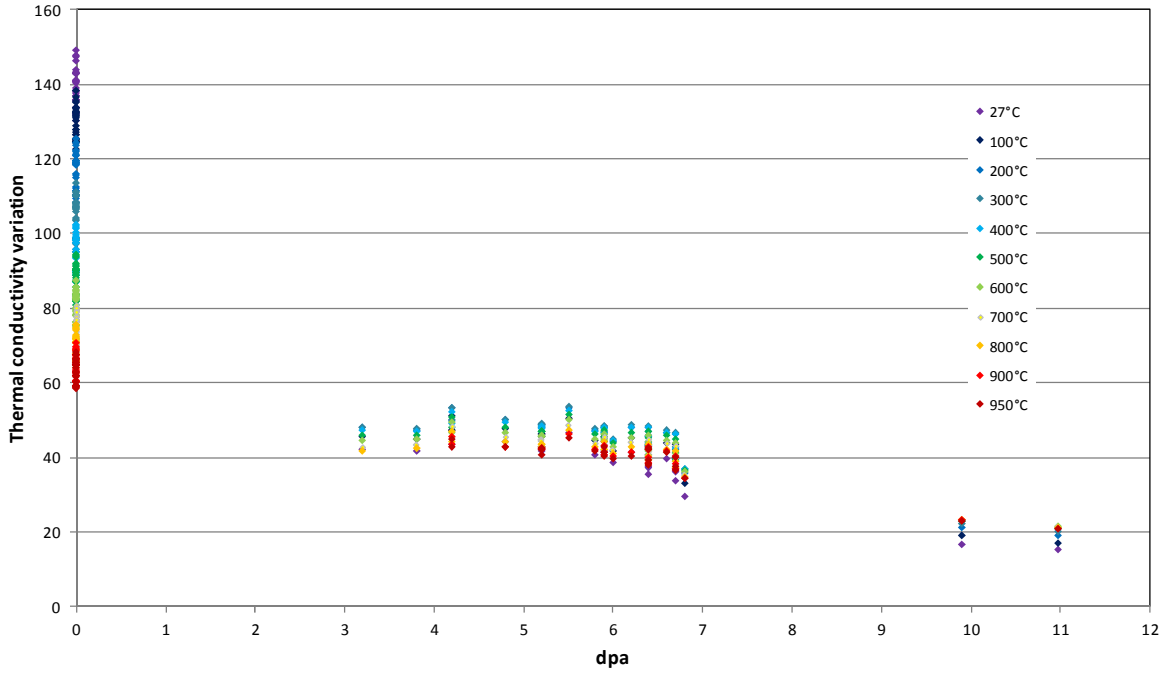

(d) NBG-18

Figure 36 – cont'd

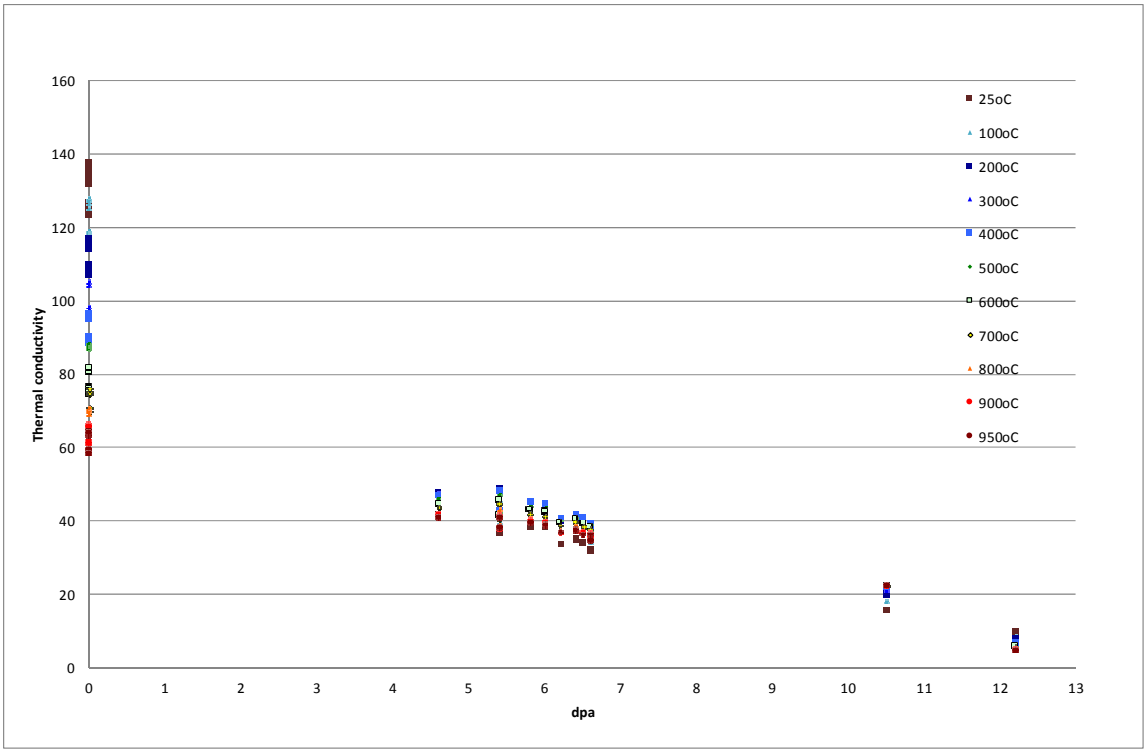

(e) NBG-25

Figure 37 – Comparison of thermal conductivity fractional changes for graphites at 950°C

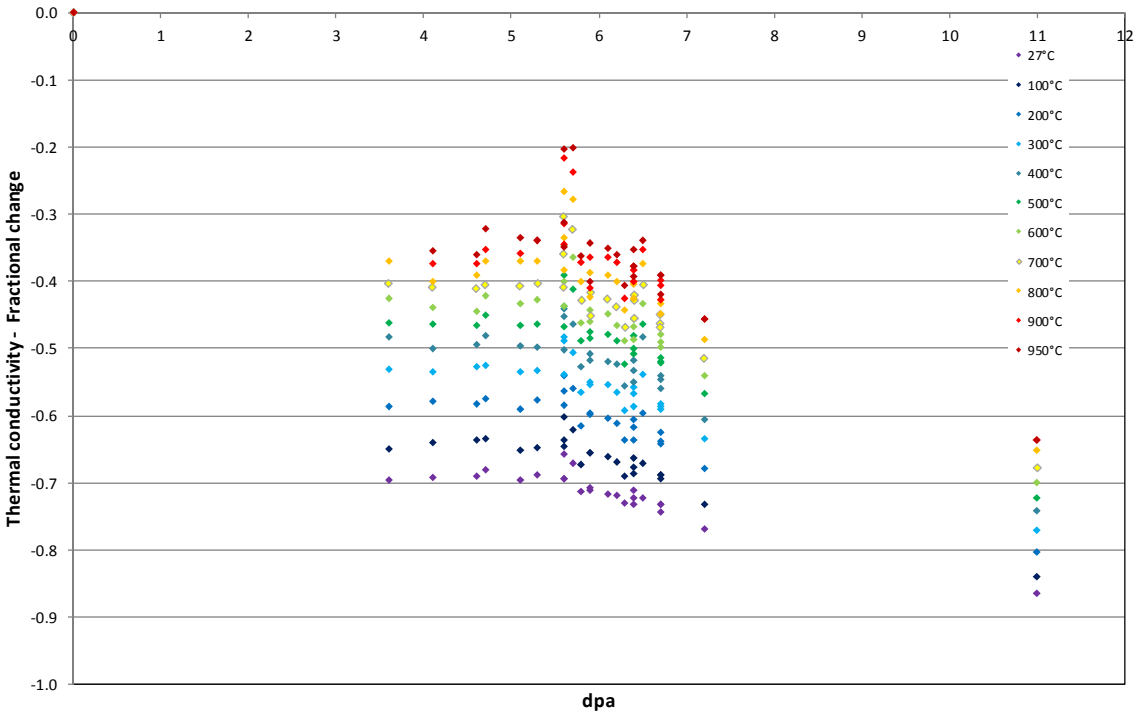

(a) NBG-10

Figure 37 – cont'd

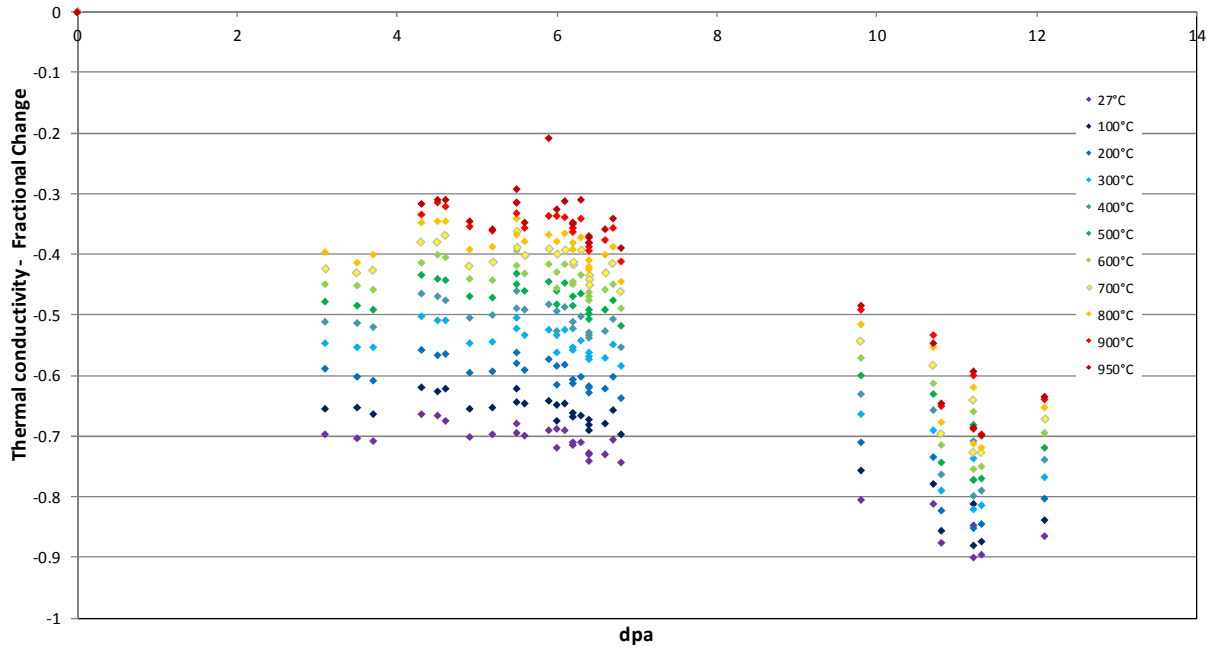

(b) PCEA

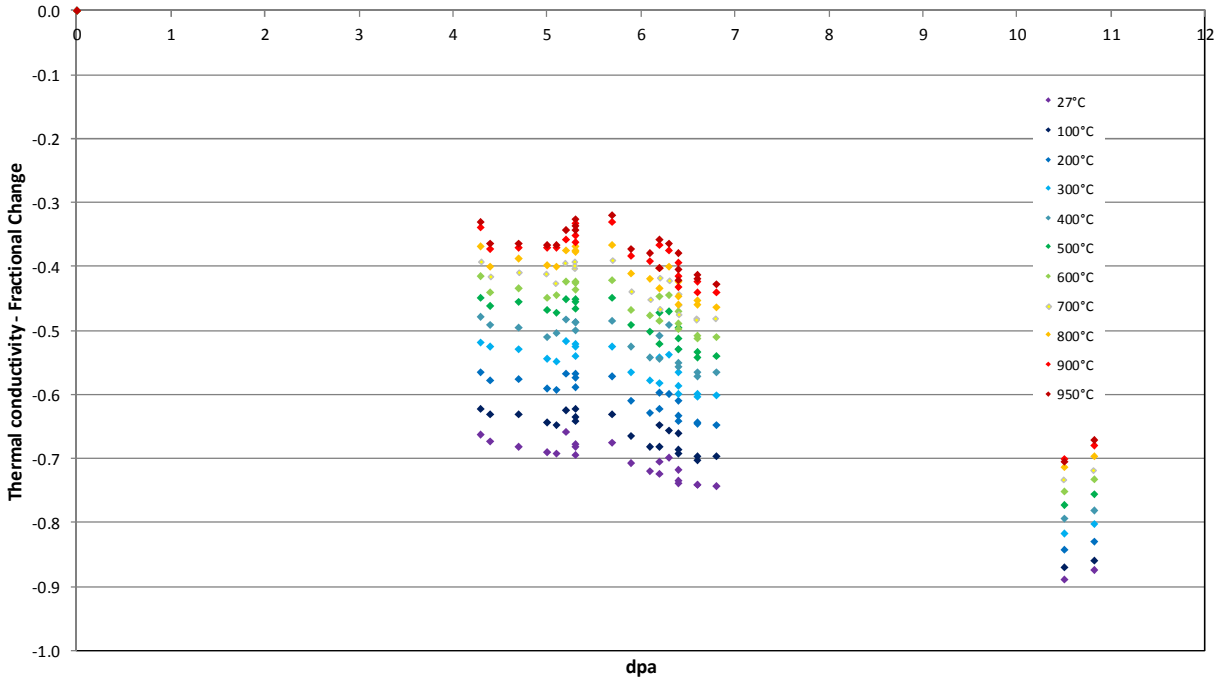

(c) PPEA

Figure 37 – cont'd

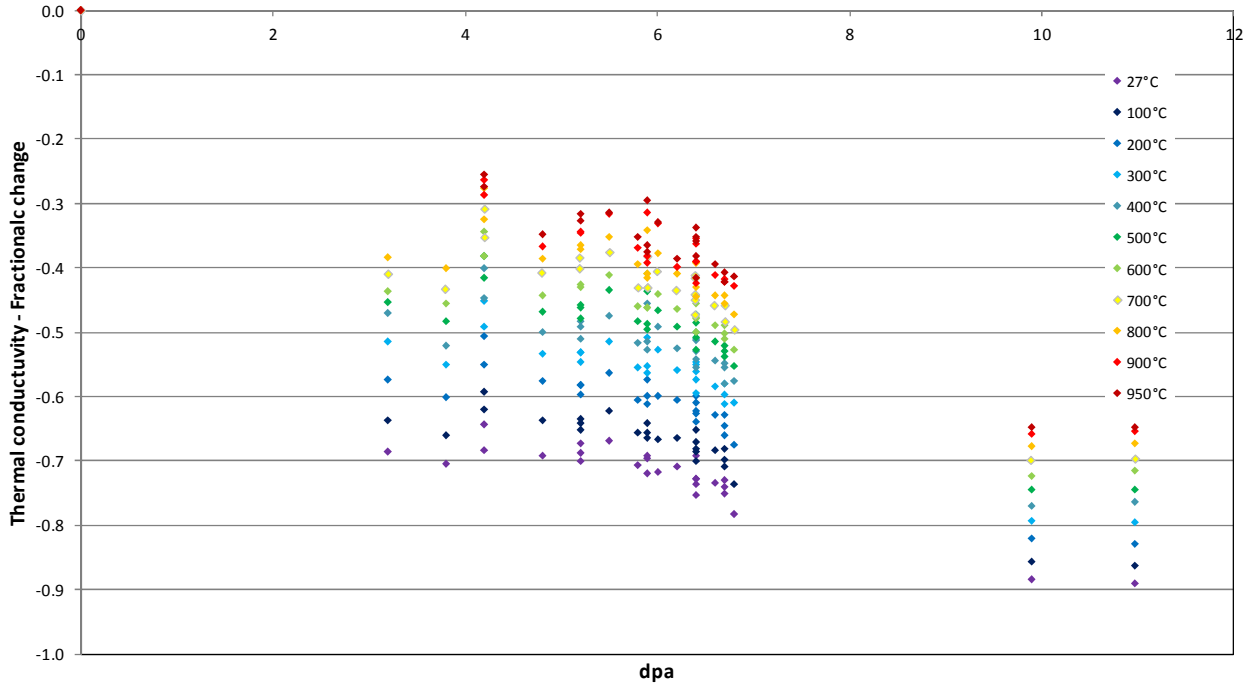

(d) NBG-18

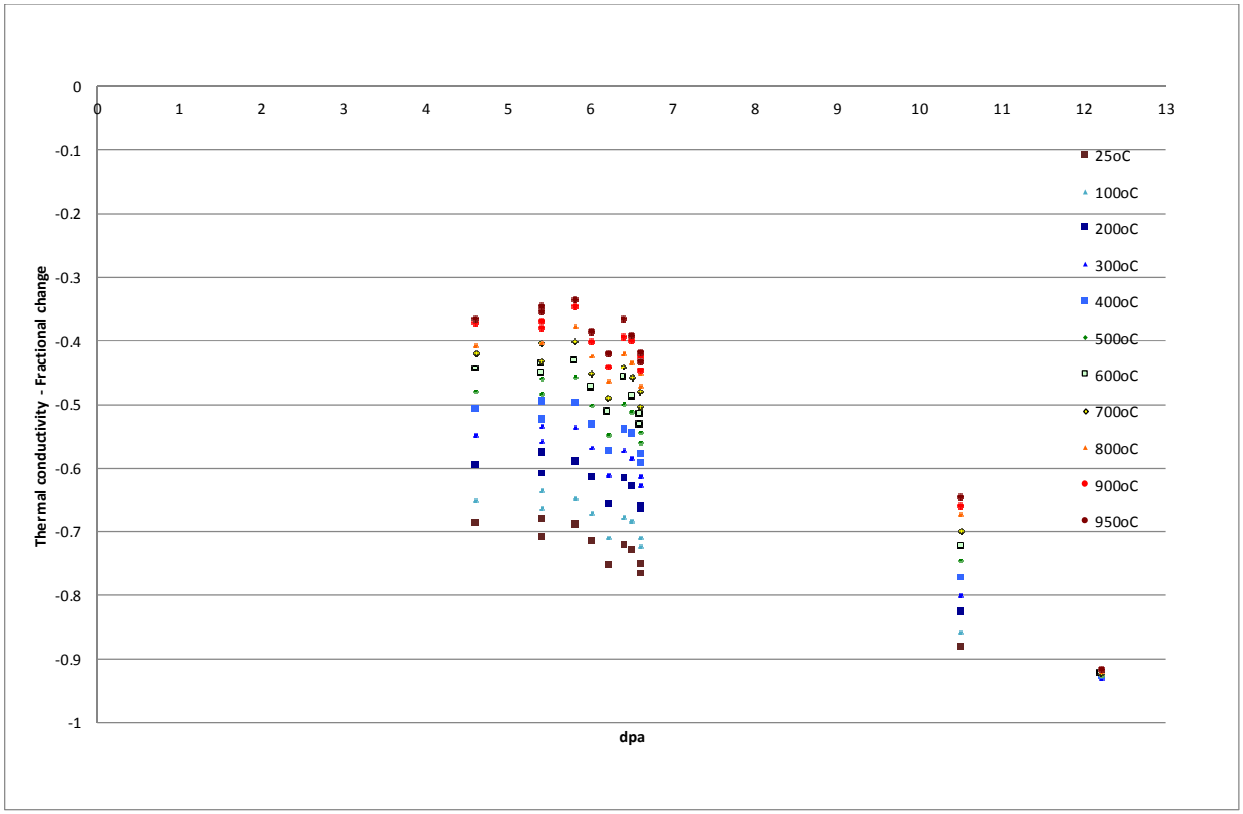

(e) NBG-25

Figure 38 – Comparison of an extruded graphite at 750ºC and 950ºC - WG

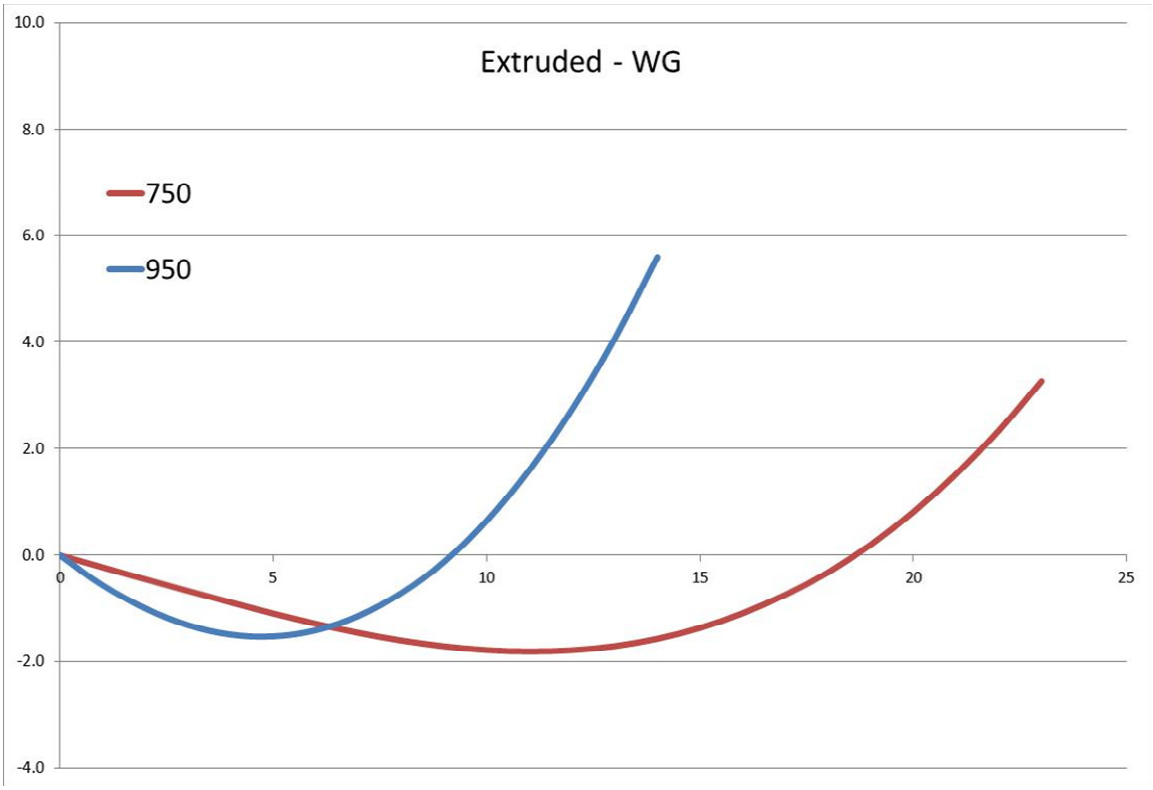

Figure 39 – Comparison of an extruded graphite at 750ºC and 950ºC - AG

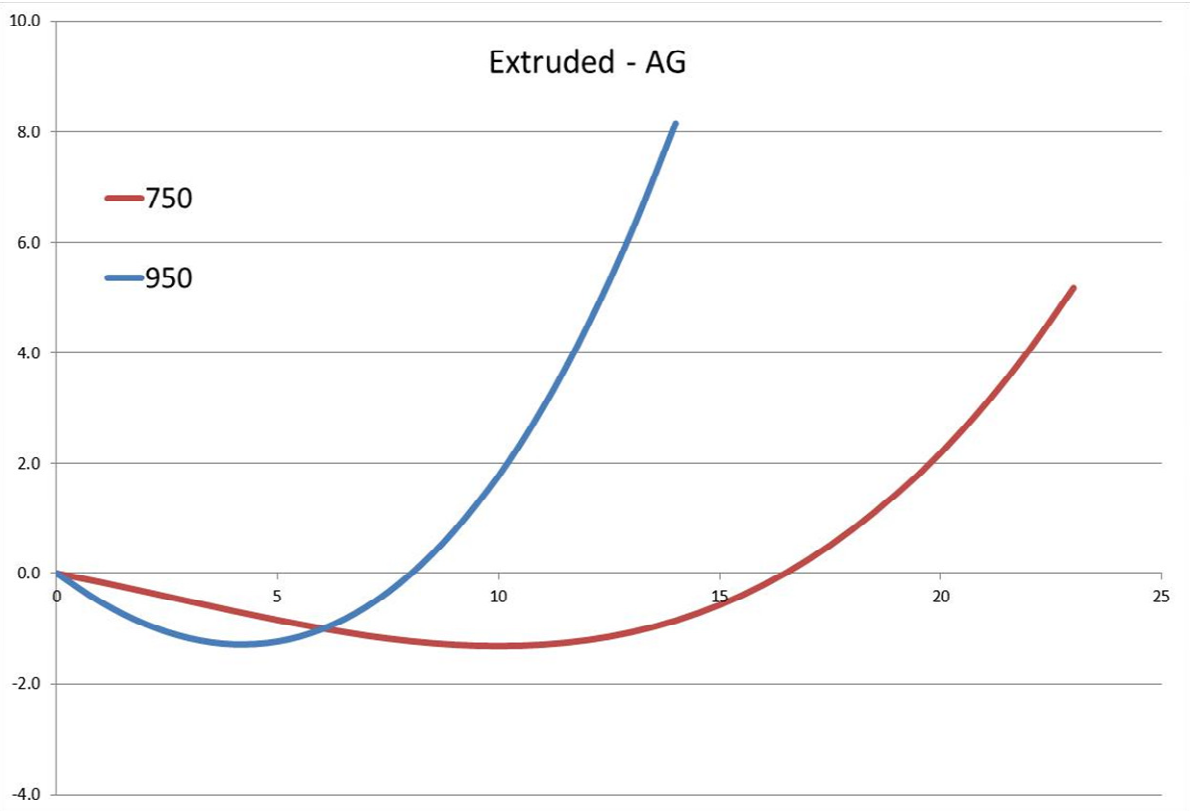

Figure 40 – Comparison of an extruded graphite at 750oC and 950oC - volume

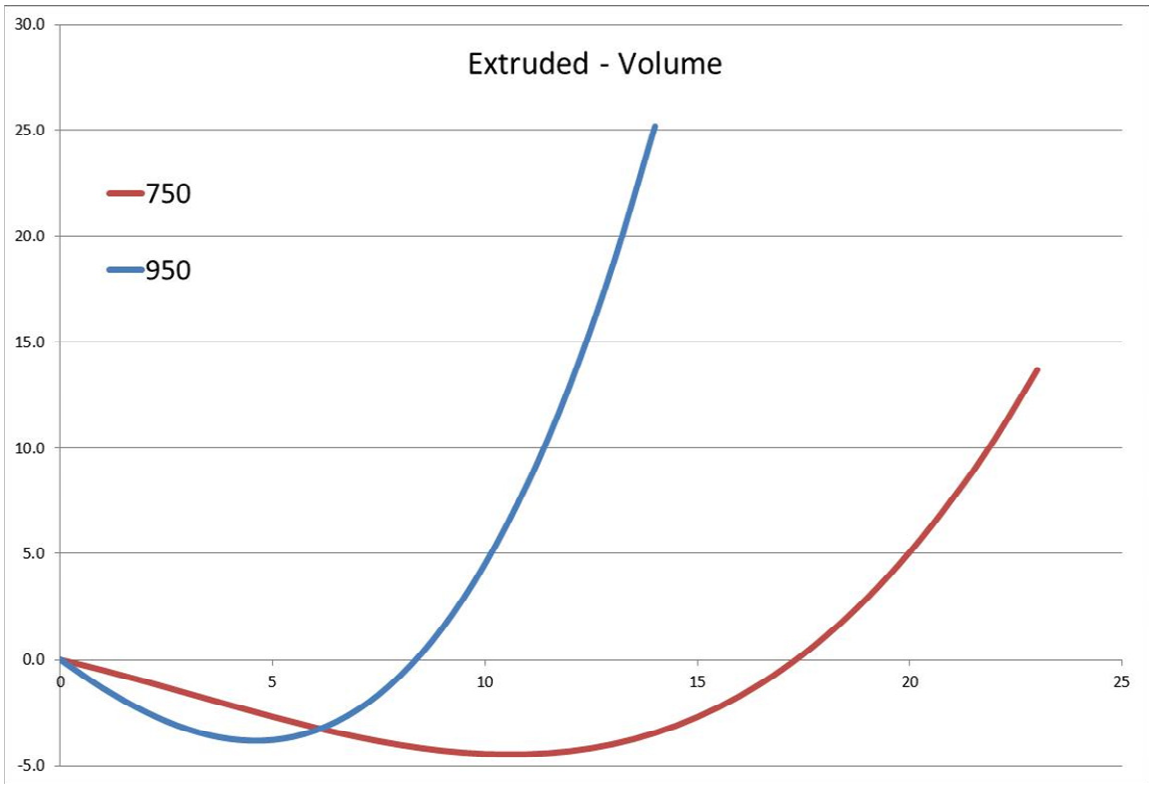

Figure 41 – Comparison of an iso-moulded graphite at 750°C and 950°C - WG

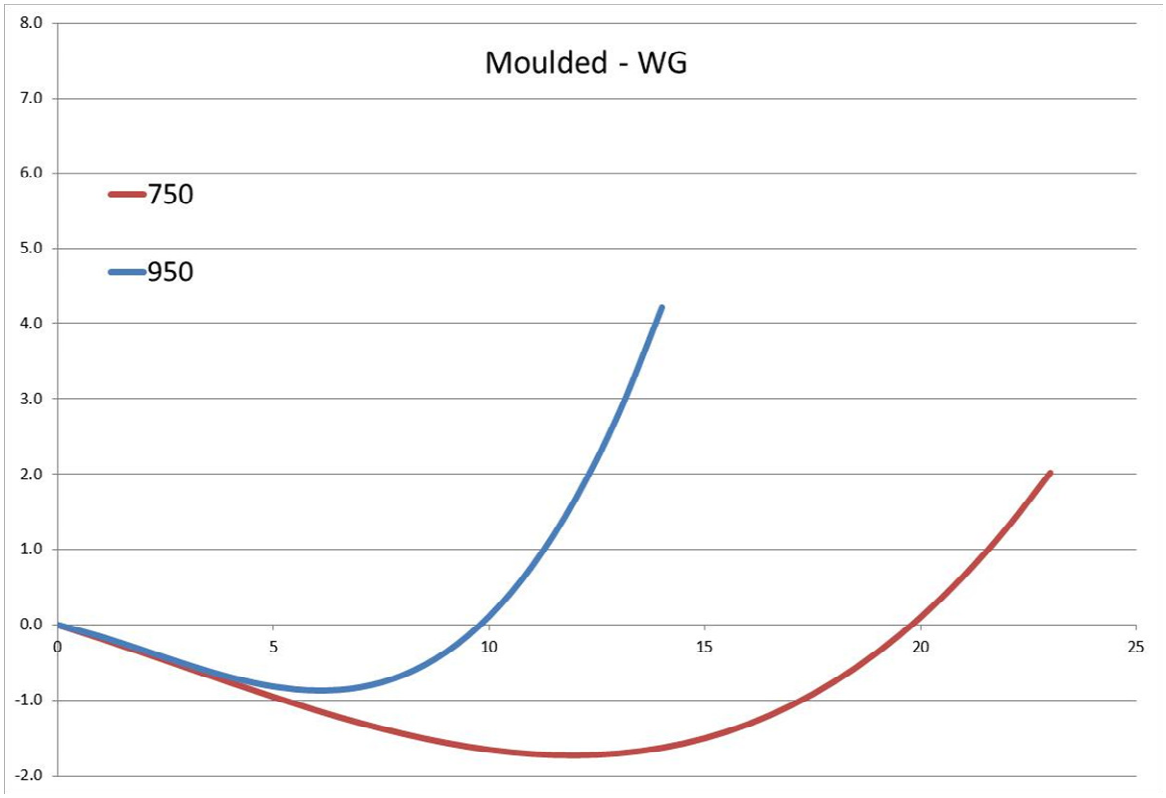

Figure 42 – Comparison of an iso-moulded graphite at 750°C and 950°C - AG

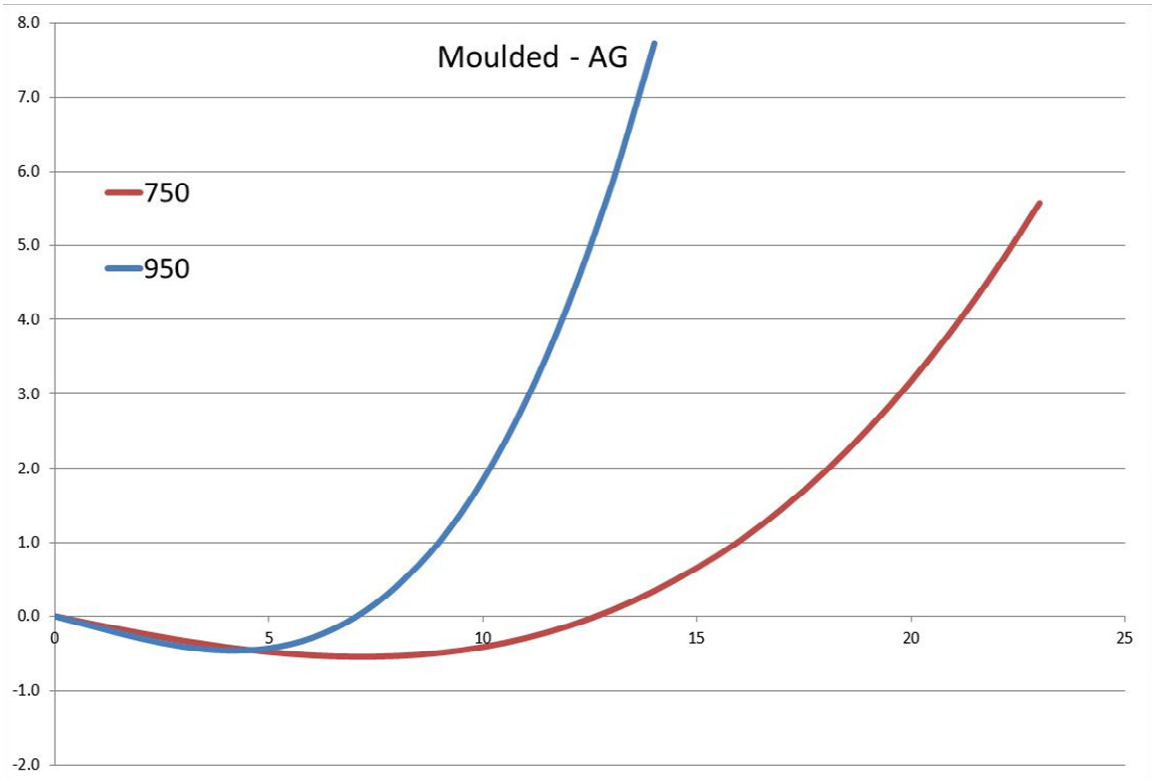

Figure 43 – Comparison of an iso-moulded graphite at 750°C and 950°C - volume